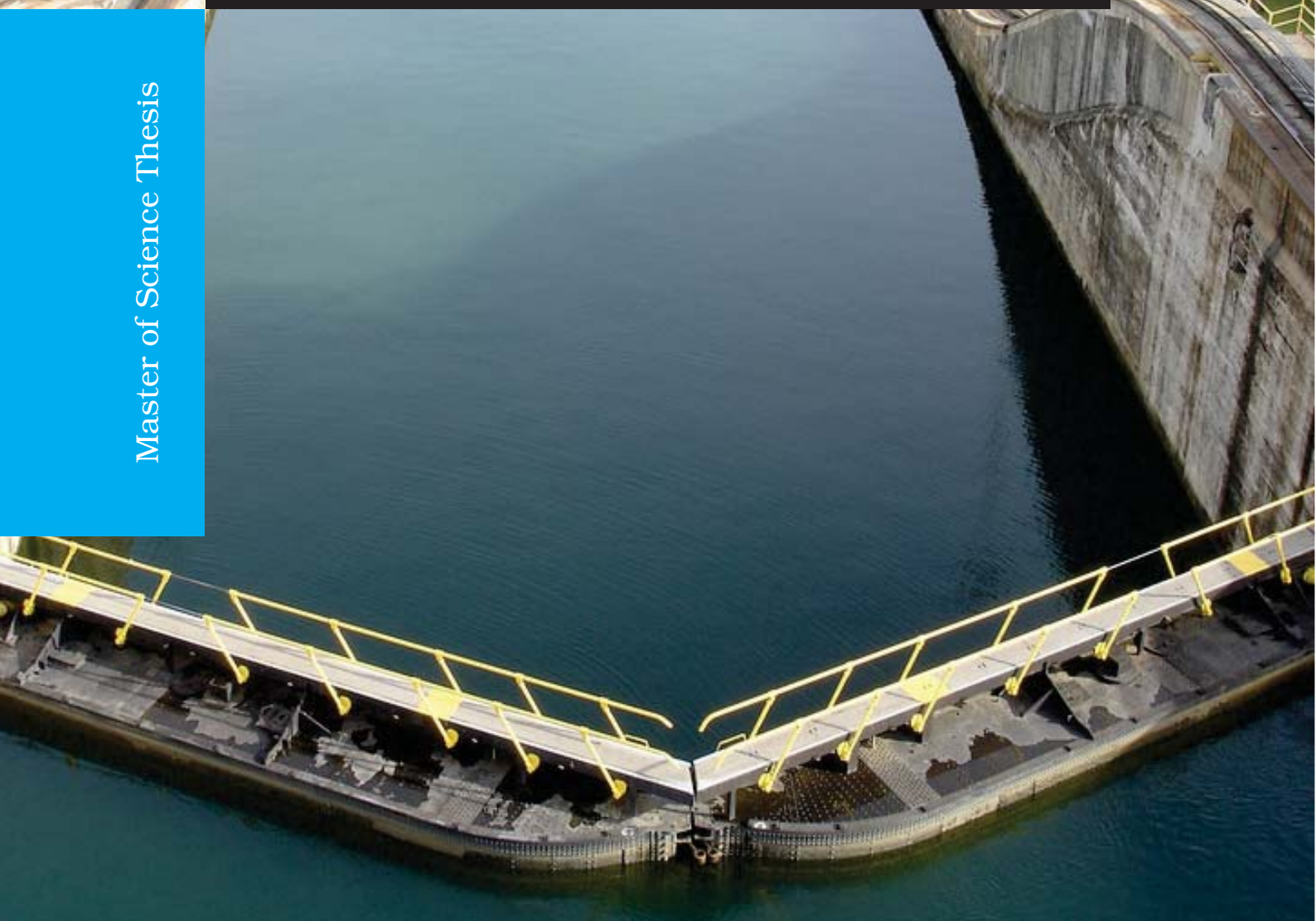


Fatigue of steel Lock Gates

Daniël Schönfeld

Master of Science Thesis



DELFT UNIVERSITY OF TECHNOLOGY

MASTER THESIS

Fatigue of steel Lock Gates

A thesis submitted to Delft University of Technology
for the degree of Master of Science in Civil Engineering

Author:

Daniël Schönfeld
Student number: 4032691
danielschonfeld@outlook.com

Thesis committee:

Delft University of Technology
Prof. dr. ir. S.N. Jonkman
dr. ir. K.J. Bakker
dr. M.H. Kolstein

TNO

dr. ir. J. Maljaars

Rijkswaterstaat

ing. J. den Toom

Delft University of Technology
Faculty of Civil Engineering and Geosciences
Department of Structural Engineering
Section of Hydraulic Engineering Structures

July 25, 2013

copyright © Daniël Schönfeld

Preface

This research project on fatigue of steel lock gates is carried out as the final phase of my master study in Civil Engineering at the Delft University of Technology. The thesis is part of the study Civil Engineering with specialization Structural Engineering - Hydraulic Engineering Structures.

This thesis has been realized with the support of TNO (Toegepast Natuurwetenschappelijk Onderzoek) and Rijkswaterstaat. I would like to thank my graduation committee, Johan Maljaars, Klaas Jan Bakker, Henk Kolstein, Bas Jonkman and Johan den Toom. I am grateful for their support and for sharing their knowledge and questions about the subject with me, which often led me to new insights and solutions for problems I encountered. I also would like to thank my colleagues at TNO for their support.

Finally I would like to express my thanks to my parents for their years of support during my study.

D.R. Schönfeld
Delft
July 2013

Summary

The Netherlands contains of more than 400 hydraulic structures, of which 120 are locks. In 2010 Rijkswaterstaat started investigations on the maintenance and operation state of the lock gates. These inspections revealed that a number of 20 to 40 cracks per lock gate have been found, with lengths from a few millimetre to 100 millimetre. Based on experience and an evaluation of the photos made during the inspections it is assumed that the cracks occur due to fatigue.

Till 1960 lock gates were fabricated with riveted joints. The standards which were used to design the steel lock gates did not take into account fatigue. Cracks that could occur in the lock gates were probably not visible from the outside. Invisible cracks could have occurred in the rivet itself but also in the plates. From the sixties lock gates are fabricated with welded joints, but the geometry of the lock gates has not changed. Cracks that have been found in welded joints are visible from the outside. These cracks could be an indication that the safety of the structures is uncertain.

In this thesis, the following research questions are investigated:

At this moment there is no good insight in the fatigue calculation of steel lock gates. The standard *EUROCODE 3* which is used at the moment, has a part dedicated to fatigue strength, but some remarks can be highlighted. The standard describes that it is only applicable to structures in atmospheric conditions. As it is clear that lock gates function in (sea) water conditions, it is questionable whether this standard can be used. Another aspect that can be highlighted is the load-spectrum. At this moment there is no guideline how to determine a load spectrum of the forces on the lock gates.

The first part of this thesis describes the forces that lock gates are subjected too. A summation is given of the observations, where the cracks have been found and consequently, which part of the lock gates should be investigated. A section is about the standard that should be used and what limitation this standard has. The second part of this thesis includes two calculations based on a simplified model of the forces lock gates are subjected too. With this simplified model the fatigue damage is investigated. The first case that is investigated is the West lock of Sambeek. For these lock gates the waterlevel spectrum is determined based on the waterlevel measurements of Rijkswaterstaat. From this spectrum a fatigue damage calculation is made. The second case that is investigated is the East lock of Terneuzen. Also for this case a waterlevel spectrum is made based on the waterlevel measurements of Rijkswaterstaat.

The results of the fatigue damage calculation based on the simplified schematisation of forces on lock gates did not match the fatigue cracks that have been found during the investigations. Some aspects that might have caused this disparity. The schematisation of the lock gate is too simplified. The calculation based on this schematisation probably gives too low stresses to determine the fatigue damage. As input parameters real measurements are used and the contribution of waves was neglected. Neglecting the influence of waves, which cause higher waterlevels and also higher stresses, also resulted in lower fatigue damage values.

A second aspect that could influence the fatigue damage is the maintenance. When (almost) no or poor maintenance is performed on the lock gates, several aspects could result in lower fatigue damage values. A poor state of the wooden sealing at the back post can contribute to other or higher stresses in the lock gate. Also the state of the coating layer is not taken into account. Over the year the coating layer gets brittle and no longer protects the full surface of the lock gates. Some lock gates are subjected to salt water conditions. Due to poor maintenance the cathodic protection system might not perform optimal. All these aspects have a negative influence on the S-N curve.

From the conclusions some recommendation can be made. The fatigue damage calculated with a simplified model can not determine correct fatigue damage values. Therefore a FEM-model should be used to determine the stresses in the lock gate. A second recommendation is to monitor the stresses in the lock gate itself. A lock gate could be fitted with strain gauges to determine the real stresses in the lock gate. These real stresses could then be compared with the result of the FEM-model and could confirm the reliability of the FEM-model. A third recommendation that can be made is to do research on the influence of the salt and fresh water condition with or without cathodic protection. It is recommended to also include rules in the EUROCODE 3 on the influence of salt and fresh water.

Contents

Preface	i
Summary	iii
List of Figures	xi
List of Tables	xiii
1 Introduction	2
1.1 Background	2
1.2 Objective	5
1.3 Outline of this thesis	6
2 Lock gates in the Netherlands	8
2.1 Description and build up of mitre gates	8
2.1.1 Ship levelling	9
2.1.2 Opening and closing	10
2.1.3 Joints	12
2.2 Forces on lock gates	14
2.2.1 Lock gate in neutral position	14
2.2.2 Lock gate moving through water	15
2.2.3 Lock gate in closed position	16
2.2.4 Moment of opening - Just after opening	20
3 Observations on lock gates in the Netherlands	26
3.1 Observations	26
3.1.1 Terneuzen	26
3.1.2 Maasbacht, Sambeek and Belfeld	30
3.2 Hypothesis	35
4 Literature study on fatigue	38
4.1 Fatigue as a Phenomenon in the material	38
4.1.1 Historical survey	38
4.1.2 Different phases in the fatigue life	39
4.1.3 S-N Curve	41
4.1.4 Fatigue strength of joints	43
4.2 Fatigue calculations according to the NEN 2063	46
4.2.1 Fatigue damage	47

4.3	Fatigue calculation according to the Eurocode 3	47
4.3.1	Fatigue damage	49
4.4	Fatigue calculation according to the DNV	50
4.5	Examples of fatigue calculations	50
5	Fatigue damage calculation	52
	Case 1: Sambeek - West	52
5.1	General information	52
5.2	Waterlevel	53
5.3	Observed cracks	55
5.4	Fatigue damage old lock gate	55
5.4.1	Detail category	56
5.4.2	Fatigue damage	57
6	Fatigue damage calculation	62
	Case 2: Terneuzen	62
6.1	General information	62
6.2	Waterlevel	62
6.3	Observed cracks	65
6.4	Fatigue damage East lock gates	68
6.4.1	Detail category	68
6.4.2	Fatigue damage	69
7	New prediction model -	74
	Waterlevel spectrum based on average waterlevels	74
7.1	New prediction model	74
7.2	Test Case; Terneuzen	77
7.2.1	Calculation of the frequency	77
7.2.2	Fatigue Damage	80
8	Conclusion and recommendations	84
8.1	Conclusion	84
8.1.1	Cause of the fatigue cracks	84
8.1.2	Waterlevelspectrum	85
8.2	Recommendations	85
	Bibliography	85
A	Tables and Figures	88
B	Examples fatigue calculation	98
B.1	Example calculation sensitivity	98
B.1.1	Example 1	98
B.1.2	Example 2	99
B.1.3	Example 3	100
B.2	Fatigue damage; NEN 2063 - RINK Report	102
B.2.1	Detail category	102
B.2.2	Waterlevel spectrum	103
B.2.3	Fatigue damage	103

C	Fatigue damage calculations of case 1 and case 2	106
C.1	Fatigue damage calculations of case 1	106
C.2	Fatigue damage calculations of case 2	108
D	Tables and Figures case Sambeek	110
D.1	Sambeek Waterlevel-difference spectrum, step of 10cm, based on measurements	111
D.2	Sambeek Old lock gate; Fatigue damage based on mean value	112
E	Tables and Figures case Terneuzen	113
E.1	Terneuzen Waterlevel-difference spectrum, step of 10cm, based on measurements	114
E.2	Terneuzen Waterlevel-difference spectrum, step of 10cm, based on new prediction model	116
E.3	Terneuzen Old lock gate; Fatigue damage based on mean value	117

List of Figures

1.1	Administrator water ways, till April 1, 2013 [17]	3
1.2	Date of build of the Locks	4
1.3	Service life of lock gates in the Netherlands	4
1.4	Crack in lock gate of Sambeek	5
2.1	Overview of mitre gates	8
2.2	Overview of a steel lock gate [14]	9
2.3	Overview of levelling options	10
2.4	Types of bearing of mitre gates [14]	11
2.5	Hydraulic cylinder gate operation mechanism [14]	11
2.6	Fabrication a rivet joints [23]	12
2.7	Shield metal arc welding [2]	12
2.8	Examples of rivet joints [23]	13
2.9	Forces in the hinges due to own weights	14
2.10	Forces on moving lock gate [14]	15
2.11	Schematic overview closed lock gate	16
2.12	Overview of forces on the cross-section of the lock gate	17
2.13	Schematisation of cross section lock gate	17
2.14	Overview of one lock gate and load transfer through the horizontal and vertical girders	18
2.15	Returning gates [14]	18
2.16	Overview of the forces on the cross-section of one lock gate	19
2.17	Time vs. Waterlevel-difference (values are fictitious)	21
2.18	Schematic overview closed lock gate	22
2.19	Bending of the lock gates in closed position and just after opening	22
2.20	Schematic representation of cross-section lock gate just after opening	22
2.21	Schematic representation of of cross-section lock gate just after opening - location of cylinder	24
3.1	Overview of the locks of Terneuzen	27
3.2	Overview of the lock gate of Terneuzen	27
3.3	Terneuzen; Crack position in lock gates inspection 1998	28
3.4	Terneuzen; Crack position in lock gates inspection 1999	29
3.5	Terneuzen; Crack position in lock gates inspection 2011	30
3.6	Cracks in horizontal and vertical girders	30
3.7	Overview of the locks Maasbracht	31
3.8	Maasbracht; Crack position in lock gates 7-12 inspection 2010	32
3.9	Maasbracht; Crack position in lock gates 1-7 inspection 2010	33

3.10	Overview of the lock complex of Sambeek	34
3.11	Sambeek; Crack position in lock gates inspection 2010	35
3.12	Founded cracks	36
4.1	Different phases of the fatigue life [19]	39
4.2	Cycle slip leads to crack nucleations [19]	39
4.3	Cross section microcrack [19]	40
4.4	Barriers to slip [19]	41
4.5	S-N Normal stress curve [based on the Eurocode 3 [21]]	42
4.6	Constant versus Variable Amplitude stress	42
4.7	S-N Curve according to Eurocode 3; NEN-EN 1993-1-9 [21]	43
4.8	Detail Categorie 40 [based on NEN-EN 1993-1-9 [21]]	44
4.9	Detail Categorie 70 and 140 [based on "Proposal Riveted Assessment of Existing steel structures, remaining fatigue life version 2, Chapter 3"]	44
4.10	Rivet vs. welded connection	45
4.11	Shield metal arc welding [2]	45
4.12	S-N Normal stress curve NEN 2063	46
4.13	S-N Normal stress curve according to the Eurocode [21]	48
4.14	S-N Shear stress curve according to the Eurocode [21]	48
4.15	DNV-RP-C203: Fatigue of Offshore Steel Structures	50
5.1	Overview of the lock complex Sambeek	52
5.2	Top view of the West and Middle locks of Sambeek, mitre gates	53
5.3	Sambeek; waterlevel presentation	54
5.4	Sambeek; Waterlevel level difference spectrum based on real measurements - steps of 10cm	55
5.5	Sambeek; Position of cracks in the lock gate	56
5.6	Sambeek; Cross-section of the old lock gate, dimensions based on Figure A.3 and A.4	57
5.7	Detail category 40 [NEN EN 1993-1-9 C2, Table 8.3-8.4]	57
5.8	Sambeek old lock gate; Waterlevellevel difference spectrum	59
5.9	Sambeek old lock gate; Fatigue damage per waterlevel difference	59
5.10	Sambeek old lock gate; Fatigue damage per waterlevel difference	59
5.11	Sambeek old lock gate; mean value of EUROCODE	60
5.12	Forces and resulting deformation	60
6.1	Overview of the locks of Terneuzen	63
6.2	Overview of the three locks of Terneuzen	64
6.3	Waterlevel locks of Terneuzen	64
6.4	Schematic situation	65
6.5	Terneuzen; Waterlevel level difference spectrum based on real measurements - steps of 10cm	66
6.6	Terneuzen; Position of cracks in lock gate	66
6.7	Terneuzen; Image front view lock gate	67
6.8	Overview of the cross-section of the locks of Terneuzen	68
6.9	*Detail category 40 of table 8.3 and 8.4, NEN-EN 1993-1-9	69
6.10	Terneuzen East lock gates; Waterlevellevel difference spectrum	70
6.11	Terneuzen East lock gates; Stresses per waterlevel difference	71
6.12	Terneuzen East lock gates; Fatigue damage per waterlevel difference	71
6.13	Terneuzen East lock gates; mean value and characteristic value	71

6.14	Forces and resulting deformation	72
7.1	Waterlevel Westerschelde transforming into sinus function	75
7.2	Terneuzen; Waterlevel difference spectrum based on real measurements - steps of 10cm	77
7.3	Waterlevel difference spectrum based on different tides, in blue the new model spectrum and in red spectrum from measurements	79
7.4	Terneuzen East lock gates; different tides based on characteristic values without partial factor for the fatigue resistance	80
7.5	Waterlevel based on measurements compared with spring tide average	81
7.6	Terneuzen East lock gates; Fatigue damage contribution per waterlevel difference	81
7.7	Terneuzen East lock gates; Fatigue damage contribution per waterlevel difference	82
7.8	Terneuzen East lock gates; Fatigue damage values of Real measurements and Spring tide	82
A.1	Recommended partial safety factors for fatigue strength	88
A.2	Example of a free hinge, old lock gate of Sambeek	89
A.3	Front view en cross-section old lock gate Sambeek	90
A.4	Cross-section old lock Sambeek, eccentricity	91
A.5	Front view en cross-section new lock gate Sambeek	92
A.6	Cross-section new lock Sambeek, eccentricity	93
A.7	DNV-RP-C203: Fatigue Design of Offshore Steel Structures	94
A.8	Equation of the effective with according to NEN 6771 13.3	95
A.9	Eurocode 3 S-N curve background document, data from experiments	96
B.1	Example 1: Load spectrum	98
B.2	Example 2: Load spectrum	100
B.3	Example 3: Load spectrum	101
B.4	Cracks in weld perpendicular and parallel to stress direction	102
B.5	Schematic situation	103

List of Tables

5.1	Sambeek; Average exceedance frequencies	54
5.2	Sambeek; Input values for the old lock gates	56
6.1	Terneuzen; Input values for the East lock gates	68
7.1	Terneuzen; Waterlevels of the different tides	77
B.1	Example 1: Fatigue damage	99
B.2	Example 2: Fatigue damage	100
B.3	Example 2: Fatigue damage	100
B.4	Terneuzen RINK; Input values	102
B.5	Terneuzen RINK; Fatigue damage, steps of 10cm , 100% ship levellings at ALW	105
B.6	Terneuzen RINK; Fatigue damage, steps of 10cm, 50% ship levellings at ALW, 50% ship levellings at AWL	105
D.1	Sambeek Waterlevel-difference spectrum, step of 10cm, based on measurements	111
D.2	Sambeek Old lock gate; Fatigue damage based on mean value	112
E.1	Terneuzen Waterlevel-difference spectrum, step of 10cm, based on measure- ments	115
E.2	Terneuzen Waterlevel-difference spectrum, step of 10cm, based on new pre- diction model	116
E.3	Terneuzen Old lock gate; Fatigue damage based on mean value	118

Chapter 1

Introduction

1.1 Background

Rijkswaterstaat is the executive arm of the Dutch Ministry of Infrastructure and the Environment. On behalf of the Minister and State Secretary, Rijkswaterstaat is responsible for the design, construction, management and maintenance of the main infrastructure facilities in the Netherlands. [16]

There are more than 400 hydraulic structures and waterways in the Netherlands. For about 250 of these hydraulic structures and waterways the operation and maintenance is the responsibility of provinces, municipalities and polder boards [18]. Rijkswaterstaat is responsible for the maintenance and operation of more than 120 locks in the main waterways of the Netherlands. Most of these locks are located in the main shipping routes. The main routes for shipping are the Maas, Rijn, Waal, IJssel and Zuid-Willemsvaart as shown in Figure 1.1. [17]

About 40% of the locks were constructed in the twenties and thirties, 40% between the fifties and eighties and the remaining part in more recent years as shown in Figure 1.2. Lock gates constructed in the twenties and thirties are made with riveted joints, since the sixties all lock gates are fabricated with welded joints. Looking at the life span of the lock gates, the majority of the gates is between 40 and 80 years old. The last 20 years a number of lock gates have been replaced based on the expiration of the life of the lock gates according to design calculations, and because the condition of the lock gates was insufficient. This is shown in Figure 1.3. Some of the locks were that old that Rijkswaterstaat started an investigation into the operation and maintenance of these locks.

In 2008 Rijkswaterstaat started the so-called RINK analyses on lock gates. All of the investigated lock gates were mitre gates. RINK, Risico Inventarisatie Natte Kunstwerken, is an analysis which gives an indication of the risk of failure of 'wet' structures. In 2009 Engineering company IV-INFRA, together with Rijkswaterstaat, started the first pilot of this RINK analysis on seven locks. In 2010 IV-INFRA (with Witteveen+Bos and Royal Haskoning) started a RAMS (Reliability Availability Maintainability Safety) performance check on 23 locks in the south of the Netherlands. The RAMS performance check consists of inspection, analysis of operation, verifying the structure with the current standard and guidelines, and the possibilities of new risks. New risks are upcoming e.g. in case of changed conditions, like discharge, remote controlling, change of maintenance contract, bigger ships with bigger ship propellers and number of levellings.[10]

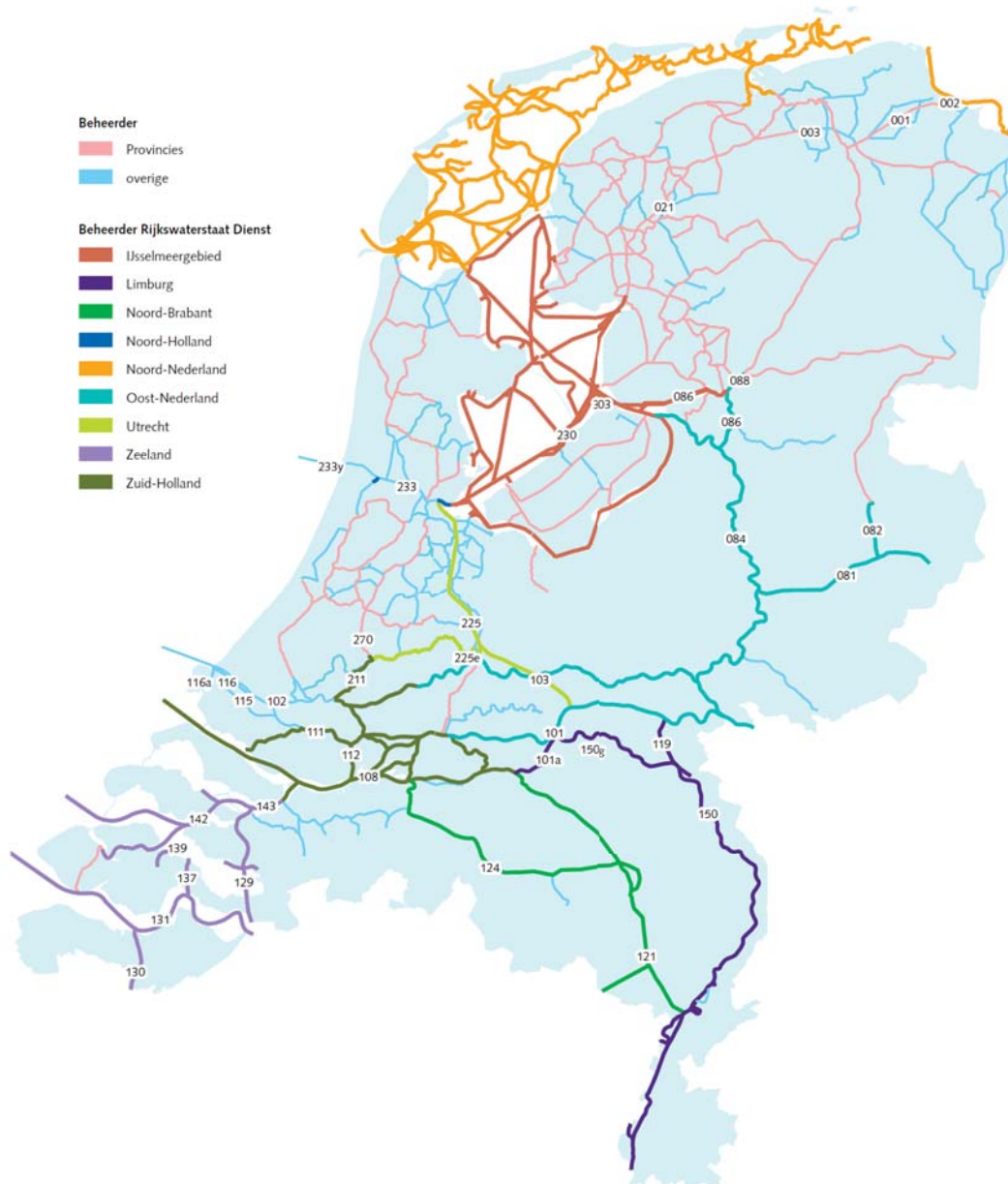


Figure 1.1: Administrator water ways, till April 1, 2013 [17]

The majority of the inspections on the lock gates was done by NEBEST Adviesgroep, who did the mapping of all the defects of the lock gates by making photographs and measuring the length of the cracks. From these inspections revealed that a number of 20 to 40 cracks per lock gate have been found, with lengths from a few millimetre to 100 millimetre. An example of a crack found is shown in Figure 1.4. This crack with a length of about 40 mil-

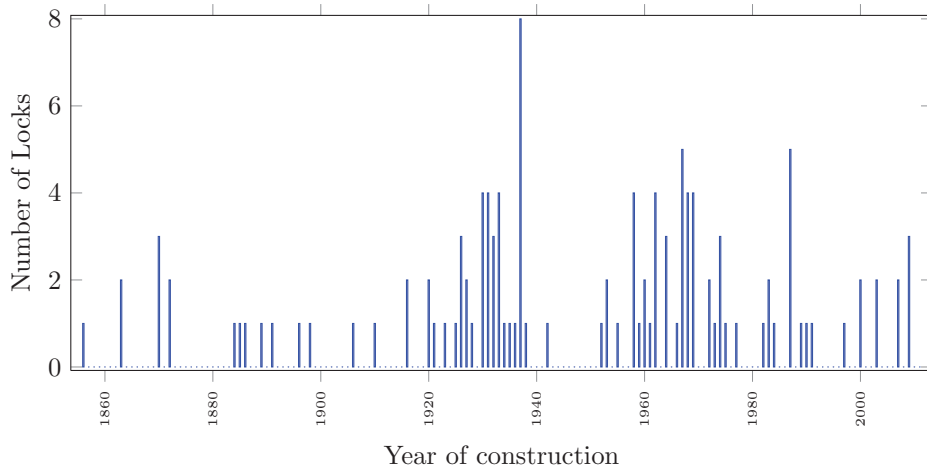


Figure 1.2: Date of build of the Locks

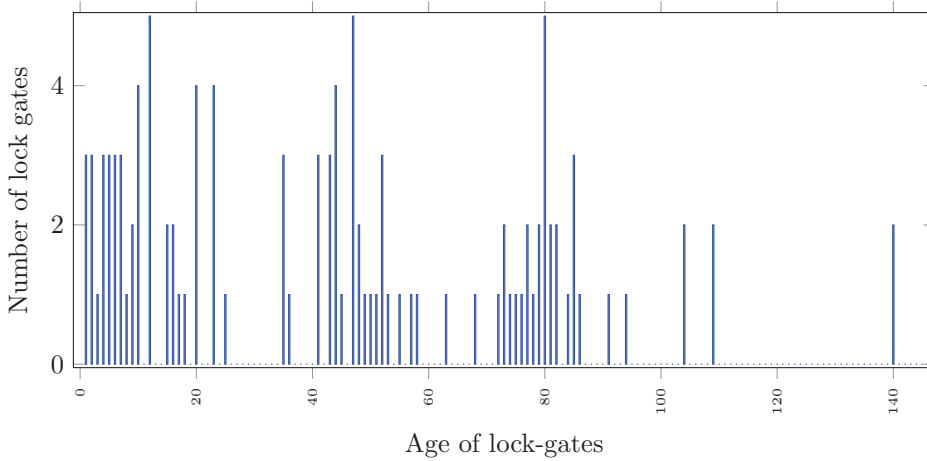


Figure 1.3: Service life of lock gates in the Netherlands

limetres is found at the open-side of the lock gate at a sharp corner in the horizontal girder. Based on experience and an evaluation of the photos from the inspections it is assumed that the cracks occur from fatigue. To be sure that it is fatigue, a crack needs to be examined by removing the crack part from the lock gate and breaking it to be able to look at the cracked surface. If striations are visible at the surface, fatigue is definitely the cause of cracking.

Rijkswaterstaat is responsible for building new structures and maintaining part of them. New structures need to be build according to the European standards and regulations. In addition, Rijkswaterstaat made their own guidelines *ROK* (*Richtlijn Ontwerp Kunstwerken*) and *RBK* (*Richtlijnen Bestaande Kunstwerken*) with specific additional requirements. These guidelines are updated regularly.

Standards and guidelines on steel structures such as *NEN 6786-requirements for the design of movable bridges* include a chapter about fatigue. *Eurocode 3 Design of steel structures* includes a part dedicated to fatigue strength, but explicitly mentions that the rules are based



(a) Lock gate [12]



(b) Crack in horizontal girder [12]

Figure 1.4: Crack in lock gate of Sambeek

on atmospheric conditions. It is clear that lock gates are located in a liquid environment and therefore it can be questioned whether it is correct to use this standard for hydraulic structures. Instead of static stresses, cyclic stresses are important for hydraulic structures with regard to fatigue. During its life span lock gates undergo thousands of cyclic stresses from cylinder forces due to opening and closing the gates and levelling stresses from the water force (levelling). At the moment it is difficult to compose a load-spectrum for the calculation of fatigue because of the different types of waterways.

To compose a waterlevel spectrum for lock gates in canals we can make use of the constant waterlevel. Multiplying the waterlevel difference to the service life we can compose the waterlevel spectrum, this is a one bar spectrum. For lock gates in rivers which have yearly fluctuating waterlevels, waterlevel data from Rijkswaterstaat can be used. By taking the daily waterlevel difference and computing this over a year, we can compute a waterlevel difference spectrum. Comparing this spectrum with the calculation of a spectrum for canals, this calculation is more time consuming.

Composing a load spectrum from the waterlevel-difference from sea going locks is more time-consuming because of the fluctuating waterlevel of the tide. The waterlevel at the seaward side of the lock gates does not only have a sinus shape for the day, due to the tide of 12 hours 25 minutes, but also has monthly fluctuations due to dead-tide and spring-tide. This means that during the day the waterlevel fluctuates from e.g. about $-3m$ to $+3m$, but for the year the maximum waterlevel can also fluctuate from $+2.75m$ to $+3.25m$. This double sinus shape makes the conversion of the waterlevel to the spectrum more difficult.

Currently there is no method to compile a model for the waterlevel spectrum. Because fatigue plays an important role, Rijkswaterstaat wants to update their guideline with fatigue rules specifically on hydraulic structures.

1.2 Objective

The investigations on the lock gates revealed that the mitre lock gates show a significant number of cracks. The first objective of this thesis is to provide information about the cause of these fatigue cracks.

The second goal of the thesis is to provide knowledge needed for computing a waterlevel difference spectrum with the available data (measurements of the waterlevels) of Rijkswa-

terstaat.

The third goal of this thesis is to provide a model based on average waterlevels to compute a waterlevel spectrum. This model should represent the waterlevel spectrum based on the waterlevel measurements of the database of Rijkswaterstaat. This model could be used by Rijkswaterstaat to update their ROK and RBK guidelines for calculations of hydraulic structures with regard to fatigue.

1.3 Outline of this thesis

This thesis is divided into two parts. Chapter 2 gives an overview of lock gates in the Netherlands. This chapter describes the build-up, design and stress calculation of lock gates. Chapter 3 summarizes the observation of several lock in the Netherlands. The cracks are highlighted in overviews. Chapter 4 gives an overview of the relevant literature to understand the phenomenon fatigue and used standards and calculations are explained. This overview should give sufficient background information to understand the research of this thesis.

The second part of this thesis consists of two cases. The first case is about the locks of Sambeek. In this case the old lock gates are examined for fatigue damage.

The second case consists of the East lock gates of Terneuzen. These lock are examined for fatigue damage. For the locks of Terneuzen a new prediction model is made to determine the waterlevel spectrum. When no detailed measurement data are available, the waterlevel spectrum can be calculated with this model based on average waterlevel input.

Chapter 2

Lock gates in the Netherlands

This chapter gives an overview on locks in the Netherlands, the description, build up and which forces are subjected on lock gates. As mentioned in Chapter 1 only mitre gates have been inspected and therefore this chapter is limited to these mitre gates.

2.1 Description and build up of mitre gates

A mitre gate is a lock gate that rotates horizontally through the water as shown in Figure 2.1. It is fixed on one side by a hinge and rotates (open and close) by pistons. In closed position the lock gates hang in the recess in the civil work as shown in Figure 2.1. By pushing out the pistons, the lock gates will rotate to the center of the lock and close the waterway. The gates have an angle of about 1 : 3; this is done for economic reasons. A bigger angle results in longer lock gates which are heavier and more expensive. The smaller the angle, the higher the forces on the civil work.

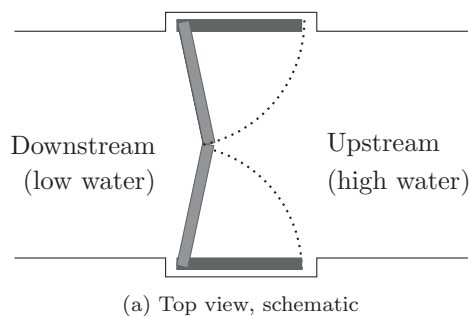


Figure 2.1: Overview of mitre gates

Figure 2.2 shows an overview of a steel mitre gate. The lock gate is built up out of vertical and horizontal girders with an open and closed side as shown in cross-section B-B from Figure 2.2. Reasons for an open and closed side are the weight of the structure (directly weight, indirectly costs) and the manufacturing process (it is difficult to weld at some places). Another reason is that a full closed mitre gate has too much buoyancy force upwards, which can cause floating of the structure. Making the structure heavier would help, but creating

an open side is easier, as this is an optimization process.

At both ends the gate has vertical posts. The post close to the rotational axis is called the 'end post', the girder at the free end (opposite of rotational axis) is called the 'front post'. At the end post over the full length, depending on the type of hinge, a rubber or wooden sealing is fitted. For a free hinge the sealing is made of wood, for a fixed hinge the sealing is made out of rubber. At the free end the sealing consists of wood because of the higher force.

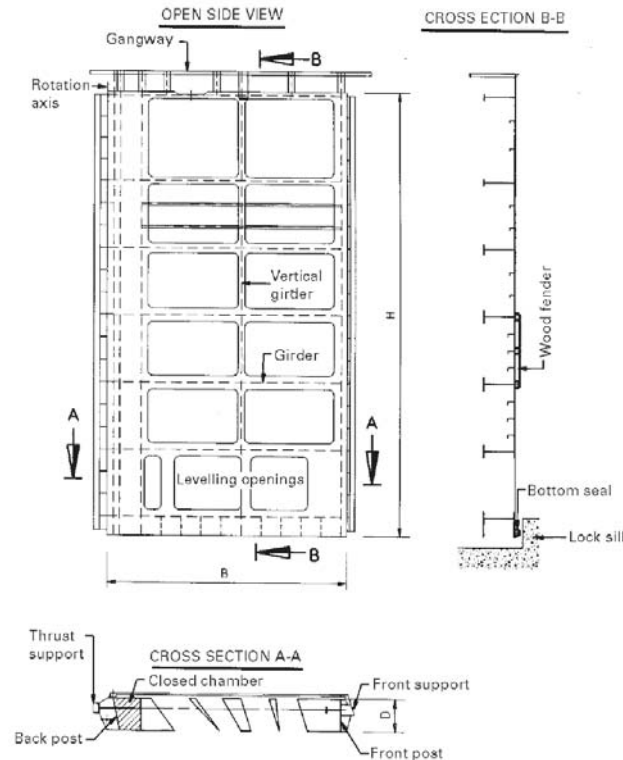


Figure 2.2: Overview of a steel lock gate [14]

2.1.1 Ship levelling

There are two options for levelling the waterlevel in the lock. The first option is the use of culverts; these are openings in the civil work through which water runs to the other side of the gates. See Figure 2.3b. By opening and closing the valves in the culverts the waterlevel can be equalized. The other option is the use of levelling-openings in the lock gates. These are openings at the lower part of the lock gates, cylinders push lock paddles, to let water through the openings. See Figure 2.3a. The majority of the mitre gates have levelling-openings because fabrication of gates with lock paddles is cheaper than a complex culvert system in the civil work.



(a) Lock paddles for the rectangular openings of the 'Kleine sluis' in IJmuiden [14]



(b) Inlet opening in upper head of the locks at Maasbracht [14]

Figure 2.3: Overview of levelling options

2.1.2 Opening and closing

For rotation the mitre gates are equipped with a pivot with pivot socket at the bottom and a rotation axis with bearing at the top. Mitre gates can be equipped with two different types of bearings, clearance-bearing and fixed-bearing, as shown in Figure 2.4. In closed position the clearance bearing uses the water force to tilt the lock gate to create a sealing to the civil work. This sealing is mostly made of wood, because the waterforce on the gate will be transported by the post to the civil work, which results in high forces. Lock gates with fixed bearing create a sealing using rubber. With fixed bearing the waterforce on the gates will be transported by the pivot and rotation axis at the top. The difference between clearance- and fixed-bearing is that with fixed bearing the forces on the gate due to the water pressure go through the hinges only. While with clearance bearing the forces will distribute over the wooden sealing to the civil work. The disadvantage of the fixed bearing is that the structure of the hinge needs to be more heavy designed, compared to a lock gate with a clearance bearing. The choice for the bearing depends on the dimensions of the lock gates. For large lock gates fixed bearing is used, because due to the large weight of the gate, the hinges will be loaded more.

To rotate the lock gates, hydraulic cylinders are mounted at the top, as shown in Figure 2.5. By pushing out the cylinders, the lock gates rotate from opened position in the recess to the center of the lock in closed position. Opening the lock gates works in the same principle, but then in reverse way.

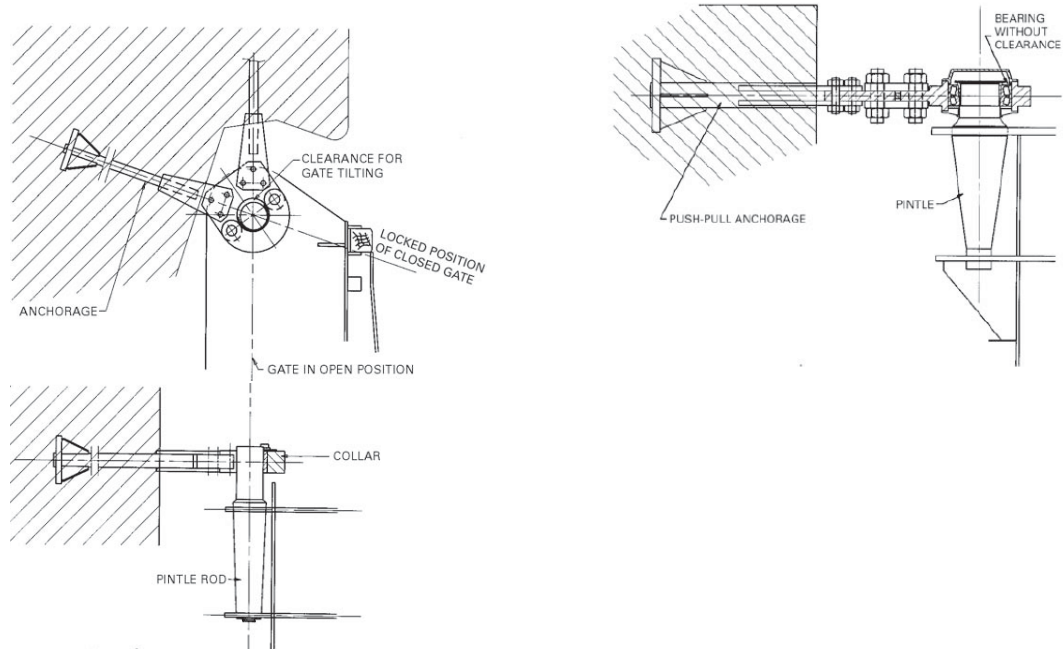


Figure 2.4: Types of bearing of mitre gates [14]

*Left top and bottom image is the clearance bearing, right top image shows the front view of a fixed bearing. The construction is almost similar with the free hinge but in this case there is no clearance. At the fixed bearing the anchorage is heavier designed, because the forces on the gates go through this hinge. In Appendix A Figure A.2 more images are shown of the hinges.



(a) Hydraulic cylinder gate operation mechanism of the 'Tweede sluis' at Lith



(b) Hydraulic cylinder gate operation mechanism of the mitre gates and sluices at Rozenburgse lock

Figure 2.5: Hydraulic cylinder gate operation mechanism [14]

2.1.3 Joints

From historical point of view the first steel lock gates were fabricated with riveted connections, which are permanent mechanical fasteners (see Figure 2.8). By hammering a preheated cylindrical, the cylindrical pen plastic deforms and fills up the hole and produces a closing head. This is shown in the Figures 2.6. After cooling down a tension force arises in the rivet, which results in a clamping force between the steel plates. By tensioning the plates, the force will be transmitted partly by friction between the plates, which reduces the shear force in the rivet.



Figure 2.6: Fabrication of rivet joints [23]

Nowadays lock gates are fabricated with welded joints. Welding is a process that melts the material; by adding filler material a pool of molten metal forms (see Figure 2.7), which after cooling down results in a strong joint. Large structures with many welds are nowadays made with automated machines. Welds in difficult corners and spots, which are hard to reach with machines, are made manually.

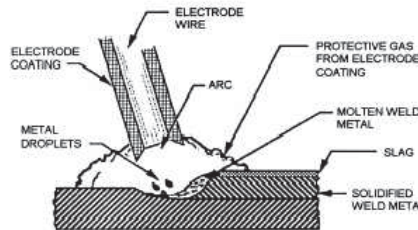
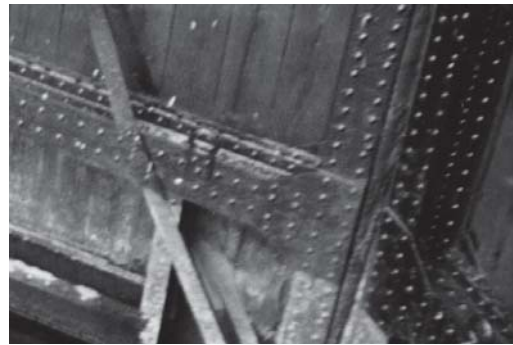


Figure 2.7: Shield metal arc welding [2]

The switch from riveted joints to welding joints was made due to the fact that the fabrication of riveted joints was very labour intensive. Every rivet needed to be preheated and hammered into the structure. This fabrication process of structures was time consuming and changing to the welding process meant that the time needed for fabrication decreased considerably.



(a) Rivet in lock gate [beeldbank.rws.nl]



(b) Rivet joints [beeldbank.rws.nl]



(c) Rivet joints [www.modernsteel.com]

Figure 2.8: Examples of rivet joints [23]

2.2 Forces on lock gates

Lock gates are subjected to different forces, depending on the position of the gates. We can distinguish different positions of the gates: the gates in opened position, the gates moving through the water, the gates in closed position and the gates just after opening. The next section gives an overview of the different forces subjected to the lock gates. A simplification is made to gain understanding about the forces. The simplification below for the calculation of the stresses is not represented 100% correctly. For the calculation of the real stresses at specific joints and connection an FEM-model (Finite Element Method -model) should be made.

2.2.1 Lock gate in neutral position

The gates in opened position (e.g. in the recess) have forces in the hinges due to the weight of the gates as shown in Figure 2.9. No additional forces are applied to the gates.

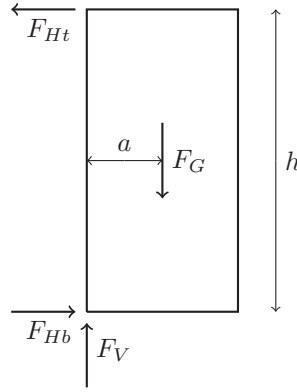


Figure 2.9: Forces in the hinges due to own weights

For calculation of the vertical force in the bottom pivot we make use of the vertical equilibrium. The vertical force in the bottom pivot is the weight of the lock gate. The equation of the vertical force in the pivot can be written as:

$$F_V = F_G$$

where:

$$\begin{aligned} F_V &= \text{Vertical force in pivot} & [\text{kN}] \\ F_G &= \text{Force of lock gate in water} & [\text{kN}] \end{aligned}$$

The horizontal forces in the hinges can be calculated by taking the moment equilibrium. The equation of horizontal force in the top bearing can be written as:

$$F_{Ht} = F_G \cdot \frac{a}{h}$$

where:

F_{Ht}	=	Horizontal force in top bearing	[kN]
a	=	Distance from rotation axis to c.o.g.	[m]
h	=	Height of the lock gate	[m]

By using horizontal equilibrium we can calculate the remaining force in the bottom pivot. The equation of the horizontal force in the bottom pivot can be written as:

$$F_{Hb} = F_{Ht} = F_G \cdot \frac{a}{h}$$

where:

F_{Hb}	=	Horizontal force in bottom pivot	[kN]
----------	---	----------------------------------	------

2.2.2 Lock gate moving through water

When closing and opening the lock gates, the gates are moving through the water. The movement is done by pistons at the top part of the lock gate. The water causes a resistance on the gates, this is shown in Figure 2.10. The speed of moving through the water is higher at the end of the gate then at the rotation axis. This results in a higher water force at the end of the gate which is shown in Figure 2.10. By moving the gate through the water the waterforce at the bottom is lower then at the top because at the bottom the water can flow under the gate (the gate has no sealing at the bottom).

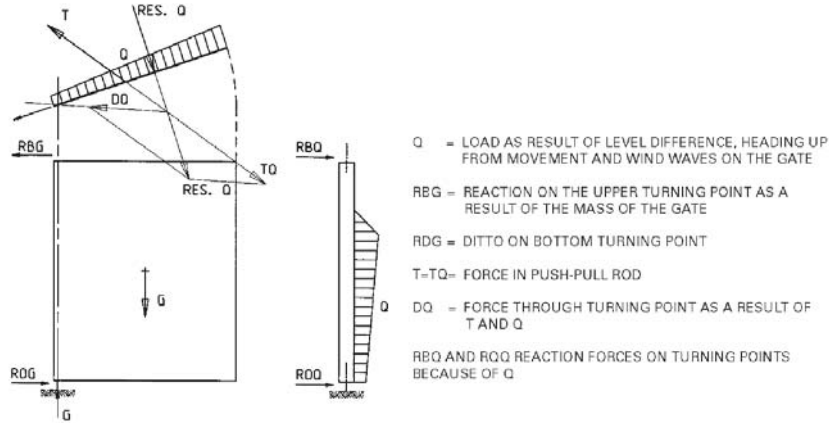


Figure 2.10: Forces on moving lock gate [14]

The equation of the force for moving the lock gate through the water is based on the equation of towing the object through water. The force of towing the objects through water can be written as [20]:

$$F_{gate} = \frac{1}{2} A c_w \rho_w v^2$$

where:

F_{gate}	=	Force for moving the gate	[kN]
A	=	Area of surface flow	[m ²]
c_w	=	Resistance coefficient (for square objects about 1.1)	[-]
ρ_w	=	Density of water	[kg/m ³]
v	=	Speed of object	[m/s]

In this equation the stresses due to torsional force are neglected. In reality there will be torsional stresses in the lock gates. The force calculated with the above equation is the total force that is needed to pull the lock gate through the water. Assuming that the cylinder is mounted at a shorter distance from the middle of the gate to the rotation centre, the force in the cylinder is larger. The force to the cylinder can be calculated by a summation of the moments. This equation is only applicable when the gate is moving through the water and the waterlevel is the same on both sides of the gate.

2.2.3 Lock gate in closed position

When the lock gates are in closed position, the waterlevel inside the lock can be levelled with the outer waterlevel. Due to the levelling there is a resulting force on the lock gate due to the waterlevel difference, as shown in Figure 2.11.

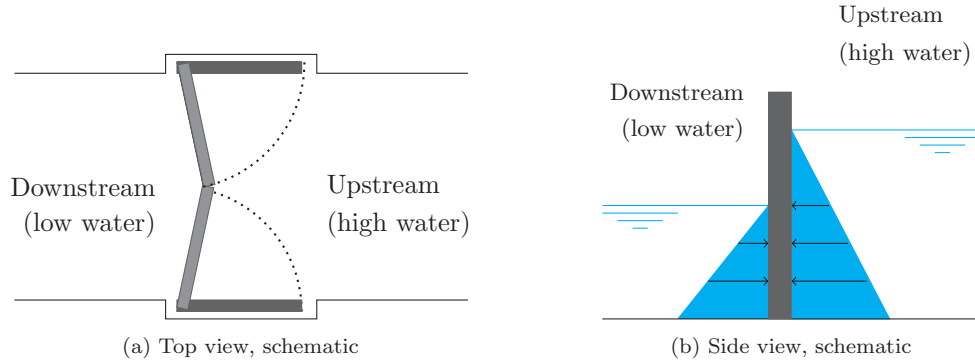


Figure 2.11: Schematic overview closed lock gate

In reality not only forces due to the waterlevel difference are governing, but also forces due to wind and (translation)waves are present on the lock gates. For simplification the forces of wind and waves are neglected in this thesis. Also the possibility that the bottom rule can lie against the barrier is neglected. This is because (almost) no information is available about the condition of the barrier and in the design of the lock gate, this aspect is not desired. It is preferred to have a good load transfer by the posts of the lock gates. The possible force of the cylinders in closed position (pushing the lock gates to a closed position) is neglected for simplicity.

A schematic presentation of the forces and reactions is given in Figure 2.12. The figure shows several forces that are applied to one lock gate; the waterforce F_W and the reaction force F_S , which is equal to force F_H . The reaction force F_S can be resolved into a force parallel to the gate F_N and perpendicular to the gate F_F . The forces F_N are applied with an eccentricity, which results in additional moments in the cross-section. These moment due

to F_N are opposite to the moments by F_W . The moment due to F_W results in a positive bending moment, the moment due to F_N results in a negative bending moment.

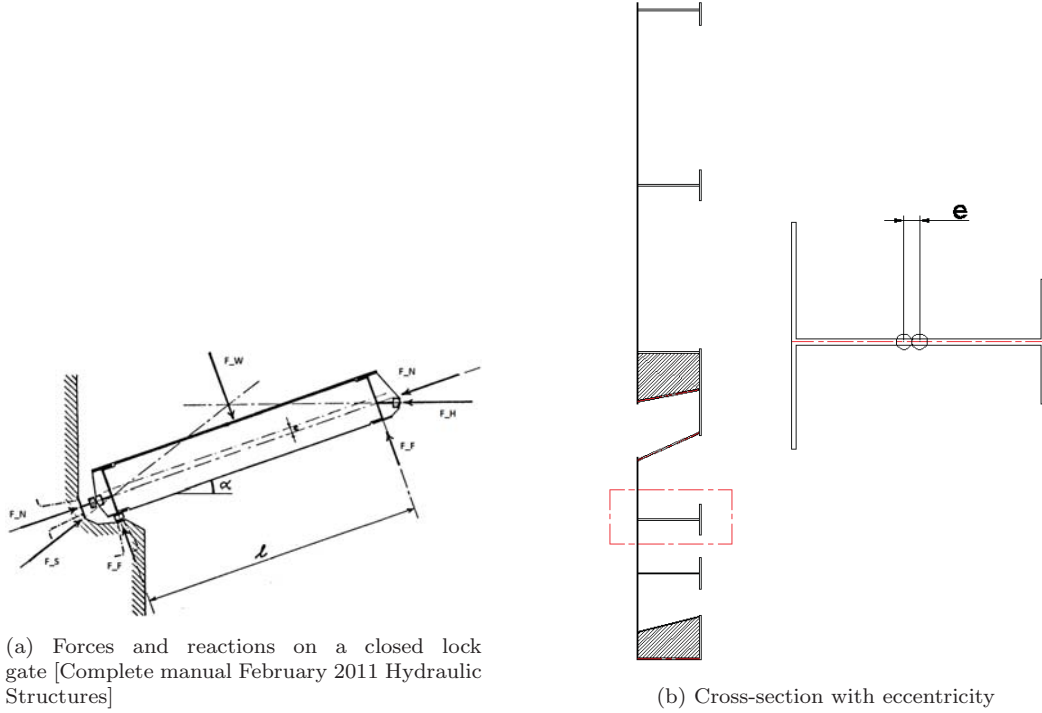


Figure 2.12: Overview of forces on the cross-section of the lock gate

For simplification we design the cross-section of one lock gate to a beam supported on two hinges as shown in Figure 2.13. In this simplification the waterforce is presented as a distributed force applied over the full cross-section, the normal forces F_N are presented with an eccentricity.

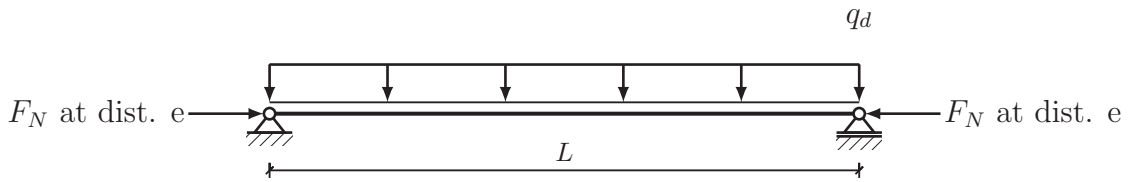


Figure 2.13: Schematisation of cross section lock gate

The waterforce on the lock gate is distributed according to Figure 2.14. The vertical girders transfer the load to the horizontal girders which then transfer the load to the outer vertical posts. At the posts the load will be transferred to the hinge and finally to the civil work. Depending on the type of the hinge, fixed or clearance bearing, the total load will be transferred by the hinge or partly by the hinge and partly by the sealing.

As shown in Figure 2.15, the load transfer in the left image is by means of sealing. In this type of lock gate a clearance bearing is applied. The waterforce pushes the lock gate to the

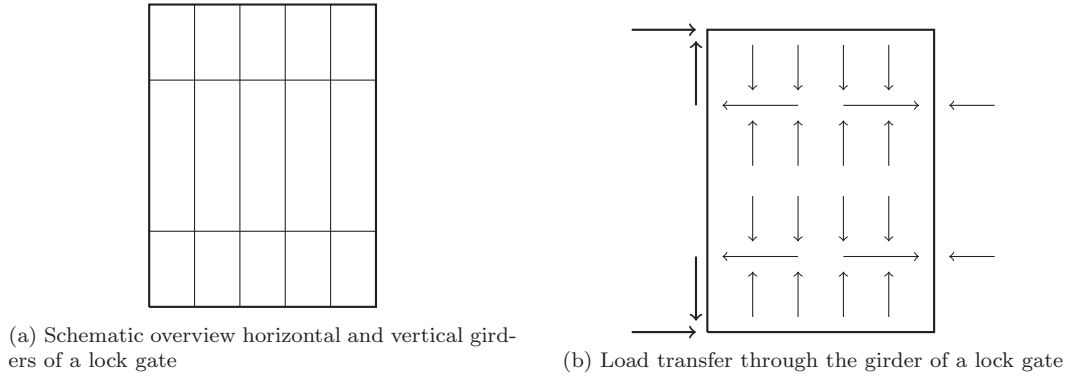


Figure 2.14: Overview of one lock gate and load transfer through the horizontal and vertical girders

civil work and the load will be transferred by the sealing. The right image in Figure 2.15 represents a lock gate with a fixed bearing: the load transfer on the lock gate is by means of the hinge. The sealing only transfers a small part of the load, enough to create a sealing.

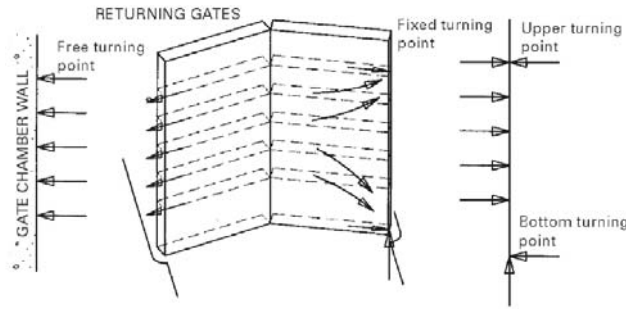


Figure 2.15: Returning gates [14]

The uniformly distributed load can be calculated from the waterlevel difference. On both sides of the gate we have a waterlevel as shown in Figure 2.16a. The maximum force is applied from the height of the downstream waterlevel to the bottom. The equation of the load distribution can be written as:

$$q_d = \rho g \Delta h \cdot h_q \quad (2.1)$$

where:

ρ	=	Density of the water	$[kg/m^3]$
g	=	Gravitational force	$[m/s^2]$
Δh	=	Waterlevel difference	$[m]$
h_q	=	Height of the part of the cross-section for the q-load	$[m]$

To determine the stresses we take a cross-section of the structure on which the highest distributed force is applied. The cross-section that should be checked is normally the second or third horizontal girder from the bottom. The first girder from the bottom cannot be

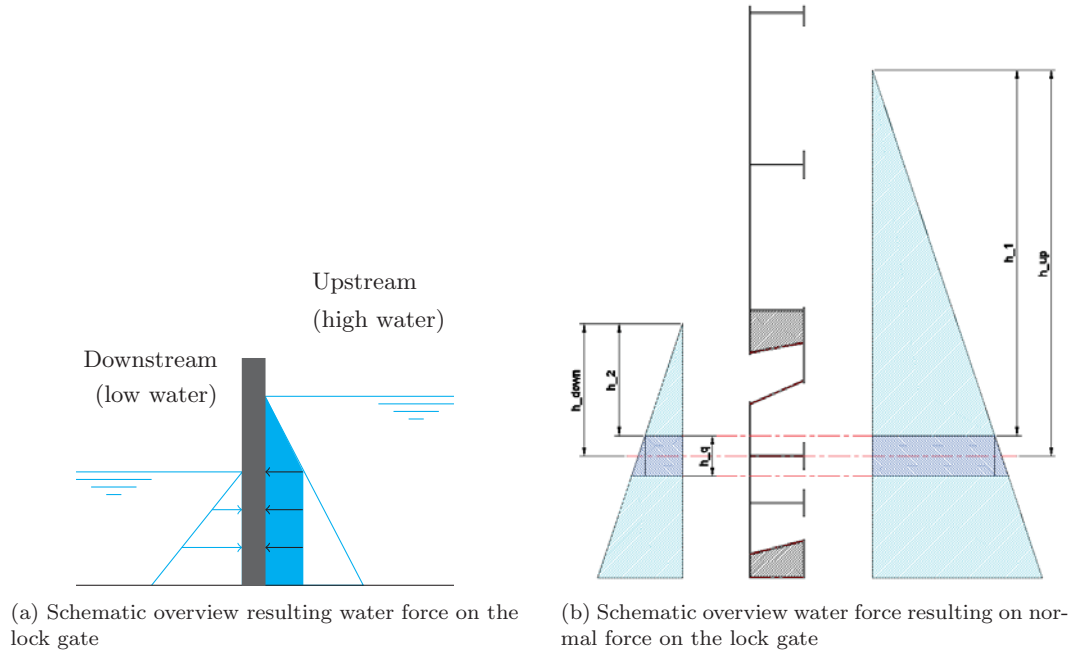


Figure 2.16: Overview of the forces on the cross-section of one lock gate

used because this girder will bend under load against the bottom rule, and the girder above the lowest waterlevel will have a less distributed force. For simplification we schematize the cross-section of the lock gate as a beam on two supports as shown in Figure 2.13. The section modulus can be determined by dividing the moment of inertia by the distance to the outer fibre. The moment of the beam on two supports can be written as:

$$M = \frac{1}{8}q_d L^2 - F_N \cdot e \quad (2.2)$$

where:

q_d	=	Uniformly distributed load	[kN/m]
L	=	Length of the gate	[m]
F_N	=	Normal force in the cross-section	[kN]
e	=	Eccentricity	[m]

The equation of the normal force in the cross-section can be expressed as:

$$F_N = \frac{F_W}{2 \cdot \tan(\alpha)} \quad (2.3)$$

where:

$$\begin{aligned} F_W &= \text{Resulting waterforce on the gate} & [\text{kN}] \\ \alpha &= \text{Angle of the gate} & [\text{degrees}] \end{aligned}$$

The equation of the resulting waterforce as shown in Figure 2.16b on the gate can be expressed as:

$$F_W = \left((\rho g h_1 A) + \left(\frac{1}{2} \rho g (h_{up} - h_1) A \right) \right) - \left((\rho g h_2 A) - \left(\frac{1}{2} \rho g (h_{down} - h_2) A \right) \right) \quad (2.4)$$

where:

$$\begin{aligned} \rho &= \text{Density of the water} & [\text{kg/m}^3] \\ g &= \text{Gravitational force} & [\text{m/s}^2] \\ h_{up} &= \text{Waterlevel upstream to centre of girder} & [\text{m}] \\ h_{downs} &= \text{Waterlevel downstream to centre of girder} & [\text{m}] \\ h_1 &= \text{Waterlevel upstream to begin part } h_q & [\text{m}] \\ h_2 &= \text{Waterlevel downstream to begin part } h_q & [\text{m}] \\ A &= \text{Area on which the force is applied } (b \cdot h_q) & [\text{m}^2] \end{aligned}$$

This equation can be rewritten in:

$$F_W = \rho g A \Delta h \quad (2.5)$$

For the calculation of the stresses at the most outer fibre we divide the moment by the section modules and the normal force by the area of the cross-section. The equation can be written as:

$$\sigma = \frac{M}{W} + \frac{F_N}{A} \quad (2.6)$$

where:

$$\begin{aligned} \sigma &= \text{Stress in outerfibre of the crossection} & [\text{kN/m}^2] \\ M &= \text{Moment on the lock gate due to waterforce} & [\text{kNm}] \\ W &= \text{Section modulus} & [\text{m}^3] \\ F_N &= \text{Normal force in the cross-section} & [\text{kN}] \\ A &= \text{Area of the cross-section} & [\text{m}^2] \end{aligned}$$

2.2.4 Moment of opening - Just after opening

Opening the lock gates should normally be applied when the waterlevel on both sides of the gate is equalized. The time for equalizing is a function of the velocity of the water through the levelling-holes. This function can be written as:

$$v = \sqrt{2g\Delta h}$$

where:

$$\begin{array}{lll} v & = & \text{Velocity of water through levelling hole} \quad [\text{m/s}] \\ g & = & \text{Gravitation force} \quad [\text{m/s}^2] \\ \Delta h & = & \text{Waterlevel difference} \quad [\text{m}] \end{array}$$

The discharge through the levelopenings is a function of the area divided by the water velocity. Dividing the discharge by the surface area of the lock, the velocity of lowering the waterlevel is calculated. The time for levelling the waterlevel, is waterlevel difference divided by the velocity of lowering the waterlevel. A plot of the time versus the waterlevel is given in graph 2.17. From the graph 2.17 we can conclude that by equalizing the waterlevels, the lower the waterlevel difference, the lower the velocity, the more time is needed to equalize the waterlevel difference. Thus, the last part of equalizing the waterlevel-difference takes a lot of time.

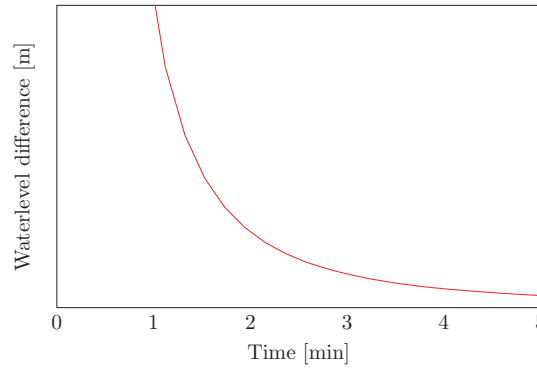


Figure 2.17: Time vs. Waterlevel-difference (values are fictitious)

Because of the time extrapolation by levelling the waterlevel, most lock-keepers open the locks before both waterlevels are equalized. This results in an extra force in the cylinders, compared to moving the gates through water with equalized waterlevels. This results in higher stress locally at the connections of the cylinder to the gates. When opening the lock gates with a waterlevel difference, the gate will bend to the other direction as shown in Figure 2.19 in the right image. The bending moment changes from direction and therefore the stresses change from tension to bending on the closed side and from bending to tension on the open side. The stresses in the gates in closed position calculated with equation 2.2 change under these circumstances. For the same cross-section, the 2nd from the bottom, the cross-section now is modelled as a beam clamped on one side (side of the rotation axis) as shown in Figure 2.20.

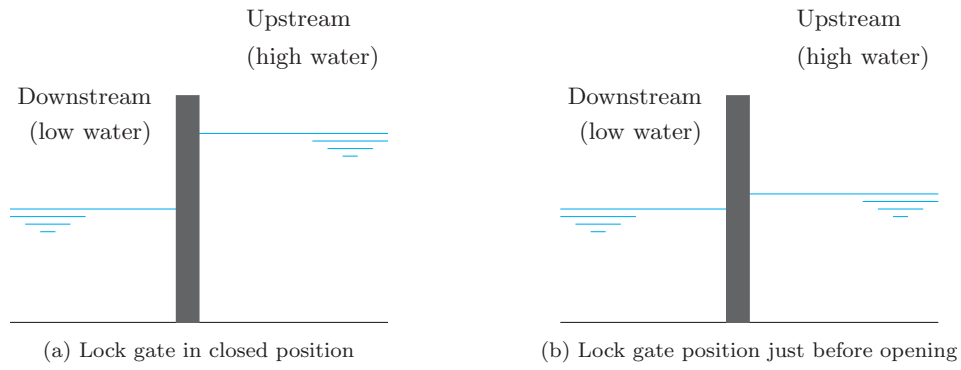


Figure 2.18: Schematic overview closed lock gate



Figure 2.19: Bending of the lock gates in closed position and just after opening

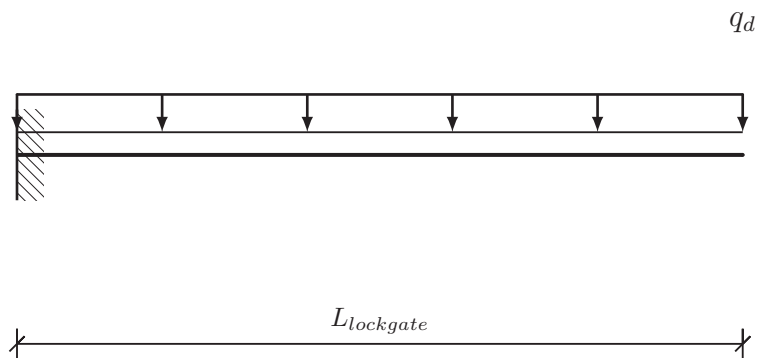


Figure 2.20: Schematic representation of cross-section lock gate just after opening

This is a simplification of the reality. In reality the lock gate will have torsional forces. These force result in higher stresses then in the simplification that here is assumed. For simplification torsional force is neglected.

The maximum moment in the cross-section (at the fixed side) can be calculated with the equation:

$$M = \frac{1}{2}q_d L^2$$

where:

$$\begin{array}{ll} q_d & = \text{uniformly distributed load} \quad [\text{kN/m}] \\ L & = \text{length of the gate} \quad [\text{m}] \end{array}$$

This is the moment at the fixed side. We are interested in the moment at midspan. The parabolic shape of the moment curve can be expressed as:

$$M(x) = \frac{1}{2}q_d x^2 - q_d x + \frac{1}{2}q_d L^2 \quad (2.7)$$

where:

$$x = \text{distance between 0 and L} \quad [\text{m}]$$

The maximum moment at midspan can be calculated by filling $\frac{1}{2}L$ into equation 2.8. The moment is:

$$M(\frac{1}{2}L) = \frac{1}{2}q_d(\frac{1}{2}L)^2 - q_l(\frac{1}{2}L) + \frac{1}{2}q_dL^2 = \frac{1}{8}q_dL^2 \quad (2.8)$$

The maximum moment in the second girder can be calculated by taking the summation of the absolute value of the moments of equation 2.2 (closed gate with waterlevel difference and normal force at eccentricity) and 2.8 (opening the gate with waterlevel difference).

Note: The maximum moment is in reality not exactly at midspan. By differentiation of the total equation and equate to 0, we find the distance where the maximum moment in the girder occurs. Because in the two equations different distributed forces q_d are used, distance of the moment changes over the vertical cross-section of the lock gate. For simplification the moments at midspan are calculated.

As mentioned before, opening the lock gates with waterlevel difference gives the cylinders higher forces, which results in higher local stress at the connection of the cylinders and the gates. A schematisation is shown in Figure 2.21.

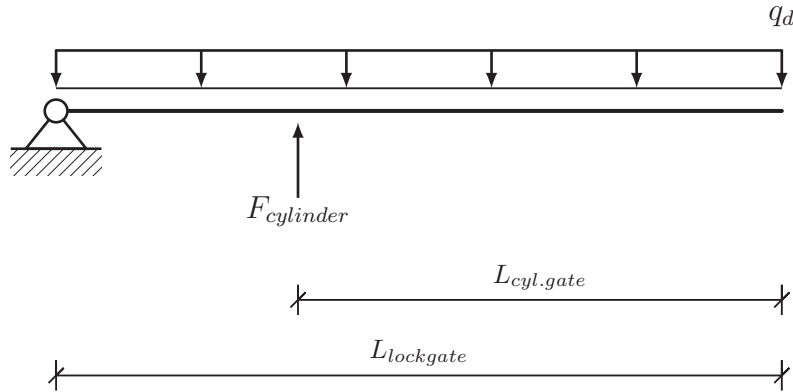


Figure 2.21: Schematic representation of cross-section lock gate just after opening - location of cylinder

The equation of the moment in the (horizontal) girder at the cylinders due to opening can be expressed with:

$$M_{cylinders} = q_{d.1} \cdot L_{cyl.gate} \cdot \frac{1}{2} \cdot L_{cyl.gate} \quad (2.9)$$

where:

$$\begin{aligned} q_{d.1} &= \text{uniformly distributed load} & [\text{kN/m}] \\ L_{cyl.gate} &= \text{length of the gate from the cylinder to end} & [\text{m}] \end{aligned}$$

The equation of the uniformly distributed load $q_{d.1}$ needs to be adjusted. Because the cylinder resists all of the waterforce, the uniformly distributed load is now taken from the total height of the lock gate. The equation can be written as:

$$q_{d.1} = \rho g h b_1 + \frac{1}{2} \rho g h b_2 \quad (2.10)$$

where:

ρ	=	Density of the water	$[kg/m^3]$
g	=	Gravitational force	$[m/s^2]$
h	=	Waterlevel difference	$[m]$
b_1	=	Height of lowest waterlevel	$[m]$
b_2	=	Height of the waterlevel difference	$[m]$

The stress in the girder at the position of the cylinder can be calculated by dividing the moment by the section modulus. The equation can be written as:

$$\sigma = \frac{M}{W} \quad (2.11)$$

Chapter 3

Observations on lock gates in the Netherlands

3.1 Observations

This section gives an overview of the observations from the inspection and maintenance reports of the lock gates taken by Nebest Adviesgroep and the RINK analysis reports of IV-INFRA. The observations in the RINK analysis of IV-INFRA under the supervision of Rijkswaterstaat have been carried out on the locks of Terneuzen. The observations of the damage inventarisation of NEBEST Adviesgroep under the supervision of Rijkswaterstaat have been performed on a number of lock gates in the Maas in the East of the Netherlands. The investigated lock gates are Maasbracht and Born, Heel, Belfeld and Sambeek. The investigated locks by NEBEST are situated in the main shipping routes of the Netherlands, in the river the Maas in the the East of the Netherlands. The river the Maas originally rises in France and flows into the North Sea in the Netherlands. The locks of Terneuzen are situated in the main route of the Westerschelde to the channel of Gent-Terneuzen and link the harbour of Gent[15] with the Westerschelde.

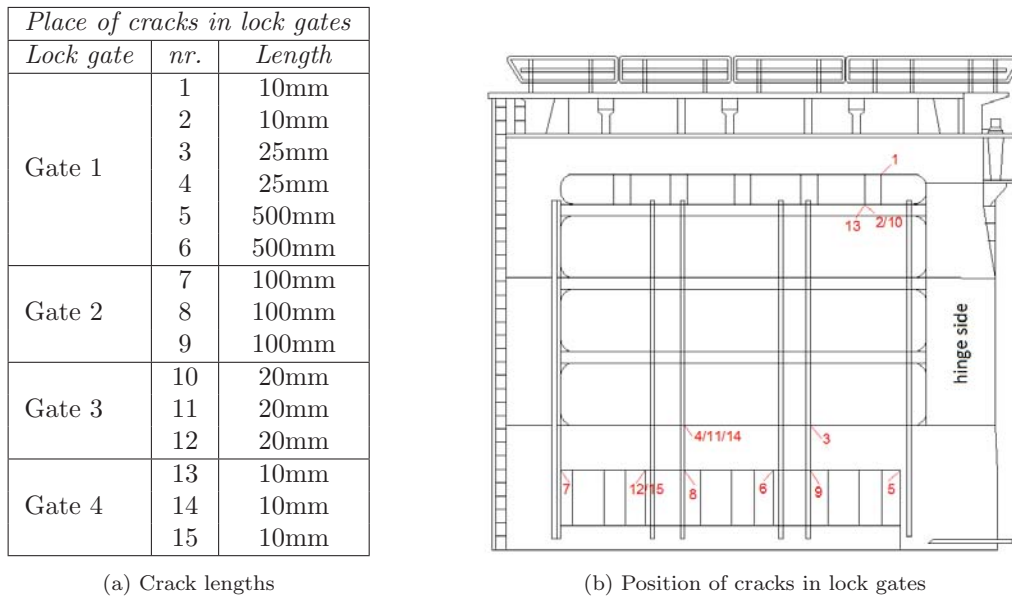
3.1.1 Terneuzen

IV-INFRA investigated the locks of Terneuzen. This lock complex consists of three locks, East, Middle and West as shown in Figure 3.1. The investigated lock is the East lock. The East lock was build in 1966 and has lock gates that are 47 years old. Because this is a see going lock, the tide plays an important factor and therefore at each side there are two ebb and two flood lock gates. The total site consists of 12 lock gates, four at each end and four in the middle, with four extra exchange gates as shown in Figure 3.1. The locks are CEMT-classes V, which means that big Rijn-Hernekanaalschip and push-vessels can use the locks. The locks are subjected to 9.000 levellings per year.

The lock has mitre gates with fixed hinges and occlusion is transmitted by rubber sealing. Rotation is effected by a piston located at the top part of the lock gate. The lock gates consist of a flatten closed side and an open side with air chambers and levelling holes at the bottom. The lock gates are made of steel with welded connections. For protection against collision, wooden beams are mounted on the front side. For corrosion protection a cathodic-protection is mounted on the lock gates. The replacement cycle is every 12 years, whereby 4 gates are exchanged with the extra set gates.

replaced once. From maintenance reports it was clear that the replacement cycle was not performed according to subscription.

The investigation over the past years was done on 13 lock gates. They were inspected visually on land (exchange gates). The gates 1, 2, 3 and 4 were inspected on land in 1998, after 32 years of service life. During this inspection a number of cracks were found as shown in Figure 3.3 [8]. Some of these cracks were so significant, e.g. 100mm to 500mm in length, that they had to be repaired. One can assume that the these cracks were repaired in 1998, but there is no proof of the repair.



(a) Crack lengths

(b) Position of cracks in lock gates

Figure 3.3: Terneuzen; Crack position in lock gates inspection 1998

*Gate 2 and 4 shown mirrored

*e.g. nr. 7 is a crack of 100mm at the bottom left of lock gate 2

Gate 9, 10, 11 and 12 were inspected on land in 1999, after 33 years of service life. During this inspection a number of cracks were found as shown in Figure 3.4. Some of these cracks were so significant, e.g. 200mm in length, that they had to be repaired. Cracks larger than 50mm were repaired and cracks less than 50mm were only repaired on specific request. One can assume that these cracks were repaired in 1999, but there is no proof of the repair. Gate 5, 6, 7, 14 and 15 were inspected on land in 2011, after 45 years of service life. During this inspection a number of cracks were found as shown in Figure 3.5. At gate 15 all the connections of the horizontal and vertical girders were cleaned and inspected. All the other gates were not fully, but only globally inspected. Possibly there are more cracks present.

The investigations revealed that at multiple lock gates significant cracks were found as shown in Figure 3.6. All cracks were at least a couple of millimetres to a few centimetres, or there was a sign of starting to crack. The Figures 3.3, 3.4 and 3.5 make it clear that most of the cracks are located in the top part and bottom part of the lock gates. The cracks in

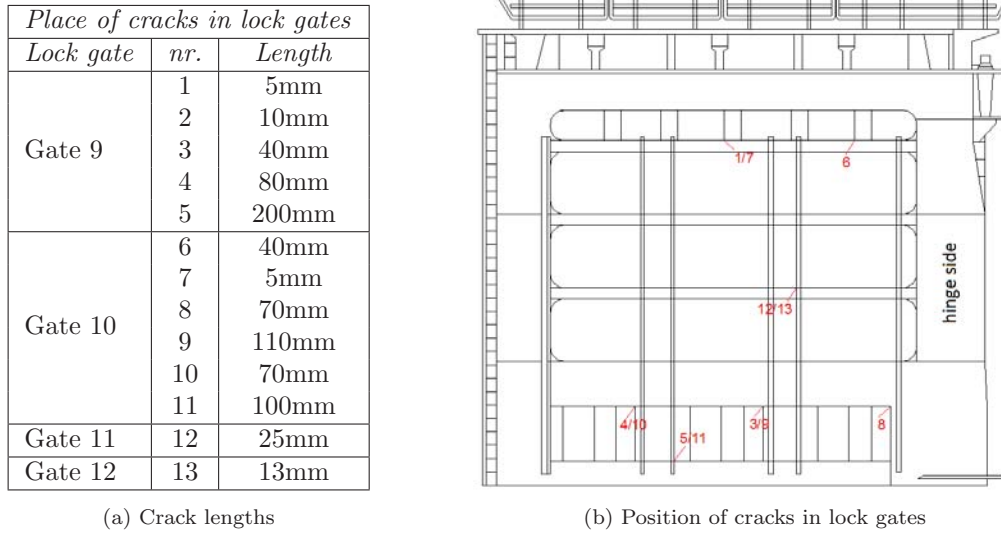


Figure 3.4: Terneuzen; Crack position in lock gates inspection 1999

**Gate 10 and 12 shown mirrored*

**e.g. nr. 7 is a crack of 5mm at the mid top of lock gate 10*

the top part as shown in Figure 3.3 are located on the exact position where the cylinder is mounted on the lock gates. The assumption being made is that the cracks in the top part at the position of the cylinder are caused by the cycles stresses of the cylinder during opening the locks with a waterlevel difference. Rijkswaterstaat confirmed that the locks of Terneuzen were opened with a waterlevel difference of 35cm over a certain period of time. This waterlevel difference caused significant forces in the cylinders, which resulted in high (cyclic) stresses at the connection to the lock gates.

The cracks in the lower part of the lock gates were found in the corners of round-off radii at the connection of the vertical and horizontal girders. It is assumed that the (cyclic) stresses of levelling are the cause of the cracks in the lower part. The maximum waterforce, the result of upstream minus downstream, is presented on the lower part of the lock gates, resulting in high cyclic stresses on this part of the lock gates.

Comparing the position of the cracks to the waterlevel as shown in Figure 6.4 reveals that the cracks in the lower part of the lock gates are located under the waterlevel and the cracks in the middle and top part of the lock gates are located in the fluctuating waterlevel, the so-called splash zone. This means that for the middle and top cracks a combination of air and salt water influences the development of these cracks over time. A protection layer and cathodic protection is used on the lock gates to reduce the influence of air and salt water condition. The maintenance state of the protection layer and cathodic protection determines the influence and growth of these cracks. In this thesis it is assumed that air and salt water have no influence on the fatigue life. However, the maintenance state of the protection layer and cathodic protection should be investigated to determine the influence in reality.

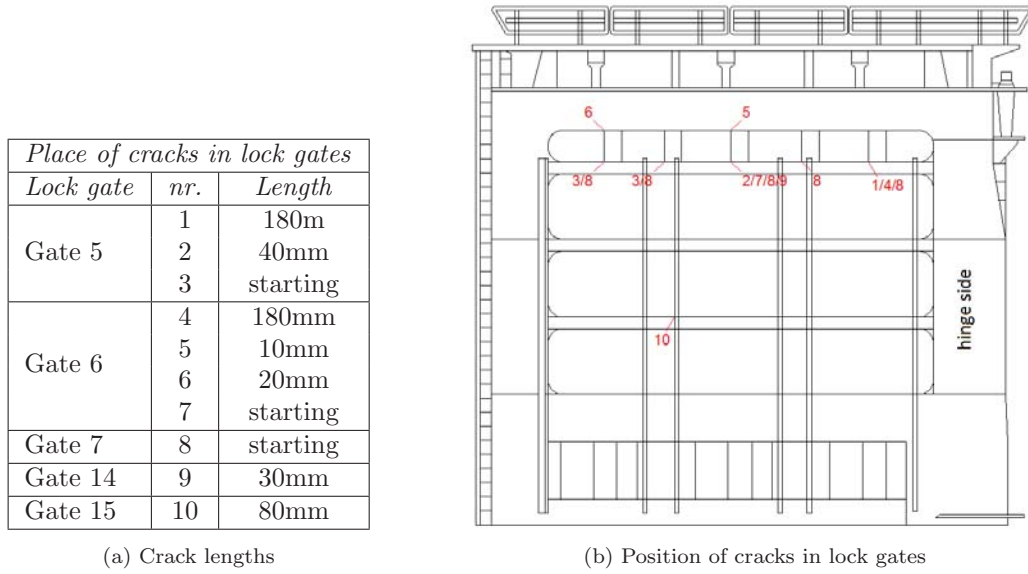


Figure 3.5: Terneuzen; Crack position in lock gates inspection 2011

*Gate 6 and 14 shown mirrored

*e.g. nr. 8 is a starting crack located in the upper horizontal girder at multiple locations of lock gate 7



Figure 3.6: Cracks in horizontal and vertical girders

*(Left: lock gate 5, Right: lock gate 6) [9]

3.1.2 Maasbacht, Sambeek and Belfeld

NEBEST Adviesgroep investigated the locks in the Maas in the East of the Netherlands. This part of the river consists of fresh water because salt water has no influence. In comparison with the lock of Terneuzen these locks only have single lock gates because of the waterlevel regulation. Upstream of the locks the water is always higher than downstream. All locks have mitre gates with free hinges and occlusion is transmitted by wooden sealing. Rotation is effected by a piston located at the top part of the lock gate. The lock gate

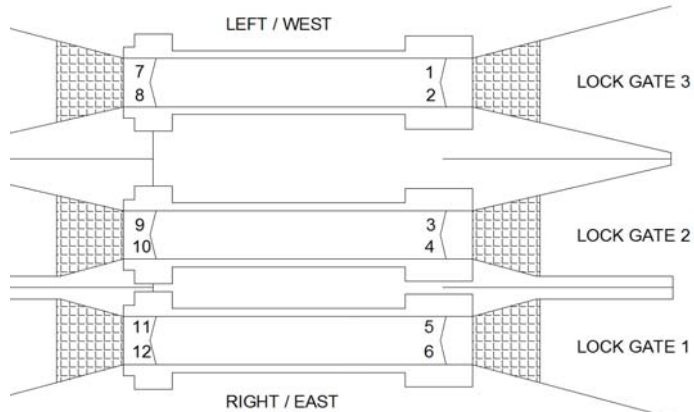
consists of a flatten closed side and a open side with air chambers and levelling holes at the bottom. The lock gates are made of steel and for protection against collisions wooden beams are mounted on the front side. The next section lists the results of the inspection reports on the lock gates of Maasbracht and Sambeek.

Maasbracht

The Lock complex of Maasbracht consist of three independent locks, East, Middle and West as shown in Figure 3.7. The locks were build in 1962 and have lock gates that are 23 years old. The locks are CEMT-classes V, which means that big Rijn-Hernekanaalschip and push-vessels can use the locks. The locks have 11.500 cycle levellings per year. The locks of Maasbracht are mitre gates with free hinges and occlusion is transmitted by wooden sealing. Rotation is effected by a piston located at the top part of the lock gate. The lock gates consist of a flatten closed side and an open side. The lock gates are made from steel with welded connections. For protection against collision a horizontal bar is located 5 metres in front of the lock gates.



(a) Top view locks of Maasbracht
[image from bing.com/maps]



(b) Position of the lock gates of Maasbracht during inspection of 2010

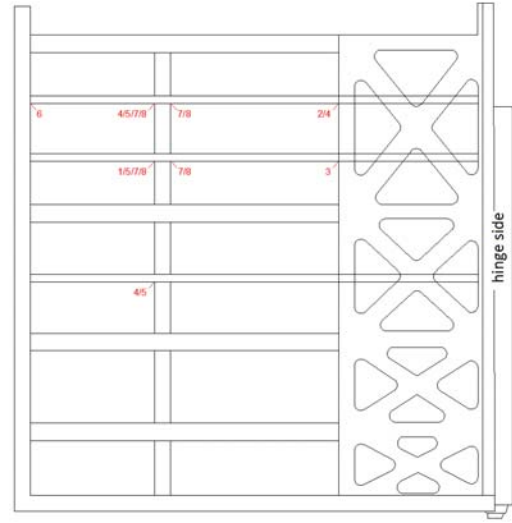
Figure 3.7: Overview of the locks Maasbracht

In Maasbracht all the lock gates have been inspected. In February 2010 the downstream lock gates 1-6 and in March 2010 the upstream lock gates 7-12 were inspected. During this inspection a number of cracks were found as shown in Figure 3.8. Because of the high number of cracks that are found in the lock gates 1-6, the cracks are summarized into compartments. The schematic lock gate (Figure 3.8) is divided into compartments, horizontal from A-C and vertical 1-11. [11]

The investigations revealed that at multiple lock gates significant cracks were found as shown in Figure 3.8 and Figure 3.9. All cracks were at least a couple of millimetres to a few centimetres in length. Even cracks in the range of over 200mm where found. Figure 3.8 makes clear that in the upstream lock gates most of the cracks are located in the centre-top part. All cracks that have been found were maximum 20mm with one crack of 40mm.

<i>Cracks in lock gates upstream</i>		
<i>Lock gate</i>	<i>nr.</i>	<i>Length</i>
Gate 7	1	10mm
	2	20mm
	3	40mm
Gate 8	no damage or cracks	
Gate 9	4	10mm
Gate 10	5	20mm
Gate 11	6	20mm
	7	10-20mm
Gate 12	8	10-20mm

(a) Crack lengths



(b) Position of cracks in lock gates

Figure 3.8: Maasbracht; Crack position in lock gates 7-12 inspection 2010

**Gate 8, 10 and 12 shown mirrored*

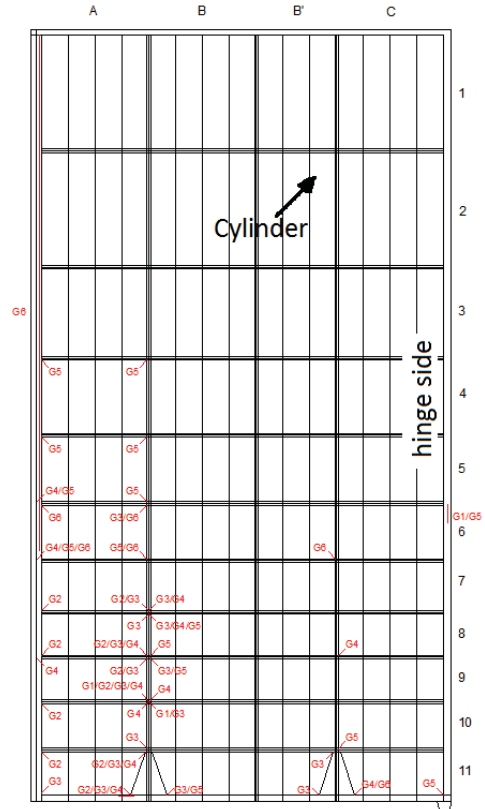
**e.g. nr. 8 is a crack of 10-20mm at the mid top of lock gate 12*

The number of cracks that have been found compared to number of cracks in Figure 3.9 is much less. Possible reason for the cracks in the upper part of the lock gate are stresses due to opening and closing the lock gates. Comparing the position of the cracks with the waterlevel reveals that the cracks in the lock gates are located in the fluctuating waterlevel, the so-called splashing zone. This means that over time a combination of air and (fresh) water influences the development of the middle and top cracks.

From Figure 3.9 we can see that most of the cracks are located in the centre-to-outer bottom part of the downstream lock gates and not in the centre of the gates. Possible reason for the cracks at this position can be that the bottom rule of the lock gates touches the sill. When touching the sill, part of the forces due to levelling will be transferred by the sill, which results in higher stresses at this part of the lock gate. Cracks from stresses of the cylinder force can be neglected. At this spot, at the connection of B' with 1-2, no cracks have been found.

<i>Cracks in lock gates downstream</i>		
<i>Lock gt.</i>	<i>Place</i>	<i>Length</i>
Gate 1	A7 B9 C6 C6	10-50mm 100-200mm
Gate 2	A12 A11 A10	10-50mm
	A9 A8 A7 C9	10-50mm
	C6 C4 C3	10-50mm
	A3 A11 A9	100-200mm >200mm
Gate 3	A11 A9 A8 B11	10-60mm
	B10 B9 B8 B6	10-60mm
	C11 C3 C2	10-60mm
	A9 B11 B10	100-200mm
	B7 A7 B7 C11	100-200mm >200mm
Gate 4	A11 A10 A9	10-70mm
	A6 A5 B7 B8	10-70mm
	C11 C8 C4 C1	10-70mm
	A8	>200mm
Gate 5	A10 A9 A6	10-60mm
	A5 A4 A3	10-60mm
	B11 C5 C4 C3	10-60mm
	C11 C10 C6	10-60mm
	B9 B8 A5 B8	100-200mm >200mm
Gate 6	A6 A5 A4	10-30mm
	B11 B6 C3	10-30mm
	C11 C6 C5	10-30mm
	A1-A6	80% crack

(a) Crack lengths



(b) Position of cracks in lock gates

Figure 3.9: Maasbracht; Crack position in lock gates 1-7 inspection 2010

*Gate 2, 4 and 6 shown mirrored

*e.g. Lock gate 3, Place B10 is a crack of 10-60mm at the mid bottom of lock gate in 'column B' and 'row 10'

Sambeek middle lock

The locks of Sambeek consist of three independent locks, an East, Middle and West Lock as shown in Figure 3.10. The West and middle locks were build in 1967 and have 46 year old lock gates, the East lock was build in 1925 and had 88 year old lock gates. The West and Middle lock gates have recently been replaced by new lock gates. The locks are located in the Maas, which is a fresh water river. The locks are CEMT-classes V and have 11.750 ship levellings per year.

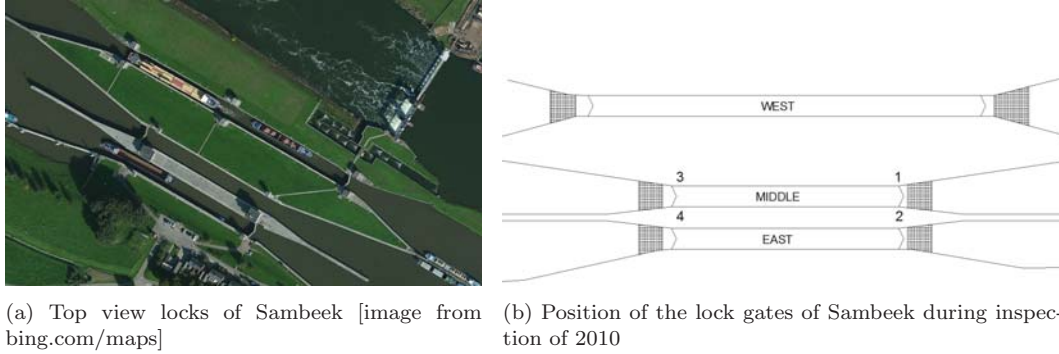


Figure 3.10: Overview of the lock complex of Sambeek

The locks of Sambeek are mitre gates with fixed hinges and occlusion is transmitted by rubber sealing. Rotation is effected by a piston located at the top part of the lock gate. The lock gates consist of a flatten closed side and an open side. In this lock the flatten closed side is on the downstream side and the open side on the upstream side. The lock gates are made of steel with welded connections and for protection against collisions wooden beams are mounted on the front side. The lock gates are not protected with a cathodic protection system.

In Sambeek only the left upstream lock gate of the West lock and all the lock gates from the middle lock have been inspected 7 times in the period of October 2010 and August 2011. Only the cracks of the middle lock gates are shown below. [12]

The investigation revealed that at multiple lock gates significant cracks were found as shown in Figure 3.11. All cracks were at least a couple of millimetres to a few centimetres on both sides of the gates, on the open side and the closed side. Because of the high number of cracks found, the cracks are summarized into compartments. The schematic lock gate (Figure 3.11) is divided into compartments, horizontal from A-G and vertical 1-5. Numbering in blue is on the closed side, numbering in red on the open side. From Figure 3.11 we can conclude that most of the cracks are located in the centre-bottom part of the lock gates. Comparing the position of the cracks with the waterlevel makes clear that the cracks in the lock gates are located below the waterlevel and thus air has no influence. It is assumed that the (cyclic) stresses of levelling are the cause of the cracks in the lower part. The maximum waterforce, the result of upstream minus downstream, is presented on the lower part of the lock gates, resulting in cyclic stresses on this part of the lock gates.

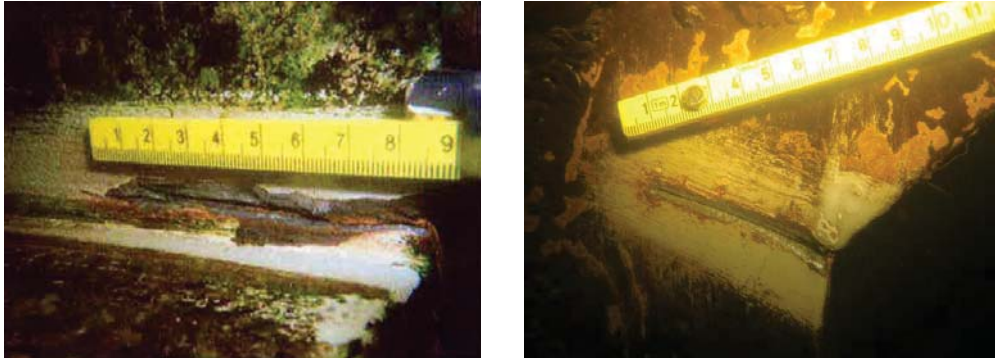


Figure 3.12: Founded cracks

**(Left: Cracks in the root of welds, Right: crack at round-off radii) [11]*

crack part from the lock gate and by breaking it to be able to have a look at the cracked surface. If striations are visible, fatigue is definitely the cause of cracking.

The cracks in the lower part of the gates are probably caused by the levelling of the water. The cracks at the top of the gates where the cylinders are mounted, are probably caused by opening the gates with waterlevel difference.

Summarized

- All the inspected lock gates show significant defects, more specific, cracks in the connections of the vertical and horizontal girders at round-off radii
- The cracks can be compared with each other: they have the same dimensions (length), the same shape and occur at the same place (weld toe or round of radii)
- Cracks that have been found in the bottom part of the lock gates; possible reason could be the levelling of the waterlevel or that the lock gates touches the sill so that the forces were transferred by this part of the gates.
- Cracks in the top part of the lock gates were probably from the cylinder force of opening the gates with waterlevel difference.
- All cracks were found in mitre gates, although there could be cracks in other types of lock gates, but they haven't been investigated

The cracks were found in different types of lock gates. The locks of Terneuzen are sea going locks, the locks of Sambeek and Maasbracht are river locks. In the Netherlands we can describe three different types of locks: sea going, river and canal locks. Canal locks have (almost) no waterlevel fluctuation. River locks have yearly waterlevel fluctuations (during the day the waterlevel is almost the same) and sea going locks have daily waterlevel fluctuation. This thesis is limited to two types of locks, river locks and sea going locks. The two cases that will be described in this thesis are the locks of Sambeek and the locks of Terneuzen.

Chapter 4

Literature study on fatigue

This chapter gives an overview of the literature on fatigue. The goal is to provide sufficient background information to understand the principle of fatigue.

4.1 Fatigue as a Phenomenon in the material

4.1.1 Historical survey

Fatigue is crack initiation under fluctuating load, which turns into crack propagation and finally can lead to failure of the structure. Already in the 19th century several serious fatigue failures were reported and the first laboratory investigations were carried out. Rankine [13] in 1843, discussed the unexpected fractures which sometime occurred in originally good railway axles after running for several years, and he attributed this behaviour to a gradual deterioration of the metal during the course of use. He demonstrated that the introduction of larger radius of curvature improved the resistance to repeated impact. Later, several researchers [7] [4] showed that beams could withstand a static load almost as great as the breaking load for as long as four years without failure. But if beams were repeatedly strained to the deflection produced by only half the breaking load, they broke in less than 1.000 reversals.

Noteworthy research on fatigue was done by August Wöhler [22] between 1858 and 1870. He was a German Engineer who did the first systematic and extensive experimental studies of fatigue behaviour of rail road axles. With his studies he laid the cornerstone for systematic approaches to the fatigue-life prediction. During his research he summarized his data in tables, which were put into diagrams later on by his successor Spangenberg. These diagrams are also known as the Wöhler diagrams, nowadays known as the S-N curve diagrams.

Until almost the end of the nineteenth century there was little knowledge of the structure of metals and the generally accepted explanation of fatigue was that the fibrous texture of metals gradually changed to a crystalline structure. Microscopic investigations by Ewing and Humfrey [3] at the end of the 19th century and the beginning of the 20th century were the first big steps of understanding the behaviour of fatigue. They found that if the limit of proportionality was exceeded, the metal deformed by slipping on certain planes within the crystals, as shown in Figure 4.2. When more research on microscopic information of the growth of small cracks became available, it turned out that nucleation of microcracks generally occurred very early in the fatigue life. [19]

Even though crack nucleation starts early, the microcracks remain invisible for a considerable part of the total fatigue life. Once cracks become visible, the remaining fatigue life of specimen is usually a small percentage of the total fatigue life. The demonstration by Forsyth [5], shows that the growth of fatigue cracks occurs in two distinct phases. Phase one is the *crack initiation period*, in which some microcracks growth occurs, but the fatigue cracks are still too small to be visible, and phase two is the *crack growth period*. Differentiating these two periods is of great importance, because several surface conditions do affect the initiation period, but have neglectable influence on the crack growth period.

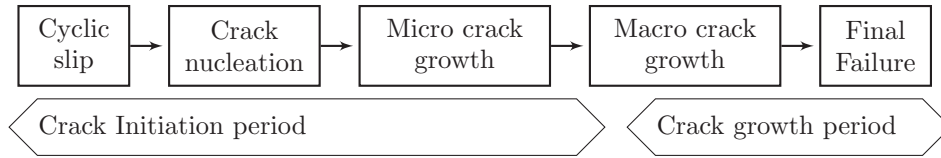


Figure 4.1: Different phases of the fatigue life [19]

4.1.2 Different phases in the fatigue life

Crack initiation

Crack initiation (and also crack growth) is a consequence of cycle slip which implies cyclic plastic deformation, in other words dislocation activities. Fatigue occurs at stress amplitudes below the yield stress. At such a (low) stress level, plastic deformation is limited to a number of grains of the (surface) material.

This microplasticity mostly occurs in the grains at the material surface, because of the lower constraint on slip. At the free surface of a material, the surrounding material is present at only one side. The other side is the environment, usually a gaseous environment (e.g. air) or a liquid (e.g. water). [19] Cyclic slip requires shear stress (see Figure cycleslip). On a microscale the shear stress is not homogeneous distributed through the material. This differs from grain to grain, depending on its sizes and shapes. When slip occurs in a grain, a slip step will be created at the material surface. The slip step implies that when a piece of new material is exposed to the environment, this new surface is immediately covered by an oxide layer in most environments. This type of monolayer adhere to the material surface can not be removed easily. Another significant aspect is that slip during the increase of the load also implies strain hardening in the slip band. As a consequence, in the unloading phase (reverse slip) a larger shear stress will be present.

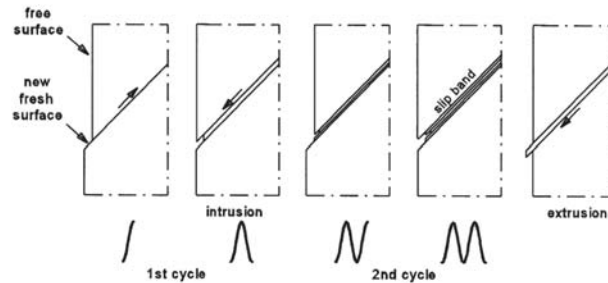


Figure 4.2: Cycle slip leads to crack nucleations [19]

In an ideal situation the slip will occur in the same slip band, which results in no fatigue. As mentioned in the previous paragraph there are two reasons why this ideal situation is not present. First, the oxide layer on the new material (after slip) can not be removed easily and second there is strain hardening in the slip band. As a result, reverse slip will not take place in the same slip band but on adjacent parallel slip planes, as shown in the second picture of Figure 4.2. Not only the lower restraint for crack initiation at the free surface is a reason for microcracks. Other reasons for crack initiation can be:

- Notch effect or holes; these produce inhomogeneous stress distributions where a peak stress occurs at the surface (stress concentrations)
- Surface roughness, corrosion pits

The most important conclusion from this theory can be written as:

In the crack initiation period, fatigue is a material surface phenomenon. [19]

Crack growth

As long as the size of the microcrack is still in the order of a single grain, the microcrack is obviously present in an elastically anisotropic material with crystalline structure and a number of different slip systems. The microcrack creates an inhomogeneous stress distribution on a microlevel with stress concentrations at the tip of the microcrack. As a result more than one slip system might be activated. If the crack is growing into the material in some adjacent grains, the constraints on slip displacement will increase due to the presence of neighbouring grains. This compared to the surface grains which only have neighbouring grains on one side. Because of the more difficult slip displacement, slip not only occurs in one slip plane but in more slip planes. The direction of the microcrack will then deviate from the initial slip band direction, generally to grow perpendicular to the loading direction, as shown in Figure 4.3.

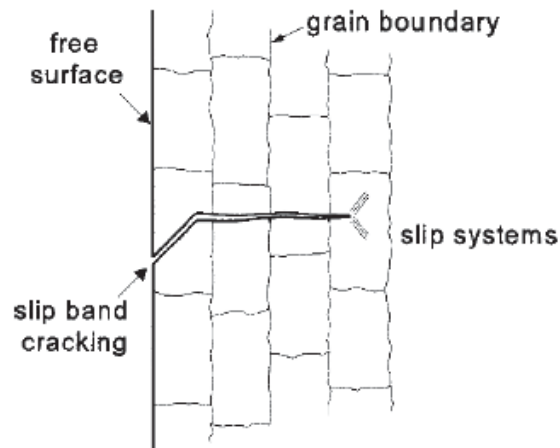


Figure 4.3: Cross section microcrack [19]

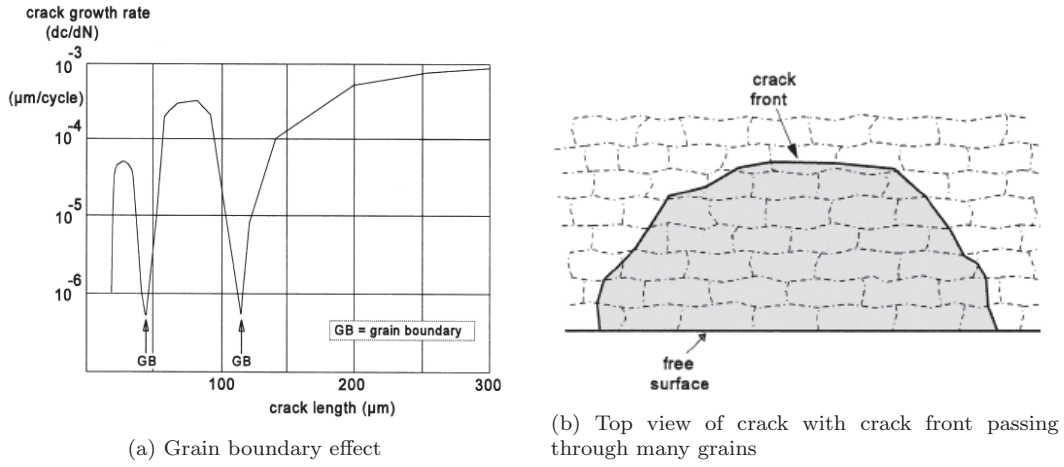


Figure 4.4: Barriers to slip [19]

Microcrack depends on the cyclic plasticity. Barriers to slip can be a threshold for crack growth. This has been observed by Forsyth [5]. As shown in Figure 4.4, the crack growth decreases when the crack tip approaches the first grain boundary. After penetrating the first grain boundary the crack growth increases until the crack tip approaches the second grain boundary. After penetrating the secondary grain boundary, the crack grows with a continuous steady rate. From the literature [5] some observations have been reported in inhomogeneous microcrack growth, which have a relatively high start growth and then slow down or even stop due to material barriers. After passing some grains, the surface aspects no longer have influence on the crack as shown in Figure 4.4. The lower restraint on cyclic slip at the surface is not applicable to the interior of the material. Secondly the roughness and other surface conditions like corrosion pits do not affect crack growth. [19]

The second important conclusion that can be made is:

Crack growth resistance when the crack penetrates into the material depends on the material as a bulk property. Crack growth is no longer a surface phenomenon. [19]

From the phases crack initiation and crack growth we can conclude two aspects:

- In the crack initiation period, fatigue is a material surface phenomenon
- When cracks penetrate into the material, the crack growth resistance depends on the bulk properties and is no longer a surface phenomenon

4.1.3 S-N Curve

The waterlevel difference consists of different values and therefore only S-N curves of variable amplitude stress are used in this thesis.

As mentioned in section 4.1.1 the fatigue strength has been put into Wöhler diagrams, also known as the S-N curve diagrams. An example of a S-N curve diagram is given in Figure 4.5.

The S-N curve can be split into two or three parts depending on the type of loading. Constant amplitude loading make use of a S-N curve of two parts, variable amplitude loading uses a S-N curve with three parts. Constant amplitude stress is stress where the amplitude does not change over time, where with variable stress the amplitude does change over time. This is shown in Figure 4.6. Constant amplitude stress only makes use of the part of the slope of $m = 3$ in the S-N curve. The other type of amplitude loading is variable amplitude stress. When variable amplitude loading occurs, the band in the spectrum with $\Delta\sigma_D$ may still cause damage. Damage occurs because the larger amplitude cycles may still start to propagate the crack. Once it starts to grow, lower cycles become effective. An example of variable amplitude stress is shown in Figure 4.6b. For variable amplitude stress, both parts of the slope $m = 3$ and $m = 5$ of the S-N curve are be used.

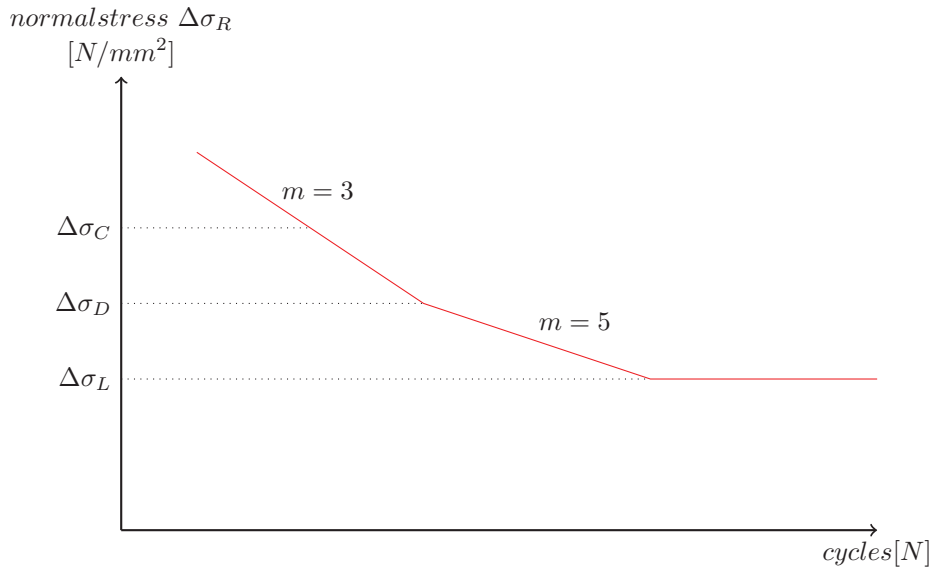


Figure 4.5: S-N Normal stress curve [based on the Eurocode 3 [21]]

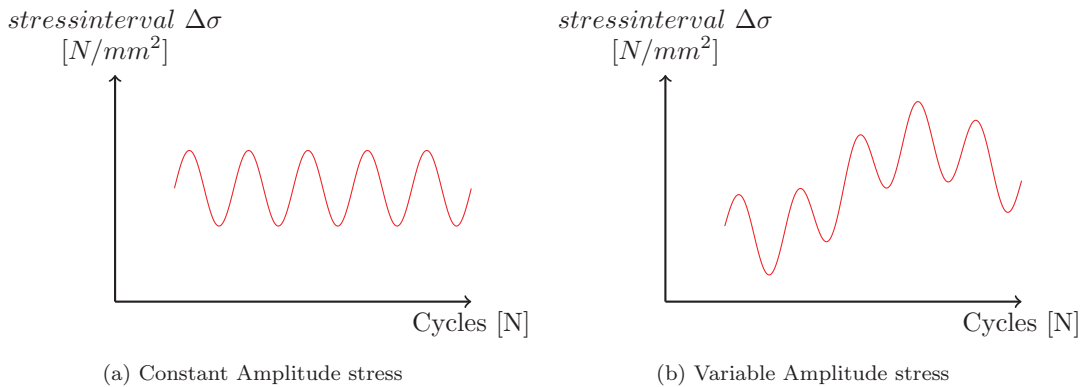


Figure 4.6: Constant versus Variable Amplitude stress

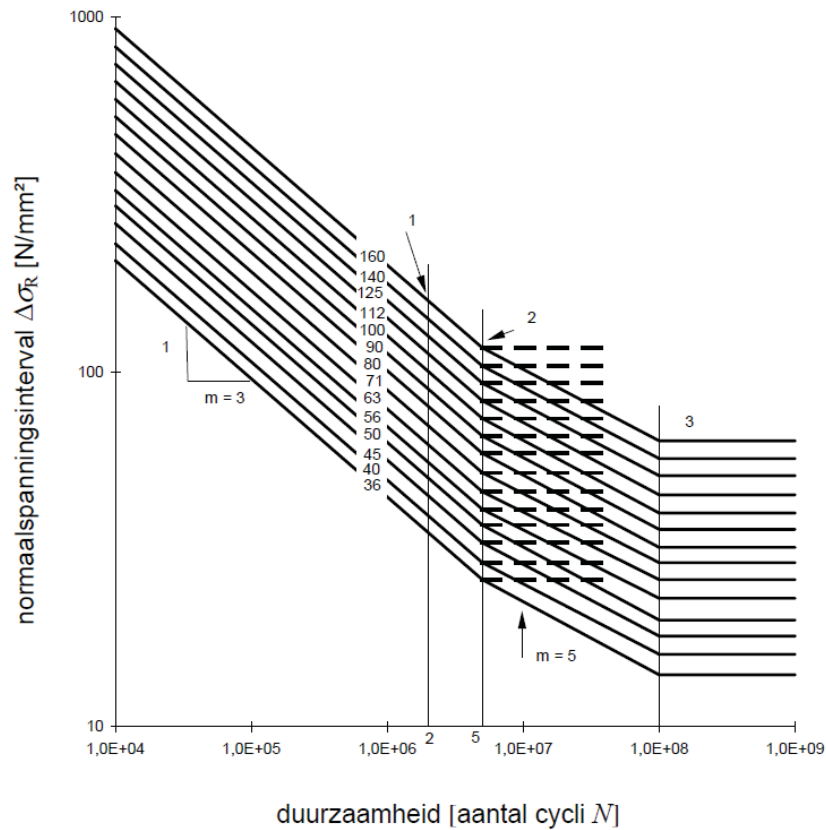


Figure 4.7: S-N Curve according to Eurocode 3; NEN-EN 1993-1-9 [21]

The S-N Curve corresponds with a typical type of joint. The better the joint resists fatigue, the higher the stress is allowed at a number of cycles, this is shown in Figure 4.13.

4.1.4 Fatigue strength of joints

Fatigue behaviour of cracks depends on the type and geometry of connections. As mentioned in section 2.1.3 the first steel lock gates where fabricated with riveted joints. In the sixties, after the welding process became more controlled, the steel lock gates where fabricated with welded joints. From historical point of view there have been some marks about the fatigue behaviour of the two different joints. The first lock gates were fabricated with perpendicular riveted joints between the horizontal and vertical girder, this is shown in Figure 2.8. These lock gates were not checked for fatigue. Cracks in riveted joints are more difficult to observe from the outside. Cracks could occur in the rivets itself or in a plate, these are not visible from outside. Because cracks in riveted joints are difficult to see from the outside, cracks were hardly or not observed in steel lock gates with riveted joints.

In the sixties when the structures were fabricated with welded joints, the joints geometry still remained the same. The geometry of the joints between the horizontal and vertical girder were still perpendicular. Cracks due to fatigue in welded joints are visible from the outside, because fatigue cracks usually occur at the root or toes.

Looking at the same geometry of the joint, the fatigue detail category (classification) of the two types of joints differ. Riveted joints have higher fatigue strength than welded joints. In Figures 4.8 and 4.9 the detail category of a typical lock gate connection (connection of the vertical to horizontal girder) is given. From the figures it can be seen that the fatigue strength of the riveted connection is stronger than the welded connection. When creating a welded connection with rounded corners it can be questionable if riveted joints are better.

40		5) Gelast, zonder overgangsronding.	
----	---	-------------------------------------	--

Figure 4.8: Detail Categorie 40 [based on NEN-EN 1993-1-9 [21]]

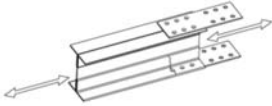


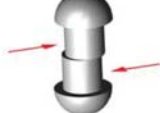
$\Delta\sigma_c$ 71 $m=5$		<u>one-shear joint with gusset plates</u>	if the calculated shear force in the rivets is lower than the minimum value of slip resistance, $\Delta\sigma_c=85$ can be used
		<u>area of the connection of a lateral bracing element to the tension flange of a girder</u>	if the restraining effect of the lateral bracing element is considered during the calculation of the applied stress range $\Delta\sigma_c = 85$ can be used
		<u>onset of a cover plate</u>	if the calculated shear force in the rivets is lower than the minimum value of slip resistance, $\Delta\sigma_c=85$ can be used
$\Delta\tau_c$ 140 $m=5$		<u>rivets in shear</u>	-

Figure 4.9: Detail Categorie 70 and 140 [based on "Proposal Riveted Assessment of Existing steel structures, remaining fatigue life version 2, Chapter 3"]

The main factors influencing the fatigue performance of riveted construction details are the stress ratio $R = \frac{\sigma_{min}}{\sigma_{max}}$, the level of clamping force present in the rivets and the level of force transmitted by the rivets through shearing of the rivets and bearing pressure in the rivet holes [1]. The higher the clamping force of the rivet, the more the force will be transmitted by friction. This results in that a crack due to fatigue is located more outside the rivet. The lower the clamping force of the rivet, the more the rivet needs to transfer the force in the connection. This leads to a crack initiation at the rivet hole.

The fabrication of rivet joints is very time and cost consuming. Every rivet needs to be preheated and hammered into shape. Especially the time consuming factor, which directly leads to costs, was one of the major aspects for changing the connections into welded joints.

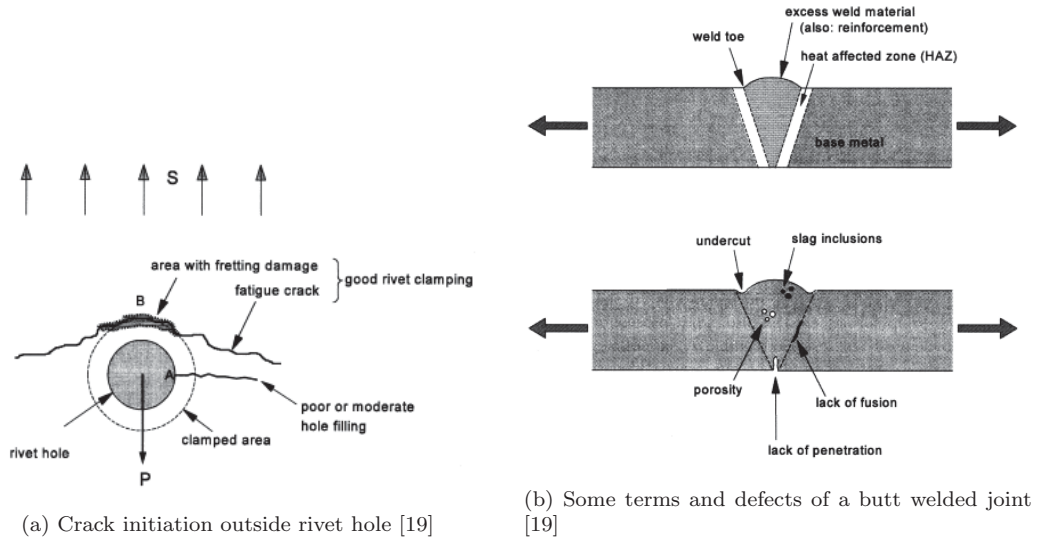


Figure 4.10: Rivet vs. welded connection

Welding is a process that melts the material; by adding filler material a pool of molten metal forms, resulting in strong joints after cooling down. The downside of welding joints is that most welding processes leave minute metallurgical discontinuities from which crack growth occurs, as shown in Figure 4.10b. Also most structural welds have a rough profile. Sharp changes in stress direction generally occur at the toes of butt welds and at the toes and roots of fillet welds. These spots are highly sensitive for fatigue. A second aspect of welding is that during welding the molten metal or the placed part being welded locally expands. After cooling down some areas contract more than other areas which leave residual stresses. These reasons lead to the fact that a welded joints is highly sensitive to fatigue.

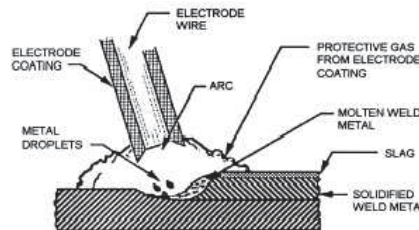


Figure 4.11: Shield metal arc welding [2]

Comparing the rivet connection to the welded connection some mark ups can be made. Before the sixties when the lock gates were fabricated with rivet connections, there were hardly any cracks found, because cracks could occur in the rivet itself or plates, that are not visible from the outside.

After the change to structures with welded connections, cracks were observed. The most important reason that welded connections are highly sensitive for fatigue, are the high residual stresses that occur after welding and the metallurgical discontinuities owing to the

welding process. Although the rivet connections have better fatigue performance, lock gates are nowadays constructed with welded joints. The reason for this is that the construction time with rivet joints is time consuming which leads to very high construction costs.

The majority of the existing lock gates are made with welded joints and also new lock gates are fabricated with welded connections. The discussed fatigue of steel lock gates in this thesis is only based on lock gates with welded connection.

4.2 Fatigue calculations according to the NEN 2063

This section describes the fatigue calculation according to the NEN 2063 standard. As mentioned, the calculation of fatigue is based on the S-N diagrams (originally made by Wöhler), see Figure 4.12. This S-N curve is split up into three parts. The first linear part from $N = 10^4$ to $N = 10^7$ cycles have a slope of $m = 3$. This part of the S-N curve is valid constant and variable amplitude stress. The second part, from $N = 10^7$ to $N = 2 \cdot 10^8$, which has a inverse slope of $m = 5$ and is only used for variable amplitude loading for which a part of the stress ranges exceed the $\Delta\sigma_k$ for $N = 10^7$. The larger stress ranges may initiate cracks, which grow further under smaller stress ranges. The third part from $N = 10^8$ is horizontal and represents the cut-off limit, below which stress ranges are assumed to give no further fatigue damage.

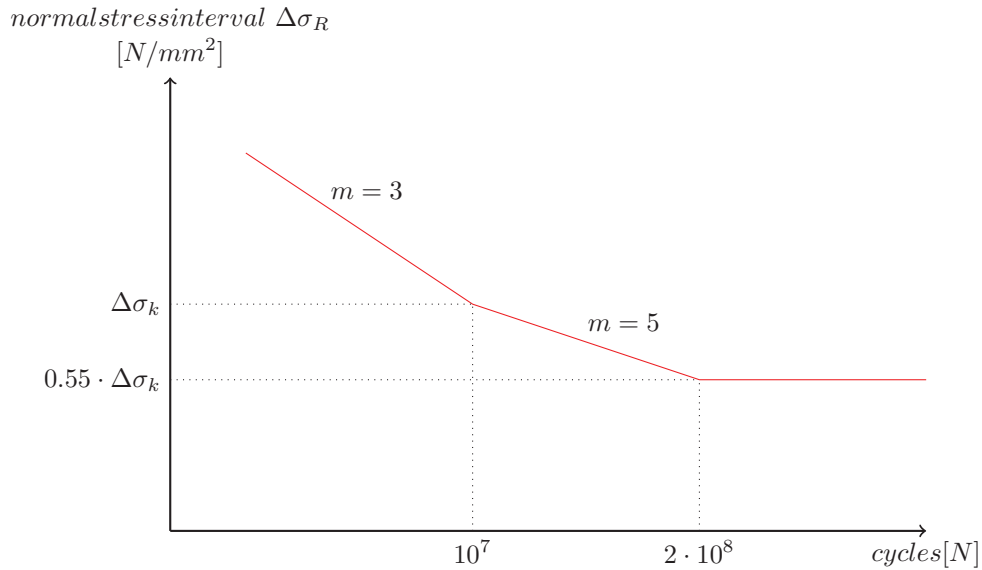


Figure 4.12: S-N Normal stress curve NEN 2063

The fatigue strength for nominal stress-intervals is displayed by a series of $(\log \Delta\sigma_k) - (\log N)$ curves, which correspond to the typical detail category, this is shown in Figure 4.7. Each detail category is a number, in N/mm^2 , that shows the reference value $\Delta\sigma_k$ for fatigue strength at 10 million cycles.

Some remarks can be highlighted regarding the NEN 2063. The NEN 2063 is not applicable for seawater conditions and the structure needs to be protected against corrosion. All the

lock gates have a coating and some of the lock gates have cathodic protection. Although lock gates have cathodic protection to ensure that sea water has no influence, it is questionable whether the used standard is applicable.

4.2.1 Fatigue damage

The calculation of the fatigue damage under variable (and constant) stresses from an S-N curve is by means of damage law. This hypothesis is based on the linear damage law that has been made analytically by Palmgren-Miner (1945). The equation for fatigue damage according to the NEN 2063 can be written as:

$$D_d = \sum_{i=1}^n \frac{n_i}{N_i} \leq 1 \quad (4.1)$$

where:

$$\begin{aligned} n_i &= \text{Number of cycles} & [-] \\ N_i &= \text{Durability (in number of cycles)} & [-] \end{aligned}$$

The durability N_i is expressed as follow:

For $\Delta\sigma_i \geq \Delta\sigma_k$ the expression can be written as follow:

$$N_i = \left(\frac{\Delta\sigma_k}{\Delta\sigma_i} \right)^3 \cdot 10^7 \quad (4.2)$$

For $0.55 \leq \Delta\sigma_i < \Delta\sigma_k$ the expression can be written as follow:

$$N_i = \left(\frac{\Delta\sigma_k}{\Delta\sigma_i} \right)^5 \cdot 10^7 \quad (4.3)$$

where:

$$\begin{aligned} \Delta\sigma_k &= \text{Characteristic fatigue strength of the detail at } 10^7 \text{ cycles} & [N/mm^2] \\ \Delta\sigma_i &= \text{Stress range} & [N/mm^2] \end{aligned}$$

The fatigue damage equation 4.1 is a calculated factor which should be smaller or equal to 1. Above 1, fatigue cracks will occur, which finally could lead to the failure of the structure.

4.3 Fatigue calculation according to the Eurocode 3

This section describes the fatigue calculation according to the Eurocode 3 NEN-EN 1993-1-9 standard. As mentioned, the calculation of fatigue is based on the S-N diagrams (originally made by Wöhler), see Figure 4.13. This S-N curve is split up to three different parts. The first linear part from $N = 10^4$ to $N = 5 \cdot 10^6$ cycles have a slope of $m = 3$. This part of the S-N curve is valid constant and variable amplitude stress. The second part, from $N = 5 \cdot 10^6$ to $N = 10^8$ which has a slope of $m = 5$ and is only used for variable amplitude loading for which a part of the stress ranges exceed the $\Delta\sigma_D$ for $N = 5 \cdot 10^6$. The larger stress

ranges may initiate cracks, which grow further under smaller stress ranges. The third part from $N = 10^8$ is horizontal and represents the cut-off limit, below which stress ranges are assumed to give no further fatigue damage.

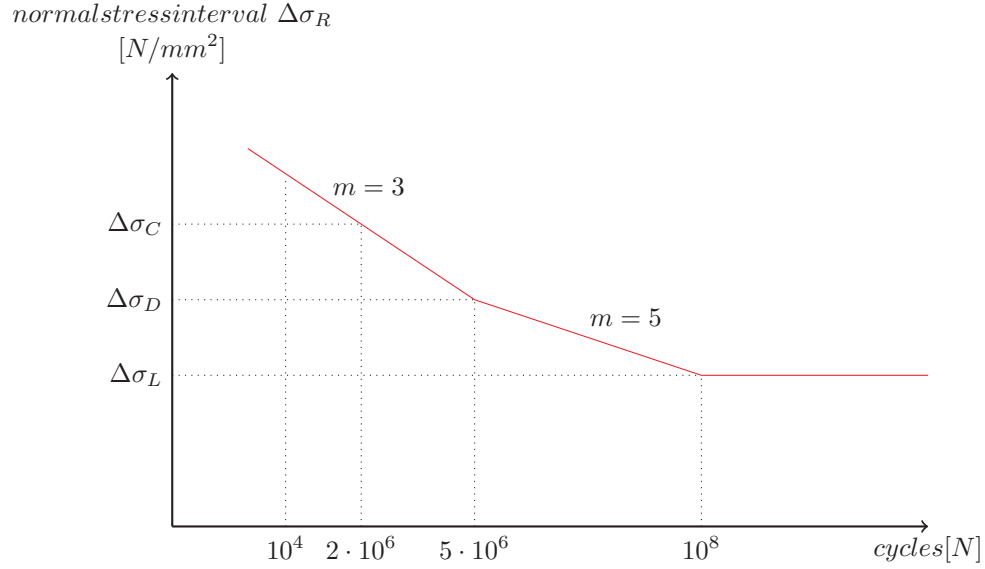


Figure 4.13: S-N Normal stress curve according to the Eurocode [21]

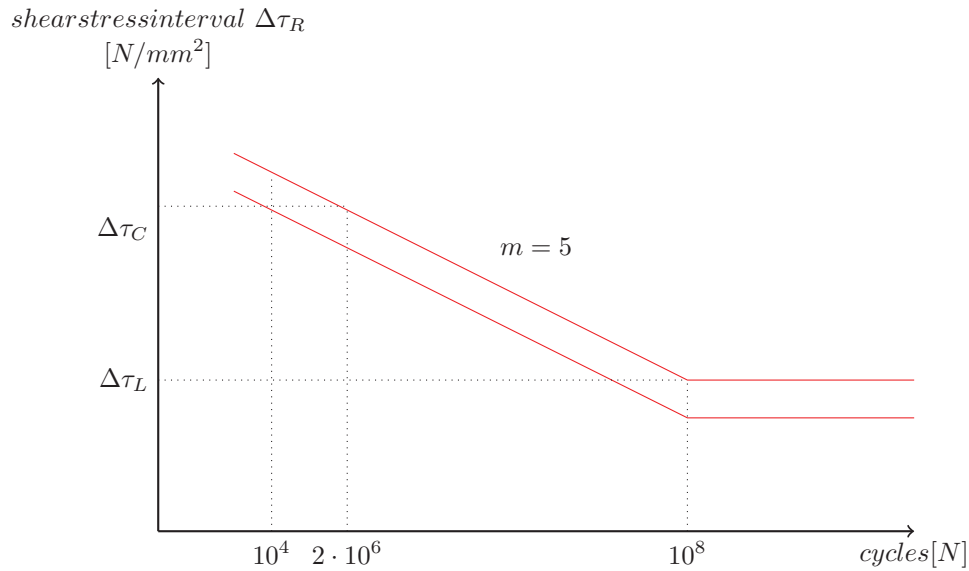


Figure 4.14: S-N Shear stress curve according to the Eurocode [21]

The fatigue strength for nominal stress-intervals is displayed by a series of $(\log \Delta \sigma_R) - (\log N)$ curves and $(\log \Delta \tau_R) - (\log N)$ curves (S-N curves), which correspond to the typical detail

category, this is shown in Figure 4.7. Each detail category is a number, in N/mm^2 , that shows the reference value $\Delta\sigma_C$ and $\Delta\tau_C$ for fatigue strength at 2 million cycles.

Some remarks can be highlighted regarding the Eurocode 3. The Eurocode 3 is only applicable for normal atmospheric conditions with corrosion protection. All the lock gates have a coating and some of the lock gates have cathodic protection. Although lock gates have cathodic protection to ensure that sea water has no influence it is questionable whether the used standard is applicable. Because only this standard is available for calculations, the calculated fatigue damage factor will be higher in reality, because of the negative influence of (sea)water conditions. An example of a lower fatigue strength due to (sea)water conditions is given in Figure A.7 in Appendix A.

4.3.1 Fatigue damage

The calculation of the fatigue damage under variable (and constant) stresses from an S-N curve is by means of damage law. This hypothesis is based on the linear damage law that has been made analytically by Palmgren-Miner (1945). The equation for fatigue damage according to the Eurocode 3 can be written as:

$$D_d = \sum_{i=1}^n \frac{n_{Ei}}{N_{Ri}} \leq 1 \quad (4.4)$$

where:

$$\begin{aligned} N_{Ei} &= \text{Number of cycles} & [-] \\ N_{Ri} &= \text{Durability (in number of cycles)} & [-] \end{aligned}$$

The durability N_i is expressed as follow:

For $\Delta\sigma_R \geq \Delta\sigma_D$ the expression can be written as follow:

$$N_{Ri} = \left(\frac{\Delta\sigma_C}{\Delta\sigma_R} \right)^3 2 \cdot 10^6 \quad (4.5)$$

For $\Delta\sigma_L \leq \Delta\sigma_R < \Delta\sigma_D$ the expression can be written as follow:

$$N_{Ri} = \left(\frac{\Delta\sigma_D}{\Delta\sigma_R} \right)^5 5 \cdot 10^6 \quad (4.6)$$

where:

$$\begin{aligned} \Delta\sigma_C &= \text{Characteristic fatigue strength of the detail at } 2 \cdot 10^6 \text{ cycles} & [N/mm^2] \\ \Delta\sigma_R &= \text{Stress range} & [N/mm^2] \end{aligned}$$

The fatigue damage equation 4.1 is a calculated factor which should be smaller or equal to 1. Above 1, fatigue cracks will occur, which finally could lead to the failure of the structure.

4.4 Fatigue calculation according to the DNV

As mentioned in the two previous sections the standards *NEN 2063* and *EUROCODE 3* have some limitations on their working field. They are both applicable in atmospheric condition. It is already clear that lock gates are not only subject to atmospheric conditions but also to fresh water and sea water conditions. The influence of these conditions is not documented in the standards. To find out what the influence of the sea and/or fresh water condition is, other standards can be used. One of these standards is the *DNV-RP-C203 Fatigue design of Offshore Steel Structures*. As shown in Figure 4.15 this standard describes a special S-N curve for structures in salt water condition with cathodic protection. When using structures without cathodic protection (or cathodic protection that does not function 100%), this S-N curve is even lower. The S-N curve of fresh water is lower than the S-N curve of sea water with cathodic protection, but higher than the S-N curve of sea water without cathodic protection.

The standard *EUROCODE 3* that is used in the Netherlands to determine the fatigue damage, does not describe (sea) water conditions with or without cathodic protection. Because these aspect are not mentioned in the standard, they will be neglected in the fatigue calculations in this thesis.

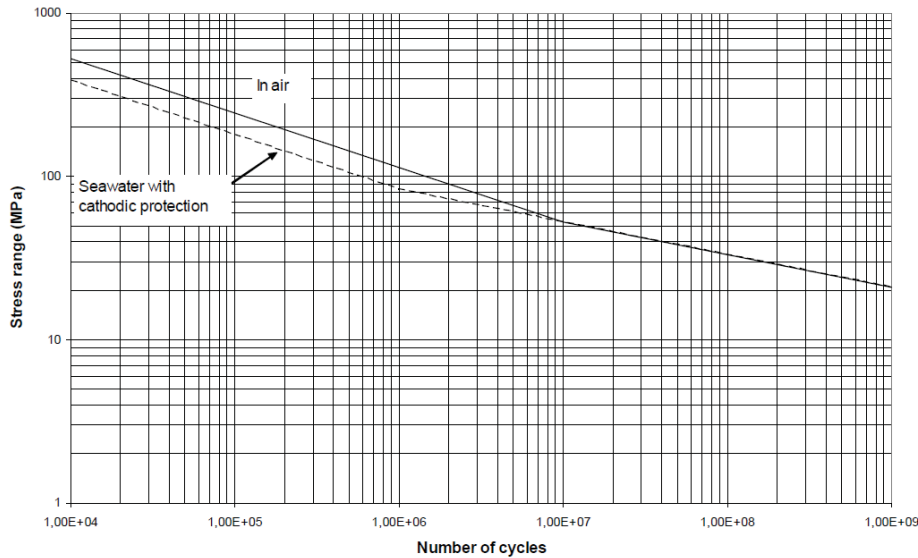


Figure 4.15: DNV-RP-C203: Fatigue of Offshore Steel Structures

4.5 Examples of fatigue calculations

In Appendix B examples are given of the fatigue damage calculation of lock gates.

Chapter 5

Fatigue damage calculation

Case 1: Sambeek - West

5.1 General information

This case is about the locks of Sambeek. The locks of Sambeek are located in the East of the Netherlands in one of the main shipping routes, river 'de Maas'. Figure 5.1 gives an overview of the lock complex of Sambeek. The East lock was build in 1925. Due to the increase in ship transport, the capacity of the lock was insufficient. By the end of the sixties the build of two extra lock was finished, the Middle and West locks. The capacity of the locks are respectively 11.744 ship movements for the East lock, 10.535 ship movements for the Middle lock and 11.146 ship movements for the East lock. All the locks consist of mitre gates as shown in Figure 5.2.



Figure 5.1: Overview of the lock complex Sambeek

**[image from bing.com/maps]*



Figure 5.2: Top view of the West and Middle locks of Sambeek, mitre gates

**[image from bing.com/maps]*

The last inspection reports made by Nebest on the middle lock gates showed that significant cracks were found. After the inspections in 2010 Rijkswaterstaat decided that the lock gates needed to be replaced. In 2011 Heijmans started with design and calculation of new lock gates to replace the old ones. In the meantime the lock gates of the Middle and West locks have been replaced. The East lock will be extended, widened and than also provided with new lock gates. Figure 5.2 gives an overview of the lock complex of Sambeek. For the calculation of fatigue we use the general information of the design and calculation reports of the new lock gates [6] made by Heijmans.

5.2 Waterlevel

As mentioned in previous section, the locks of Sambeek are located in the river the Maas. The Maas is a river with relatively constant waterlevel. It fluctuates upstream over the year from +10.80m NAP to +13.90m NAP and downstream from +7.65m NAP to +13.70m NAP (highest measurements recorded on December 22nd 1993 at 07.00 hours). The average waterlevel (AWL) downstream is +8.00m NAP and upstream +10.80m NAP. Figure 5.3a gives an overview of the waterlevel over a period of 5 days. It shows that the waterlevel does not fluctuate during the day, but only over the year. An overview of the data is shown in Table 5.1. To give an impression, the waterlevel data are presented in Figure 5.3b.

From the database of Rijkswaterstaat upstream and downstream measurements of the lock of Sambeek are available. Downstream measurements have been taken until now, but upstream only measurements have been taken till 1988. For the calculation of the waterlevel-difference spectrum the waterlevel data from 1980 till 1988 are used. The reason for using more years is to get a more accurate average per year. It is possible that at some years higher values occur, therefore a more accurate average can be determined by using the data of multiple years. For the calculation of the waterlevel spectrum the number of data points have been counted per waterlevel spectrum. For example the number of data points from -3.13m NAP

<i>Exceedance frequency</i>	<i>Downstream [m]</i>	<i>Upstream [m]</i>
1x per 1.250 year	14.30	14.50
Highest known measurement 22 dec. 1993 7h	13.70	13.90
1x per 100 year	13.40	13.60
1x per 10 year	12.55	12.85
1x per 2 year	11.55	11.85
1x per year	11.00	11.40
AWL	8.00	10.80
AWL Summer	7.75	10.80
Lowest known measurement	7.65	10.80

Table 5.1: Sambeek; Average exceedance frequencies

*Data from www.rijkswaterstaat.nl, AWL = Average Waterlevel, AWL Summer = Average Waterlevel Summer

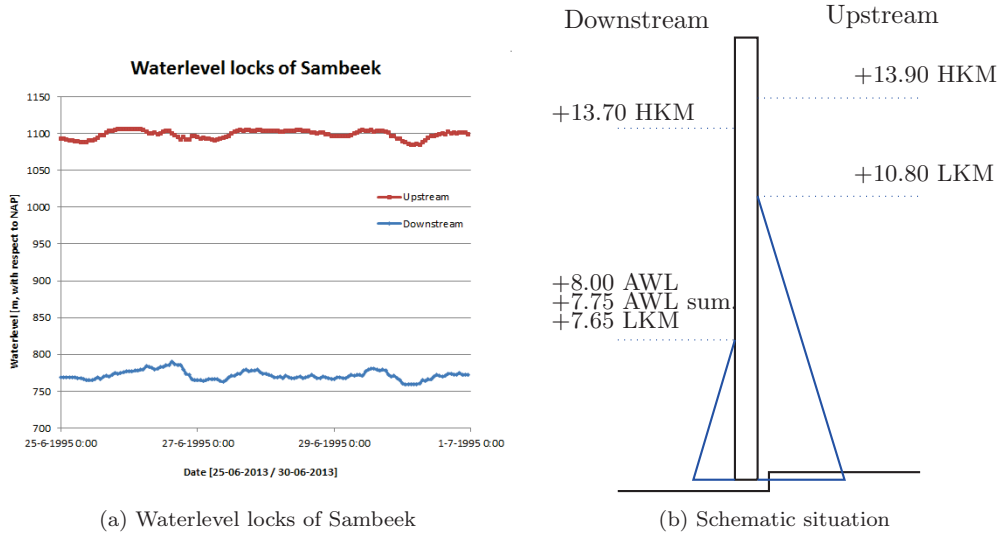


Figure 5.3: Sambeek; waterlevel presentation

*[measurement from http://www.rijkswaterstaat.nl/geotool/waterhoogte_tov_nap.aspx]

*LKM = Lowest known measurement, AWL summer = Average waterlevel summer, AWL = Average waterlevel summer, HKM = Highest known measurement

to -3.03m NAP have been counted over the 9 years (1980-1988), this are 5 data points. Dividing this value by the total number of measurements, 3.288 (total number of days in the 9 years), results in the percentage, namely $1.0560 \cdot 10^{-5}$. Multiplying this percentage with the total number of ship levellings per year results in the number of ship levellings that take place between -3.13m NAP and -3.03m NAP. In Appendix D Table D.1 the total number of ship levellings has been calculated. Figure 5.4 gives a presentation of the data.

As shown in Figure 5.4 the majority of ship levellings take place at a waterlevel-difference of about +320cm. The peak at +30cm is likely due to extreme high waterlevel upstream.

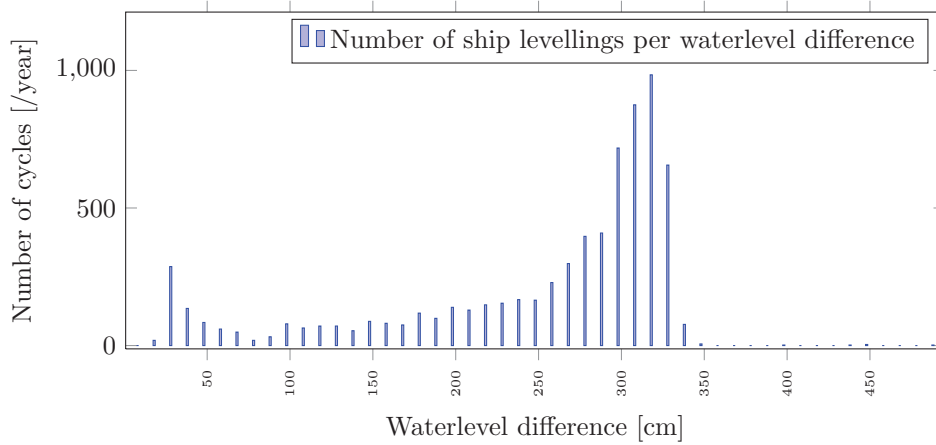


Figure 5.4: Sambeek; Waterlevel level difference spectrum based on real measurements - steps of 10cm

At high waterlevel the spillway will overflow and the water downstream will rise, therefore the waterlevel difference reduces.

5.3 Observed cracks

The inspection reports revealed that a number of cracks have been found on the Middle lock of Sambeek, for reference see Chapter 3. The cracks found in the lock gates are shown in Figure 5.5. The cracks have been found in the lower part of the lock gates at the corners and round-off radii of the connection between the horizontal and vertical girders. The cracks in the lower part of the lock gates are assumed to be caused by the ship levellings (waterlevel difference). In the top part of the lock gates cracks have been found at the free end stem post; this could be the result of objects between the lock gates. The other cracks in the middle of the top part could have been the result of opening and closing the lock gate. When opening and closing the gates, high forces of the cylinder are subjected to this part of the gates.

The measurement of the cracks on the lock gates were done on the old gates. In 2010 the gates have been replaced by new lock gates. The design of the new gates is based on the old gates. The majority of the cracks have been found in the second and third girder, therefore only these two girders will be checked in the fatigue damage calculation.

5.4 Fatigue damage old lock gate

This section gives an overview of the fatigue damage calculation for the old lock gate. Table 5.2 lists the different parameters for the calculation of the fatigue damage. The fatigue damage calculation is based on the Eurocode 3 NEN-EN 1993-1-9. This fatigue calculation is based on two different calculations. The first model is a fatigue damage calculation based on mean value from the scatter of the experiments of the S-N curve. The second calculation is based on the characteristic value of the Eurocode 3 S-N curve without partial safety factor.

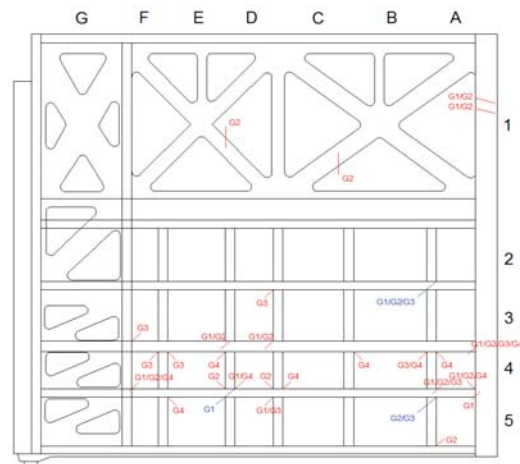


Figure 5.5: Sambeek; Position of cracks in the lock gate

The life span that is used in the calculation for the lock gates is 43 years, $N_{year} = 43$ year. In total 11.747 ship levellings took place each year, in one direction a value of 60% is used, namely $T = 7048$ levellings per year. The detail can be compared with detail category 40 of Table 8.3 and 8.4 of NEN-EN 1993-1-9 Figure 5.7. For the section modulus a value of $W = 3807618 \text{ mm}^3$ is used, this value is calculated from the image of Figure 5.6. Dimensions are based on old drawings. For the gravitational force $g = 9.81 \text{ m/s}^2$ is used.

<i>Description</i>	<i>Sign</i>	<i>Value</i>	<i>Unit</i>
Service life	T_{43}	43	year
Number of levellings	N	11.747	[-]
Detail category	$\Delta\sigma_C$	40	N/mm^2
Partial factor for fatigue resistance	γ_s	1.00	[-]
Stress concentration factor	γ_c	1.00	[-]
Section modulus	W	3807618	mm^4
Effective height	h_q	875	mm
Length lock gate	L	8900	mm
Density water	ρ_{water}	1025	kg/m^3
Gravitational force	g	9.81	m/s^2

Table 5.2: Sambeek; Input values for the old lock gates

5.4.1 Detail category

The characteristic value of the fatigue strength of the detail is based on the stress direction and the typical connection where the cracks have occurred. From the observation it was clear that cracks have occurred at sharp corners and round-off radii of the vertical and horizontal girders. The stresses in the girder at the connection are parallel and perpendicular to the welds. This is also shown in section 3.1.2. This fatigue damage calculation is based on the NEN-EN 1993-1-9. The characteristic value of the fatigue strength for the second calculation

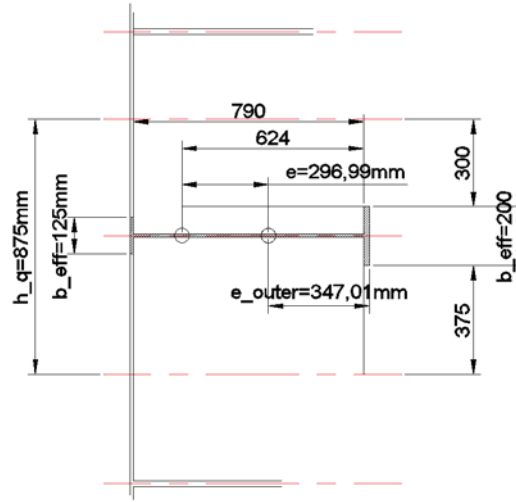
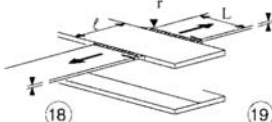


Figure 5.6: Sambeek; Cross-section of the old lock gate, dimensions based on Figure A.3 and A.4

can be taken from Figure 5.7. The detail category states $\Delta\sigma_R = 40 \text{ N/mm}^2$ at 10^7 cycles.

40		18) Stompe las in dwarsrichting bij kruisende flenzen. 19) Met overgangsstralen volgens tabel 8.4, detail 4	Details 18) en 19) De vermoeingssterkte van de doorgaande component moet zijn getoetst via tabel 8.4, detail 4 of detail 5.
----	---	--	--

(a) Cracks in weld perpendicular to stress direction

40		5) Gelast, zonder overgangsroning.	
----	---	------------------------------------	--

(b) Cracks in base material perpendicular to stress direction

Figure 5.7: Detail category 40 [NEN EN 1993-1-9 C2, Table 8.3-8.4]

For the first calculation the mean value of the fatigue strength of the detail needs to be calculated. In Appendix A Figure A.9 the scatter data of this detail category 40 is presented. From this scatter plot a mean value is calculated as shown in Figure A.9. From this mean value a new slope and detail category is calculated. The new detail category states $\Delta\sigma_R = 74.65 \text{ N/mm}^2$ at $2 \cdot 10^6 \text{ N/mm}^2$ with a slope of $m = 3.4602$.

5.4.2 Fatigue damage

The stress calculation is based on equations 2.1, 2.2, 2.6, 2.3, 2.5 and 2.8. From the waterlevel-difference the distributed force is calculated. This force is directly used in the moment equation and equation to determine the stresses. The normal force in the structure at an eccentricity is determined from the result of the upstream waterforce minus the downstream waterforce. By using equation 2.3 the normal force is calculated. This normal force is applied over this part of the cross-section.

With equations 4.4, 4.5 and 4.5 the fatigue damage is determined.

As mentioned in section B.1 the choice of the correct load spectrum is of high importance. For the fatigue damage calculation of the lock of Sambeek different waterlevel steps have been used. Steps of 10, 20, 50 and 100cm have been used to see how large the influence is of the fatigue damage.

A calculation of one step waterlevel difference can be found in Appendix C section C.1.

Figure 5.8 represents the total number of cycles over 43 year per waterlevel difference. Figure 5.9 represents the stress in the cross-section per waterlevel difference. Figure 5.10 represents the influence of the fatigue damage per waterlevel difference. From the last figure we can conclude that the relative high number of cycles at +30cm have (almost) no influence on the fatigue. The largest contribution to the fatigue damage is from the waterlevel difference of +3.20m. In Figure 5.11 the red line represents the fatigue damage of the old lock gate based on the mean value of the scatter plot of the experiments. From this figure we can conclude that the calculated fatigue damage is below the value of 1. From the chapter Observations it can be concluded that cracks have occurred in the lock gate. Therefore it is expected that the fatigue damage value should be higher (> 1) than the calculated value in Figure 5.11.

The conclusion is that the observed fatigue damage cannot be predicted with the simplified model used for this fatigue damage calculation. A number of aspects could be the reason for this.

The schematisation of the lock gate was too simplified. The moments due to torsional, as result of the deformation according to Figure 5.12, have not been taken into account. Due to torsional moments the stress will increase and therefore the value of the fatigue damage will increase. Also the assumption made in Figure 2.20 might be too conservative. The torsional force in the lock gate due to opening with a waterlevel difference is also probably not that simple modelled. Higher waterlevels due to waves which results in higher stresses also influence the fatigue damage negatively.

The influence of maintenance is also not taken into account. When (almost) no or poor maintenance is performed on the lock gates, a number of aspects could result in lower fatigue damage values. A poor state of the wooden sealing at the back post (which results in a different load transfer of the normal forces in the lock gate to the civil work) can contribute to other or higher stresses in the lock gate. Also the state of the coating layer is not taken into account. Over the year the coating layer gets brittle and no longer protects the full surface of the lock gates. This gives a negative influence on the S-N curve. The lock gates are subjected to fresh water conditions. As mentioned in the chapter about fatigue, the influence of fresh water also has a negative influence on the S-N curve.

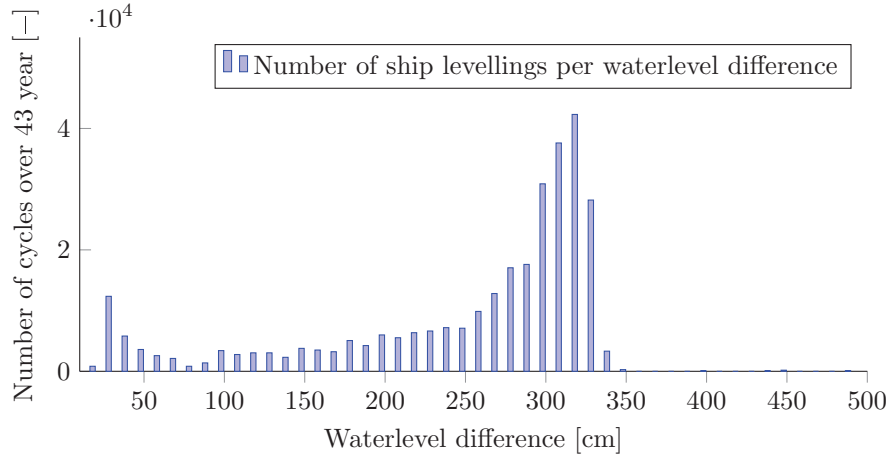


Figure 5.8: Sambeek old lock gate; Waterlevel difference spectrum

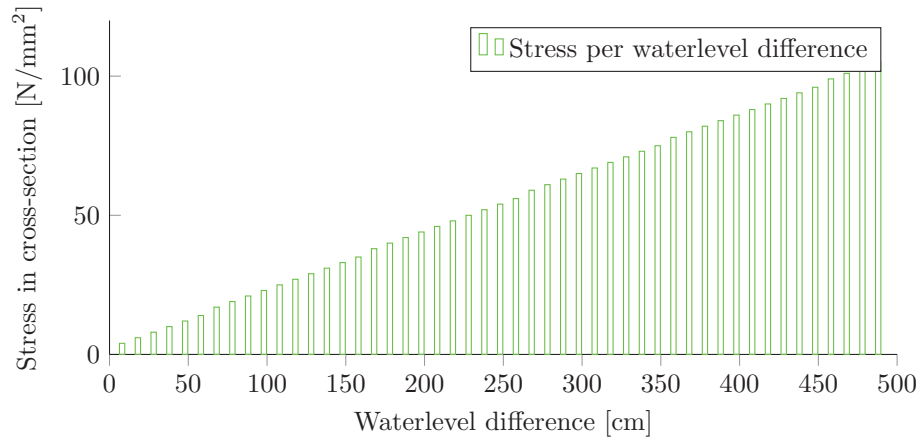


Figure 5.9: Sambeek old lock gate; Fatigue damage per waterlevel difference

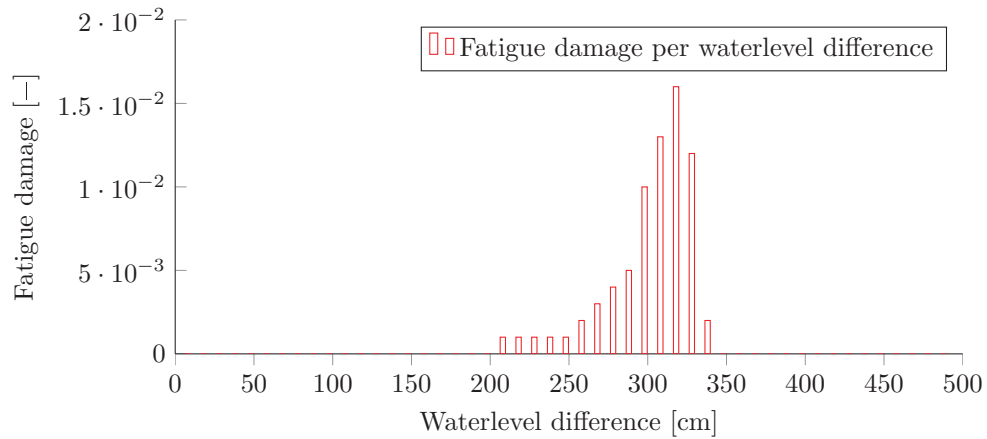


Figure 5.10: Sambeek old lock gate; Fatigue damage per waterlevel difference

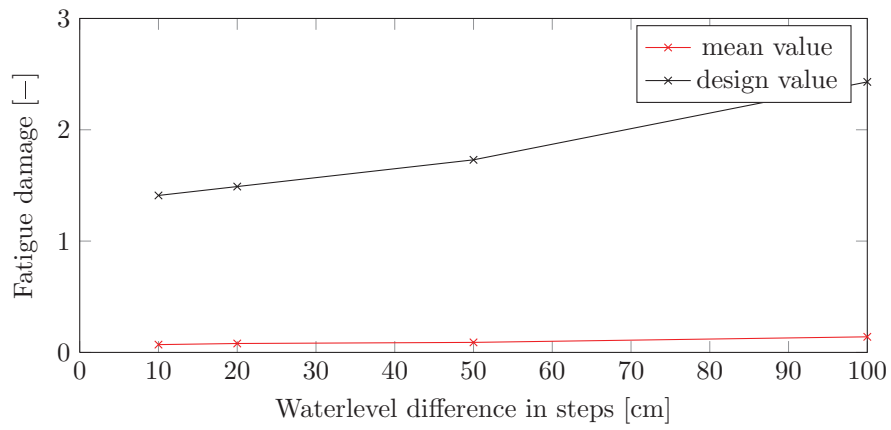


Figure 5.11: Sambeek old lock gate; mean value of EUROCODE

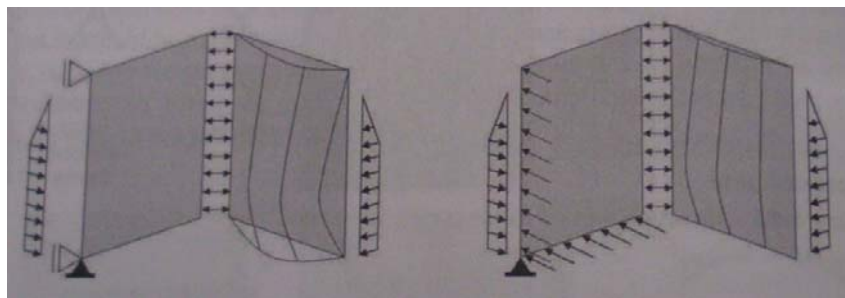


Figure 5.12: Forces and resulting deformation

Hydraulic Structures - Locks, March 2011, W.F. Molenaar

Chapter 6

Fatigue damage calculation

Case 2: Terneuzen

6.1 General information

This case is about the locks of Terneuzen. The locks of Terneuzen are located in the South-West of the Netherlands in the province Zeeland. The locks are located in the canal Gent-Terneuzen and form the link between the Westerschelde and the city Gent in Belgium. Figure 6.1 gives an overview of the lock complex of Terneuzen.

The middle lock was build in 1910. Due the increase in ship transport the capacity of the lock was insufficient and by the end of the sixties the build of two extra locks was finished, the East and West locks. The capacity of the lock are respectively 8.900 ship movements for the middle lock, 9.500 ship movements for the West lock and 14.000 ship movements for the East lock. The Middle and West locks consist of rolling gates and the West lock consists of mitre gates (two sets, namely ebb and flood mitre gates) as can be seen in Figure 6.2. The locks of Terneuzen are sea-going locks. This means that at one side of the locks the waterlevel is fluctuating during the day according to the tide. The other side, the upstream side, is in this case a relatively constant waterlevel. An example is given in Figure 6.3.

6.2 Waterlevel

As mentioned in the section with general information, the locks of Terneuzen are sea going locks. This means that one side of the locks are influenced by the (sea)tide. In this case the downstream side of the locks are located in the area of the Westerschelde where a sea tide occurs. As shown in Figure 6.3 the waterlevel downstream of the locks fluctuates from -2.00m NAP to +2.60m NAP over a period of 12h25min. The tide that occurs is always 12h25min. or 745 minutes. The maximum and minimum values of the peaks are not always the same, but fluctuate over time, at its lowest point from -2.30m NAP to -1.80m NAP and at its highest from +2.15m NAP to 2.60m NAP. An impression of the waterlevel over a period of 5 days is given in Figure 6.3 (even values of -3.13m NAP and +3.98m NAP are registered, resp. at 13th December 2008 and at the 9th November 2007).

From the database of Rijkswaterstaat measurements are available from 1945. Till 1970 every

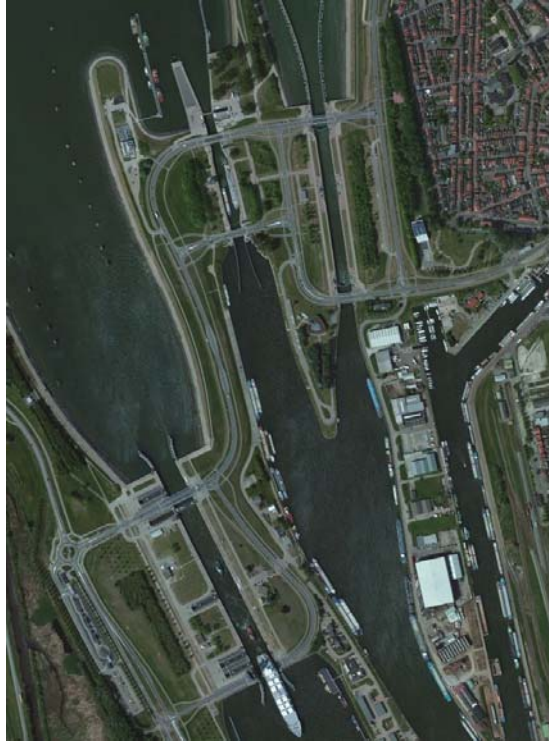


Figure 6.1: Overview of the locks of Terneuzen

**[image from bing.com/maps]*

3 hours a measurement was taken, from 1970 till 1986 every hour measurements have been taken and from 1986 till now every 10 minutes measurements have been taken. To get a precise waterlevel spectrum based on real waterlevel measurements, only the values with an interval of 10 minutes have been taken.

For the calculation of the waterlevel spectrum the waterlevel data from 2008 till 2012 are taken. The reason to take more years is to get a better average per year. It is possible that at some years higher values occur, therefore by using the data of multiple years a more accurate average can be determined. For the calculation of the waterlevel spectrum the number of data points have been counted per waterlevel spectrum. For example the number of data points have been calculated with a waterlevel difference step of 10cm. In this case the number of data points is counted from -3.13m NAP to -3.03m NAP over the 9 years, 5 data points were found. Dividing this value by the total number of measurement, 473.472, we have the percentage namely $1.0560 \cdot 10^{-5}$. Multiplying this percentage with the total number of ship levellings per year results in the number of ship levelling that take place between -3.13m NAP and -3.03m NAP. In Appendix D Table E.1 the total number of ship levellings have been calculated. The waterlevel-difference spectrum is shown in Figure 6.5. From this figure we can conclude that a large number of ship levelling occur at a waterlevel-difference of 350cm and at 30cm. There is a cut-off at +0m NAP. This is because only measurements have been taken till +2.13m NAP. Above this value the flood-lock gates are used and therefore this data is not taken into account.

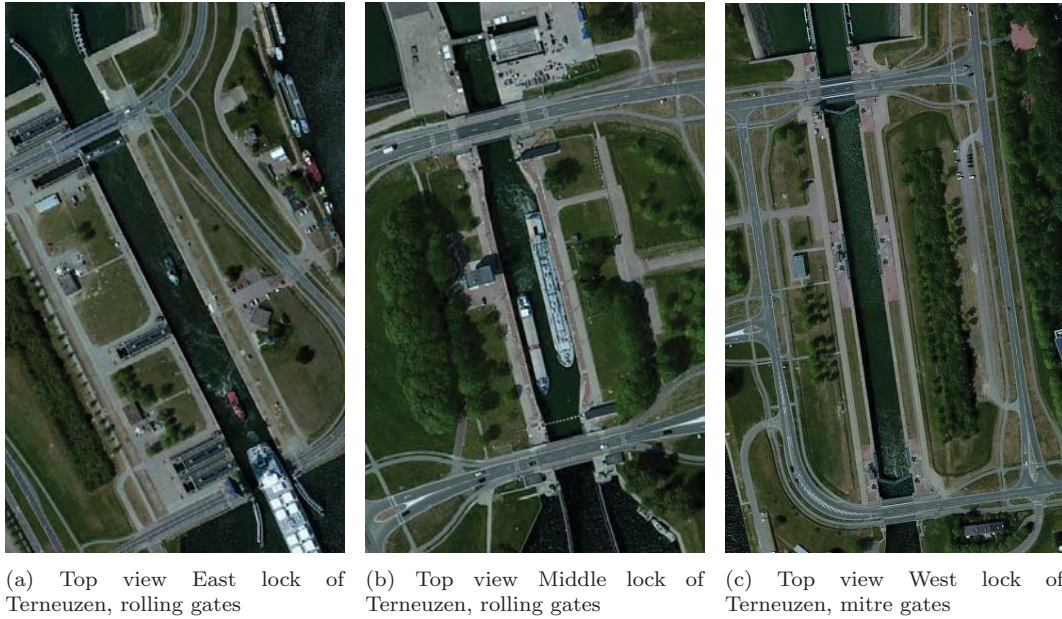


Figure 6.2: Overview of the three locks of Terneuzen

**[image from bing.com/maps]*

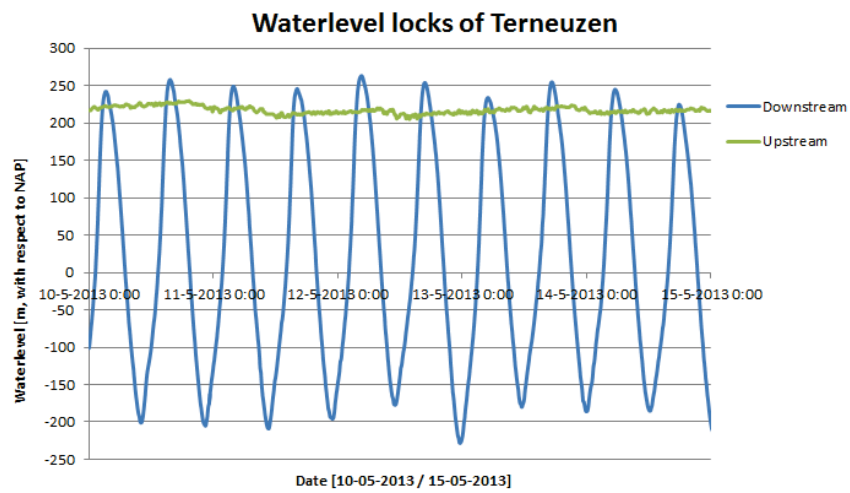


Figure 6.3: Waterlevel locks of Terneuzen

**[measurement from http://www.rijkswaterstaat.nl/geotool/waterhoogte_tov_nap.aspx]*

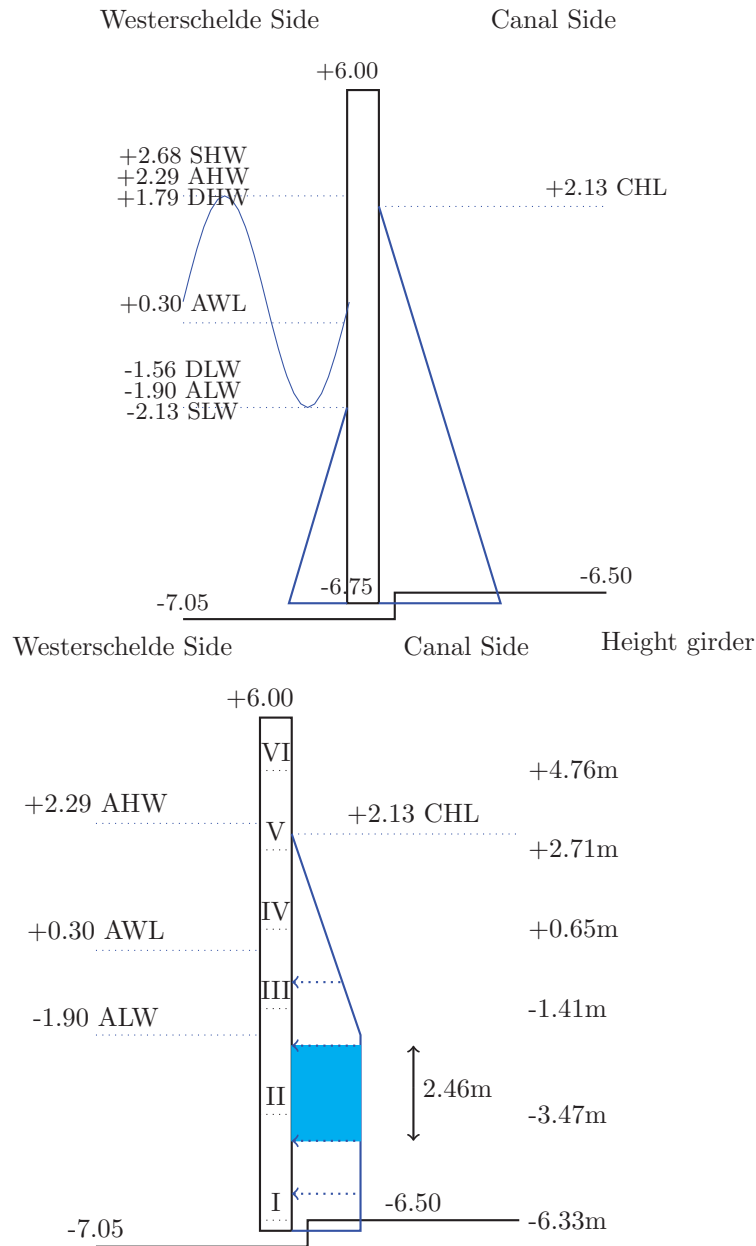


Figure 6.4: Schematic situation

*CHL = Canal Waterlevel, AHW = Average High Waterlevel, ALW = Average Low Waterlevel, SHW = Springtide High Waterlevel, SLW = Springtide Low Waterlevel, DHW = Deadtide High Waterlevel, DLW = Deadtide Low Waterlevel

6.3 Observed cracks

From the inspection reports on the East lock of Terneuzen a number of cracks have been found, for reference see Chapter 3 section 3.1.1. The cracks found in the lock gates of

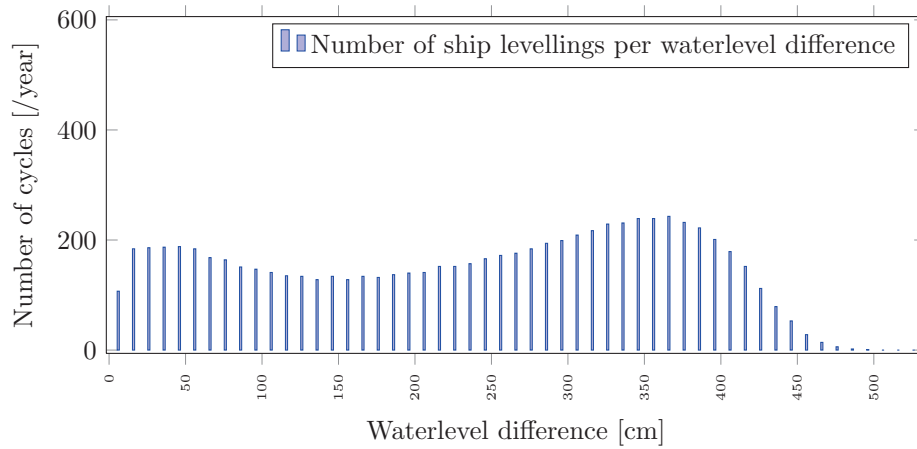


Figure 6.5: Terneuzen; Waterlevel level difference spectrum based on real measurements - steps of 10cm

Terneuzen are shown in Figure 6.6. The cracks have been found in the lower part of the lock gates at the corners and round-off radii of the connection between the horizontal and vertical girders. The cracks in the lower part of the lock gates are assumed to be caused by the ship levellings (waterlevel difference). Only in the lower part of the lock gate the force of the waterlevel difference is the highest, this can be seen in Figure 6.4. In the top part of the lock gates, cracks have been found at the location of the cylinder. The cracks could be caused by opening and closing the lock gates. When opening and closing the gates, high forces of the cylinder are subjected to this part of the gates.

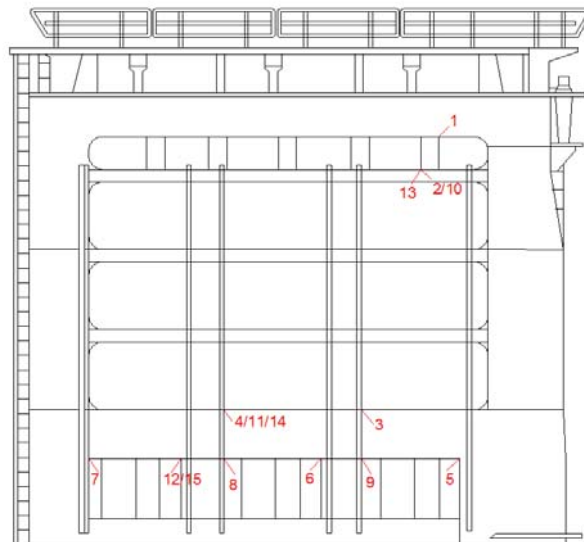


Figure 6.6: Terneuzen; Position of cracks in lock gate



Figure 6.7: Terneuzen; Image front view lock gate

**image from www.google.nl/maps streetview Terneuzen locks.*

The cracks in the upper right part of the lock gate near the hinge are assumed to be from the piston forces from opening and closing the gates. At this part of the lock gate the piston is mounted, this can be seen in the image of Figure 6.7. As mentioned in Chapter 3 the lock gates of Terneuzen were opened with a waterlevel difference of 35cm. Opening the lock gates with a waterlevel difference will give the pistons a higher force (waterlevel difference results in an opposite direction force on the pistons), which results in higher forces at the location of the pistons.

6.4 Fatigue damage East lock gates

This section gives an overview of the fatigue damage calculation for the East lock gates. Table 6.1 lists the different parameters for the calculation of the fatigue damage. The fatigue damage calculation is based on the Eurocode 3 NEN-EN 1993-1-9.

The life span that is used in the calculation for the lock gates is 43 years, $T_{year} = 43$ year. In total 14.000 ship levellings took place each year, in one direction a value of 60% is used, namely $N = 8.400$ levellings per year. The detail can be compared with detail category 40 of Table 8.3 and 8.4 of NEN-EN 1993-1-9 Figure 6.9. For the section modulus a value of $W = 21.688 \cdot 10^6 \text{ mm}^3$ is used, this value is taken from the design report page 9. For the gravitational force $g = 9.81 \text{ m/s}^2$ is used.

Description	Sign	Value	Unit
Service life	T_{year}	43	year
Number of levellings	N	8400	per year
Detail category	$\Delta\sigma_C$	40	[-]
Partial factor for fatigue resistance	γ_s	1.00	[-]
Stress concentration factor	γ_c	1.0	[-]
Section modulus	W	$21.688 \cdot 10^6$	mm^3
Effective width	h_q	2.46	m
Length lock gate	L	12.743	m
Density water	ρ_{water}	1025	kg/m^3
Gravitational force	g	9.81	m/s^2

Table 6.1: Terneuzen; Input values for the East lock gates

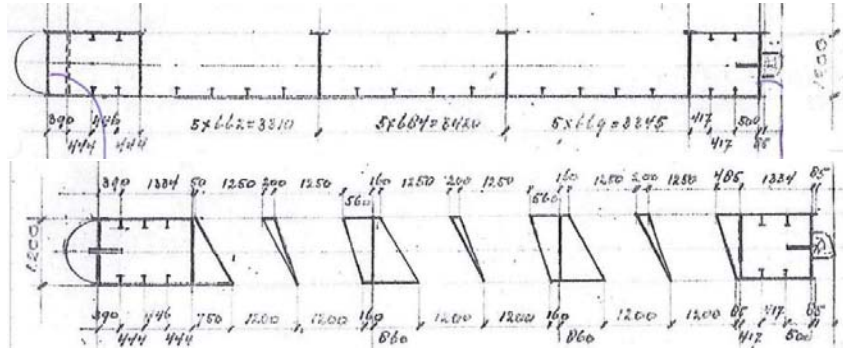


Figure 6.8: Overview of the cross-section of the locks of Terneuzen

6.4.1 Detail category

The characteristic value of the fatigue strength of the detail is based on the stress direction and the typical connection where the cracks have occurred. From the observation it was clear that cracks have occurred at sharp corners and round-off radii in the vertical and horizontal girders. The stresses in the girder at the connection are parallel and perpendicular

to the welds. This is also shown in section 3.1.1. The fatigue damage calculation of the real waterlevel spectrum is based on the NEN-EN 1993-1-9. The typical connection of the cracks found is compared with detail 40 of Table 8.3 and 8.4, the detail category can be seen in Figure 6.9. The detail category states $\Delta\sigma_R = 40 \text{ N/mm}^2$ at $2 \cdot 10^6$ cycles.

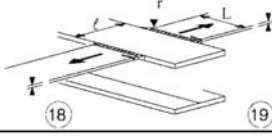

40		18) Stompe las in dwarsrichting bij kruisende flenzen. 19) Met overgangsstralen volgens tabel 8.4, detail 4	Details 18) en 19) De vermoeingssterkte van de doorgaande component moet zijn getoetst via tabel 8.4, detail 4 of detail 5.
(a) Cracks in weld perpendicular and parallel to stress direction			
40		5) Gelast, zonder overgangsroning.	
(b) Cracks in weld perpendicular and parallel to stress direction			

Figure 6.9: *Detail category 40 of table 8.3 and 8.4, NEN-EN 1993-1-9

For the calculation the mean value of the fatigue strength of the detail needs to be calculated. In Appendix A Figure A.9 the scatter data of this detail category 40 is presented. From this scatter plot a mean value is calculated as shown in Figure A.9. From this mean value a new slope and detail category is calculated. The new detail category states $\Delta\sigma_R = 74.65 \text{ N/mm}^2$ at $2 \cdot 10^6 \text{ N/mm}^2$ with a slope of $m = 3.4602$.

6.4.2 Fatigue damage

The stress calculation is based on equations 2.1, 2.2, 2.6, 2.3, 2.5 and 2.8. From the waterlevel-difference the distributed force is calculated. This force is directly used in the moment equation and equation to determine the stresses. In the structure there is a normal force present. This normal force is at the neutral axis (for reference see Figure 6.8) of the structure and there this force does not contribute to the moment in the structure. With equations 4.4, 4.5 and 4.5 the fatigue damage is determined.

As mentioned in section B.1 the choice of the correct load spectrum is of high importance. For the fatigue damage calculation of the lock of Terneuzen different waterlevel steps have been used. Steps of 10, 20, 50 and 100cm have been used to see how large the influence is of the fatigue damage.

A calculation of one step waterlevel difference can be found in Appendix C section C.2.

Figure 6.10 represents the total number of cycles over 43 year per waterlevel difference. Figure 6.11 represents the stress in the cross-section per waterlevel difference. Figure 6.12 represents the influence of the fatigue damage per waterlevel difference. From the last figure we can conclude that the relative high number of cycles at +30cm have (almost) no influence on the fatigue. The largest contribution to the fatigue damage is from the waterlevel difference of +3.50m. In Figure 6.13 the red line represents the fatigue damage of the old lock gate based on the mean value of the scatter plot of the experiments. From this figure we can conclude that the calculated fatigue damage is below the value of 1. From the section

Observations it can be concluded that cracks have occurred in the lock gate. Therefore it is expected that the fatigue damage value should be higher (> 1) than the calculated value in Figure 6.13.

The conclusion is that the observed fatigue damage cannot be predicted with the simplified model used for this fatigue damage calculation. A number of aspects could be the reason for this.

The schematisation of the lock gate was too simplified. The moments due to torsional, as result of the deformation according to Figure 5.12, have not been taken into account. Due to torsional moments the stress will increase and therefore the value of the fatigue damage will increase. Also the assumption made in Figure 2.20 might be too conservative. The torsional force in the lock gate due to opening with a waterlevel difference is also probably not that simple modelled. Higher waterlevels due to waves which results in higher stresses also influence the fatigue damage negatively.

The influence of maintenance is also not taken into account. When (almost) no or poor maintenance is performed on the lock gates, a number of aspects could result in lower fatigue damage values. A poor state of the wooden sealing at the bottom (which results in different torsional moments in the lock gate) can contribute to other or higher stresses in the lock gate. Also the state of the coating layer is not taken into account. Over the year the coating layer gets brittle and no longer protects the full surface of the lock gates. This gives a negative influence on the S-N curve. The lock gates are subject to salt water conditions. As mentioned in the chapter about fatigue, the influence of salt water also has a negative influence on the S-N curve. The maintenance of the cathodic protection system can also contribute a negative influence on the S-N curve. When the cathodic protection system is not performing optimal, due to poor maintenance, a lower value of the S-N curve should be used.

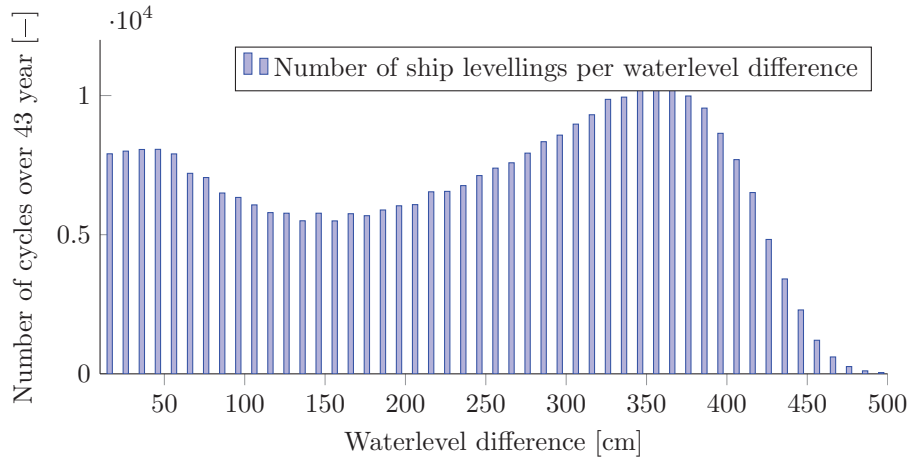


Figure 6.10: Terneuzen East lock gates; Waterlevellevel difference spectrum

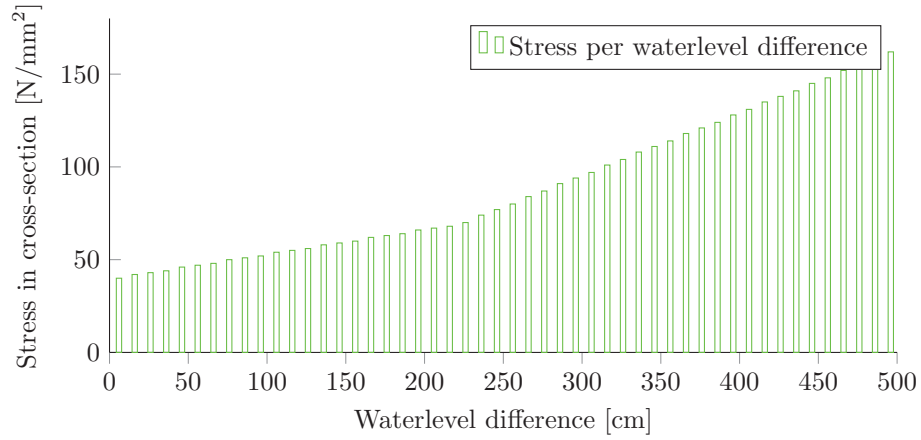


Figure 6.11: Terneuzen East lock gate; Stresses per waterlevel difference

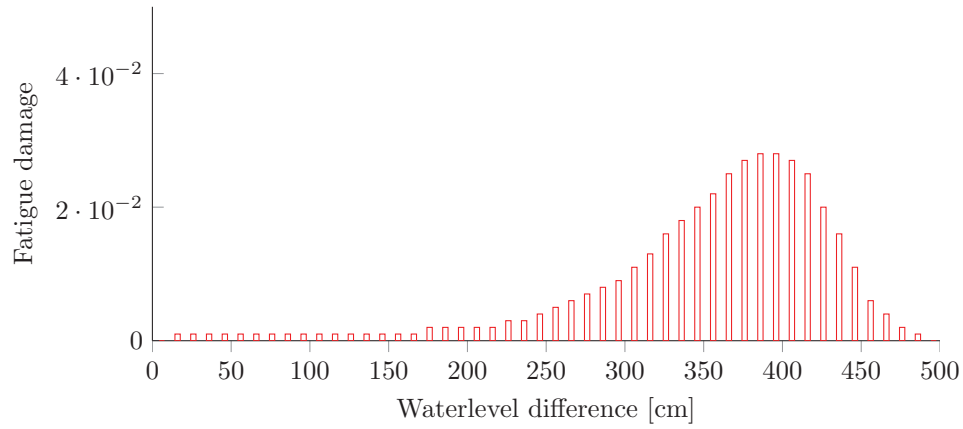


Figure 6.12: Terneuzen East lock gates; Fatigue damage per waterlevel difference

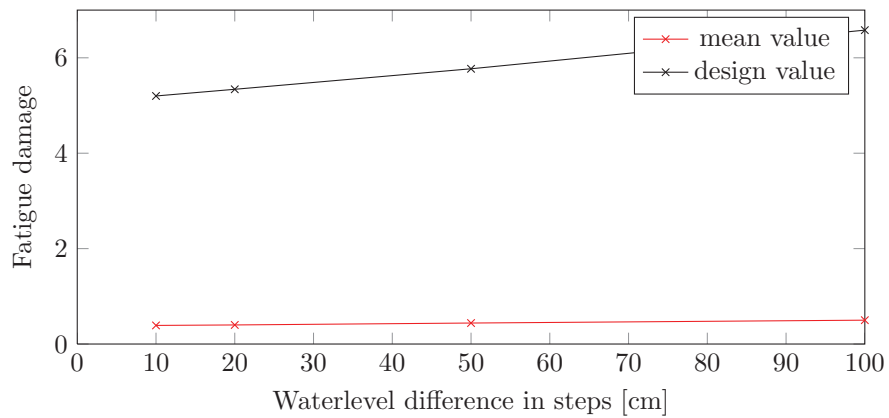


Figure 6.13: Terneuzen East lock gates; mean value and characteristic value

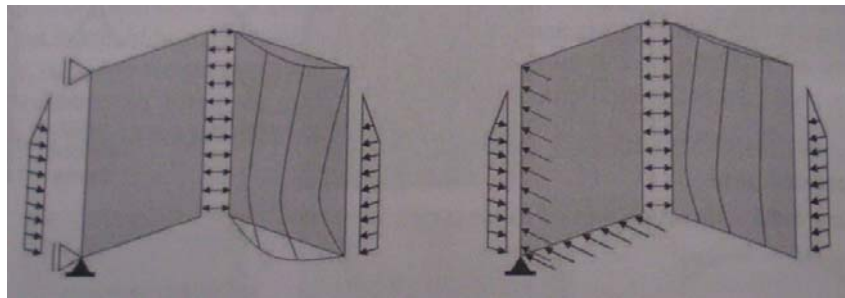


Figure 6.14: Forces and resulting deformation

Hydraulic Structures - Locks, March 2011, W.F. Molenaar

Chapter 7

New prediction model - Waterlevel spectrum based on average waterlevels

As mentioned in the previous chapter and in Appendix B it is important to construct a correct waterlevel spectrum. In this chapter a new model is presented based on the average waterlevels, that could be used if no waterlevel measurements are available.

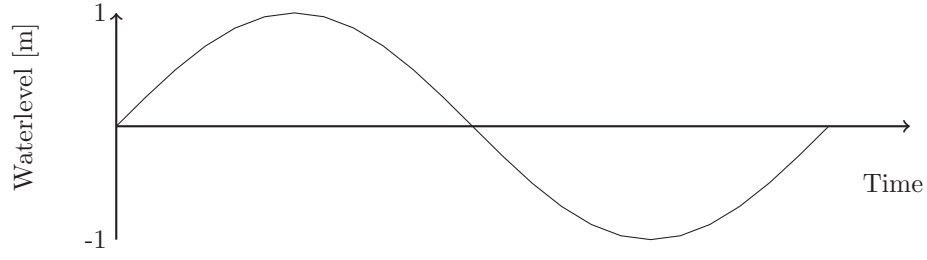
7.1 New prediction model

If no measurements are available and a waterlevel spectrum needs to be made, it is difficult to estimate the contribution of each step. The scope of this chapter is to create a model from waterlevel data (like the average waterlevel), that represents the waterlevel spectrum from real measurements. This model could be used to create a waterlevel spectrum for sea going locks.

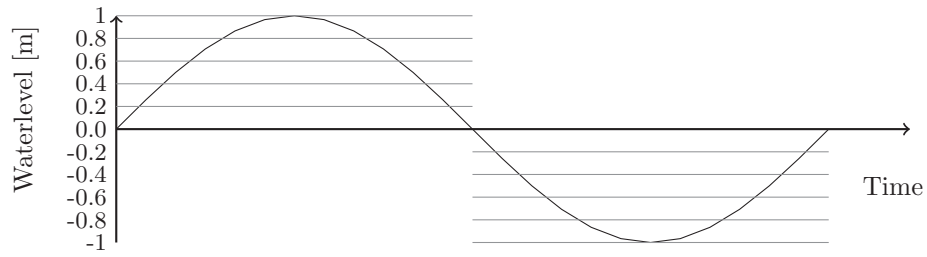
To determine the waterlevel downstream we simplify the real waterlevel to an equivalent waterlevel in the form of a sinus shape as shown in Figure 7.1a. To determine the contribution of the different waterlevel steps, the shape is divided into parts. In Figure 7.1b the waterlevel is split up into parts of 20cm; it could also be split up into smaller parts like 10cm or larger parts in the range of 40cm to 100cm (1m). In Figure 7.1c the contribution of the different parts is marked up in red. From this Figure can be concluded that the contribution of the part from 0.8m to 1.0m has the highest period, compared to the other parts. This period gives the longest time where ship levellings could occur. The size of the contribution of the different parts can be calculated by taking the time period of the different parts and dividing them over the total tide time.

Writing this shape function into a formula, we take the standard equation of a sinus and shape it into the correct function to calculate the contribution of the different steps. The equation of the sinus shape can be written as:

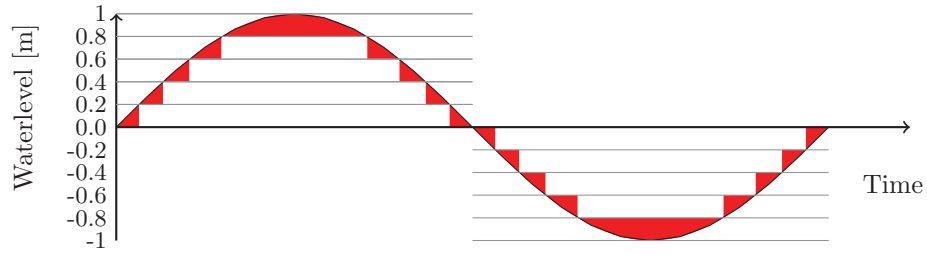
$$y = A \cdot \sin(x) \tag{7.1}$$



(a) Sinus shape function, comparable with the waterlevel of the Westerschelde



(b) Sinus shape function; divided into phases



(c) Sinus shape function; contribution of the different phases

Figure 7.1: Waterlevel Westerschelde transforming into sinus function

Writing this equation into a form that represents the waterlevel we change the variable into input variable. Equation 7.1 can be rewritten as:

$$H_w = h_{shift} + A \cdot \sin\left(\frac{2\pi}{P} \cdot x\right) \quad (7.2)$$

where:

H_w	=	Waterlevel (with respect to NAP)	[m]
h_{shift}	=	Shifted average in vertical direction	[m]
A	=	Amplitude	[m]
x	=	Time	[min]
P	=	Period (in this case 745min)	[-]

For the calculation of the contribution (time) we have to rewrite the equation in the form of T. This equation becomes:

$$T_i = \frac{P}{\pi} \left(\arcsin \left(\frac{Hw_{i+1} - h_{shift}}{A} \right) - \arcsin \left(\frac{Hw_i - h_{shift}}{A} \right) \right) \quad (7.3)$$

where Hw_{i+1} and Hw_i represent the waterlevels. These waterlevels are calculated by taking the waterlevel difference from the maximum and minimum waterlevel and divide this in $1/n$ steps, for $i = 1..n$.

This new prediction model is calibrated on the locks of Terneuzen. The next section gives an overview of the calculation.

7.2 Test Case; Terneuzen

The new prediction model is tested on the locks of Terneuzen. Before the calculation a number of assumptions is made. The waterlevel upstream is relatively constant and therefore it can be assumed to be +2.13m NAP (the same value as used in the calculation of measurements in the previous chapter). As input variables for equation 7.3, three different types have been used: spring tide, average tide and dead tide. Figure 7.2 represents the waterlevel spectrum based on measurements.

<i>Tide</i>	<i>HW level [cm]</i>	<i>LW level [cm]</i>
Average tide	229	-190
Spring tide	268	-213
Dead tide	179	-156

Table 7.1: Terneuzen; Waterlevels of the different tides

*HW level = High waterlevel, LW level = Low water level

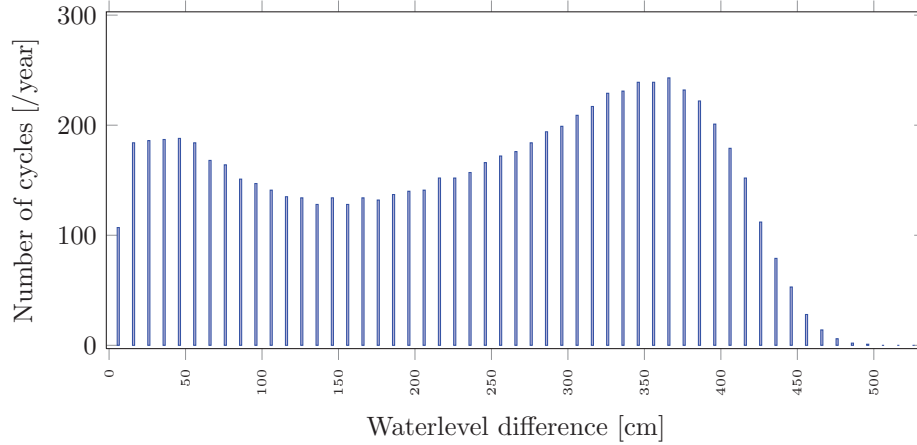


Figure 7.2: Terneuzen; Waterlevel difference spectrum based on real measurements - steps of 10cm

7.2.1 Calculation of the frequency

In this section the calculation of one of the steps of the new prediction model is shown. The values are based on the spring tide model.

The vertical shift which represents the nominal line can be written as:

$$h_{shift} = \frac{268 - (-213)}{2} + 213 = 27.5cm$$

The amplitude equation can be written as:

$$A = 268 - h_{shift} = 268 - 27.5 = 240.5cm$$

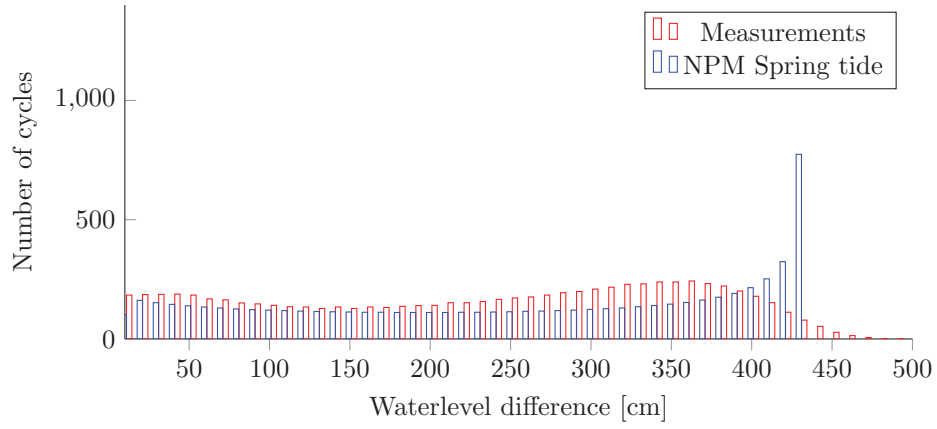
The period of step -213cm NAP to -203cm NAP is calculated using the following equation:

$$T_i = \frac{745}{\pi} \left(\arcsin \left(\frac{-203 - (-27.5)}{240.5} \right) - \arcsin \left(\frac{-213 - (-27.5)}{240.5} \right) \right) = 69min$$

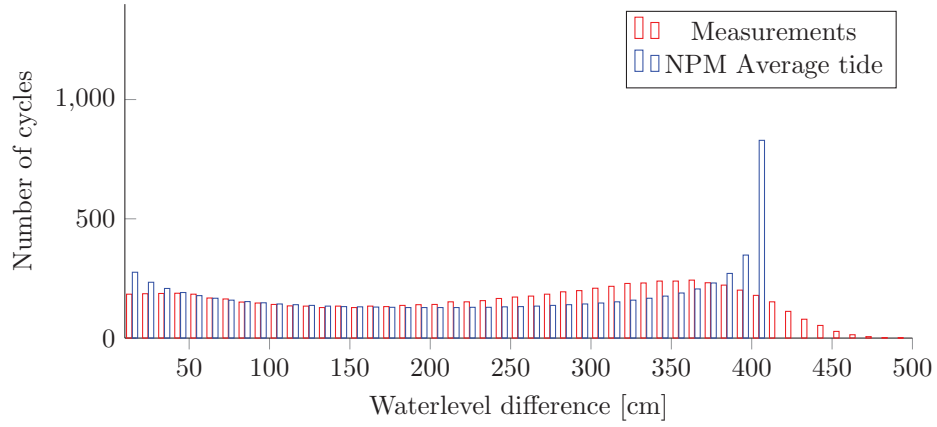
Dividing this time with the total time (745min), results in the percentage of this period ($69/745 = 0.0926$). Multiplying this percentage with the total number of levellings per year, the number of ship levellings is computed between -213cm NAP and -203cm NAP ($0.0926 \cdot 8400 = 774$).

The waterlevel spectra of the three different tides are presented in Figure 7.3. The blue bars represent the waterlevel spectrum from the three tides and the red bars represent the waterlevel spectrum based on measurements.

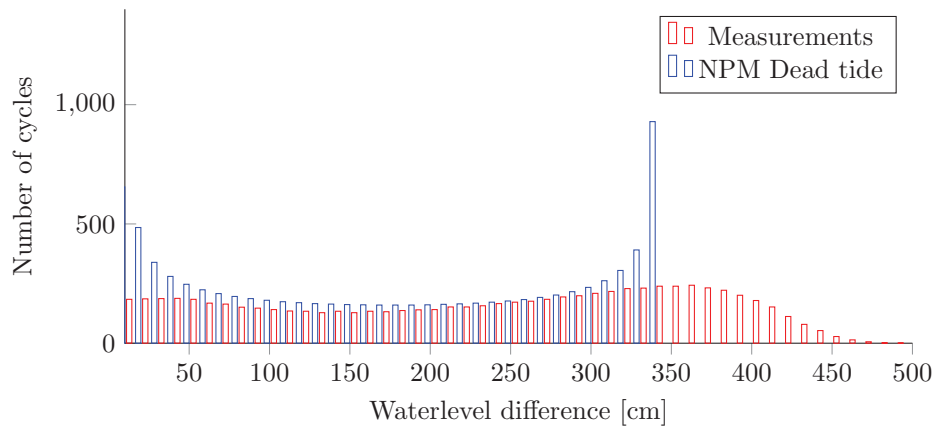
From the figure it can be concluded that with these three tides, a fatigue damage calculation can be made. The next section gives the results of the calculations.



(a) Terneuzen; Waterlevel difference spectrum based on spring tide



(b) Terneuzen; Waterlevel difference spectrum based on average tide



(c) Terneuzen; Waterlevel difference spectrum based on dead tide

Figure 7.3: Waterlevel difference spectrum based on different tides, in blue the new model spectrum and in red spectrum from measurements

7.2.2 Fatigue Damage

For the calculation of the fatigue damage, the input parameter of the cross-section is used from the previous chapter, section 6.4, Table 6.1. In the previous two chapters the conclusion of the fatigue damage was that with the manual calculation no accurate values can be computed. This chapter is about how to determine a waterlevel spectrum when no measurements are available. Therefore the fatigue damage values are indicative.

As mentioned in section B.1 the choice of the correct load spectrum is of high importance. For the fatigue damage calculation of the lock of Terneuzen different waterlevel steps have been used. Steps of 10, 20, 50 and 100cm have been used to see how large the influence is of the fatigue damage.

In Figure 7.4 the green line represents the dead tide, the black line the average tide, the red line the spring tide and the blue line represents the fatigue damage value of the real measurements. From this figure it can be concluded that the fatigue damage based on the different tides does not present sufficiently accurate values.

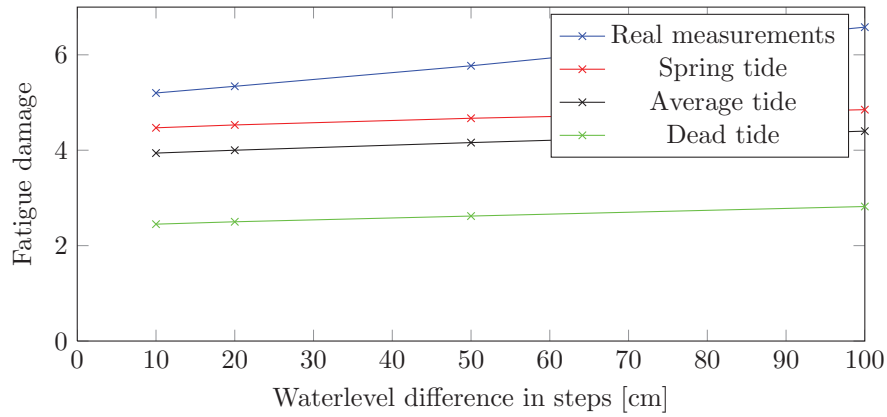


Figure 7.4: Terneuzen East lock gates; different tides based on characteristic values without partial factor for the fatigue resistance

Figure 7.5 shows a period of 1 year (2008) where the waterlevel of the Westerschelde and the spring tide is presented. From this figure it can be concluded that a part of the waterlevel; below the spring tide waterlevel, is not taken into account in the fatigue damage calculation. This can also be seen in Figure 7.6. Figure 7.6 also shows the part of the waterlevel difference between 250cm and 380cm, which has a major contribution to the fatigue damage value. The function of the new prediction model needs to be adjusted. Adding an adjusting factor γ_w to the waterlevel height of equation 7.3 should lead to a better fatigue damage value. Because the waterlevel height is adjusted, the amplitude also will change.

By tweaking (increasing) the value γ_w the fatigue damage will change. The value representing the fatigue damage of the measurement at best is $\gamma_w = 1.12$. The new fatigue damage contribution is presented in Figure 7.7. In this Figure the part of the blue bar that exceeds the red bars, between 200cm and 420cm is about the same as the red bar exceeds the blue bar between 420cm and 460cm. Although the shape of the red bars do not follow the shape of the blue bar, the summation of the fatigue damage is about the same.

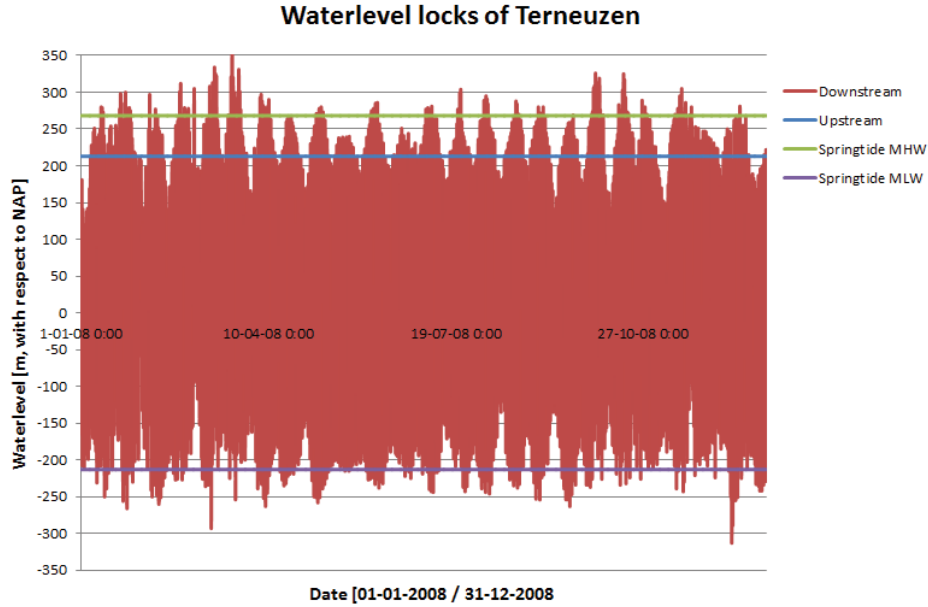


Figure 7.5: Waterlevel based on measurements compared with spring tide average

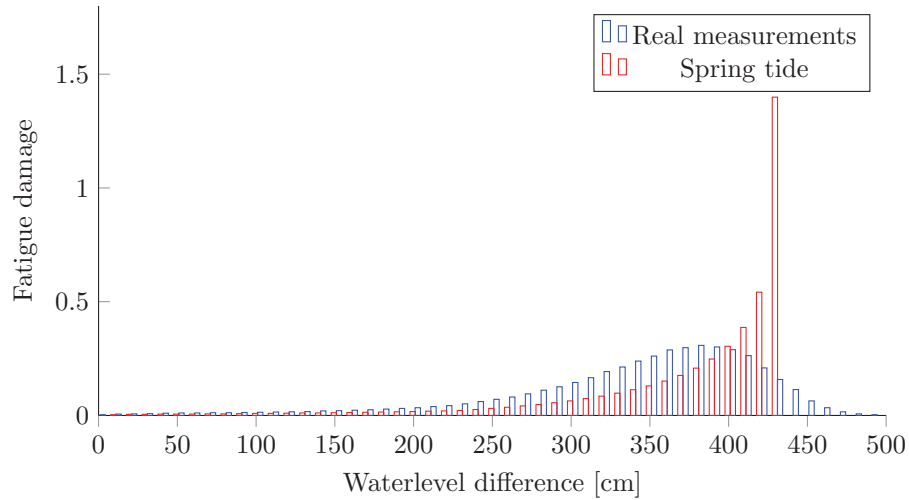


Figure 7.6: Terneuzen East lock gates; Fatigue damage contribution per waterlevel difference

The fatigue damage values are presented in Figure 7.8. A remark can be made about the new prediction model. The fatigue damage values are only valid when using waterlevel steps till 20cm. Above 20cm the fatigue damage values do not match with the fatigue damage values of the real measurements. The reason why the fatigue damage values with steps larger then 20cm do not match is because the shape of the curves do not match perfectly. In the new prediction model an assumption is made that the tide height does not change over the year (always spring tide), where in reality there are different tides (average tide, dead tide). This new prediction model could be used to produce a waterlevel spectrum when no

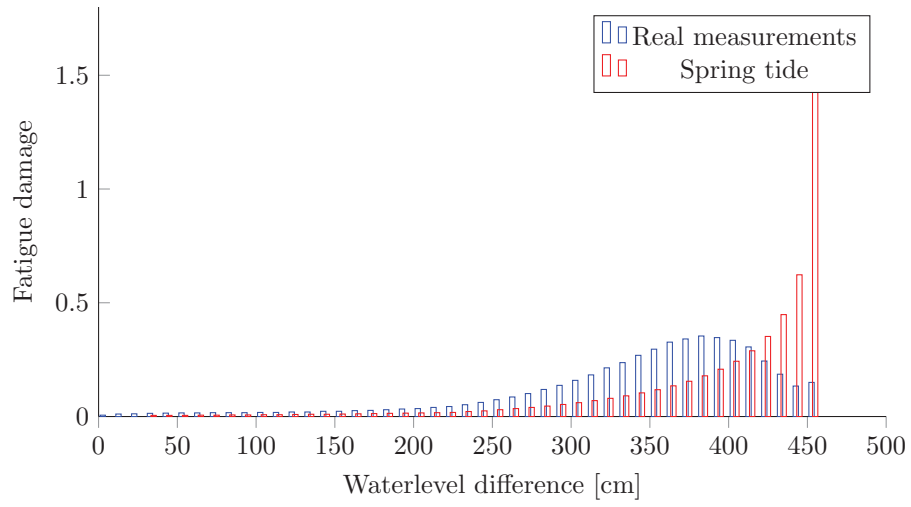


Figure 7.7: Terneuzen East lock gates; Fatigue damage contribution per waterlevel difference

waterlevel measurements are available.

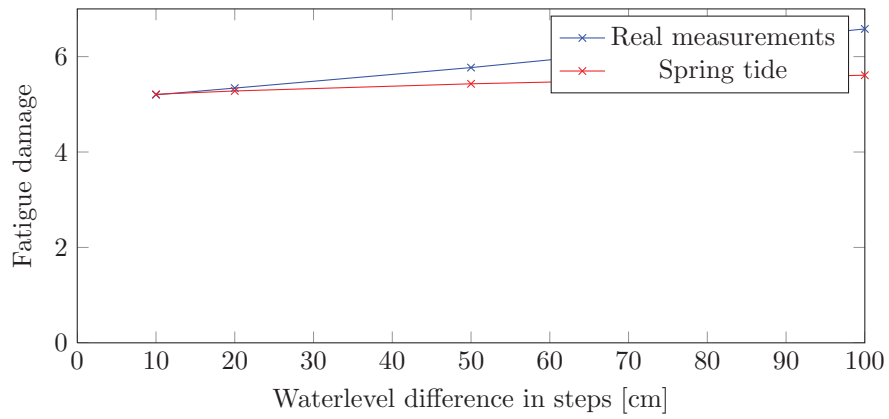


Figure 7.8: Terneuzen East lock gates; Fatigue damage values of Real measurements and Spring tide

Chapter 8

Conclusion and recommendations

8.1 Conclusion

As mentioned in the introduction, on a number of lock gates (mitre gates) cracks have been found. Based on experience and an evaluation of the photos from the inspections, it is assumed that the cracks occur from fatigue. From this hypothesis two research questions were made.

8.1.1 Cause of the fatigue cracks

The first objective of this thesis is to provide information about the cause of these fatigue cracks.

The conclusion is that the observed fatigue damage cannot be predicted with the simplified model used for the fatigue damage calculations. A number of aspects could be the reason for this.

Calculation model

The schematisation of the lock gate was too simplified. The moments due to torsional, as result of the deformation according to Figure 5.12, have not been taken into account. Due to torsional moments the stress will increase and therefore the value of the fatigue damage will increase. The torsional force in the lock gate due to opening with a waterlevel difference is also probably not that simple modelled. Higher waterlevels due to waves also contribute to higher stresses and influence the fatigue damage negatively.

Maintenance state of the lock

The influence of maintenance is also an important aspect. When (almost) no or poor maintenance is performed on the lock gates, a number of aspects could result in lower fatigue damage values. A poor state of the wood (sealing) at the back post or at the bottom can contribute to other or higher stresses in the lock gate. Also the state of the coating layer is not taken into account. Over the year the coating layer gets brittle and no longer protects the full surface of the lock gates. This gives a negative influence on the S-N curve. Some lock gates are subject to salt water conditions. The influence of salt water also has a negative

influence on the S-N curve. The maintenance of the cathodic protection system can also contribute to a negative influence on the S-N curve. When the cathodic protection system is not performing optimal, due to poor maintenance, a lower value of the S-N curve should be used.

8.1.2 Waterlevelspectrum

The second objective of this thesis is to provide knowledge needed for computing a waterlevel difference spectrum with the available data (measurements of the waterlevels) of Rijkswaterstaat.

By using the measurements of the waterlevel from the database of Rijkswaterstaat a waterlevel difference spectrum can be computed. The calculation itself is simple to do and gives good result. The spectrum can be determined with steps of 10, 20, 50 and 100cm.

The fatigue damage calculation with these different steps gives different values. It is clear that using waterlevel difference steps of 100cm results in the largest fatigue damage values. This large step could lead to a calculation that is too conservative. The optimum of the waterlevel steps would be between 20cm and 50cm. The step of 20cm gives an increase (compared to using steps of 10cm) of the fatigue damage value of 3%. Where using steps of 50cm results in an increase of about 12%. Although there are many uncertainties in the initial fatigue damage calculation, using a value of 20 cm would give accurate enough results.

8.2 Recommendations

From the conclusions some recommendation can be made. The fatigue damage calculated with a simplified model can not determine correct fatigue damage values. Therefore a FEM-model should be used to determine the stresses in the lock gate. A second recommendation is to monitor the stresses in the lock gate it self. A lock gate, e.g. Terneuzen, could be fitted with strain gauges to determine the real stresses in the lock gate. These real stresses could then be compared with the result of the FEM-model and could confirm the reliability of the FEM-model.

A second recommendation that can be made is to do research on the influence of the salt and fresh water conditions on lock gates with or without cathodic protection. The standard *DNV* already describes lower S-N curves, due to the influence of water. It is recommended to also include rules in the EUROCODE 3 on the influence of salt and fresh water.

Bibliography

- [1] Assesment of existing steel structures, remaining fatigue life, paper.
- [2] Corrosionist. Shielded metal arc welding. [http://www.corrosionist.com/shielded_metal_arc_welding_\(smaw\).htm](http://www.corrosionist.com/shielded_metal_arc_welding_(smaw).htm).
- [3] J. A. Ewing and J.C. Humfrey. *The Fracture of Metals under Repeated Alternations of Stress*. Phil. Trans. Roy. Soc., 1903.
- [4] W. Fairbairn. *Experiments to Determine the Effect of Impact, Vibratory Action and Long-Continued Change of Load on Wrought Iron Girders*. Phil. Trans. Roy. Soc., 1843.
- [5] P. J. E. Forsyth. *A Two-Stage Process of Fatigue Crack Growth*. 1961.
- [6] Heijmans. Hoofdberekening stalen puntdeuren oostsluizen. Technical report, Heijmans.
- [7] E. A. Hodgkinson. *Report of the Commissioners Appointed to Enquire into the Application of Iron to Railway Structures*. H.M.S.O Command Paper No. 1123, 1849.
- [8] IV-INFRA. Aanvullend onderzoek oostsluis terneuzen (54e-001-01) uitgangspunten. Technical report, IV-INFRA.
- [9] IV-INFRA. Analyserapport staalbouw - oostsluis terneuzen (54e-001-01). Technical report, IV-INFRA.
- [10] IV-INFRA. Rink: Iv-infra opnieuw het beste aanbod. <http://www.iv-groep.nl/nl/nieuws/131-nieuws-ivinfra/121-rink-iv-infra-opnieuw-het-beste-aanbod.html>, Februari 2013.
- [11] NEBEST. Schade-inventarisatie drielingsluis maasbracht. Technical report, NEBEST.
- [12] NEBEST. Sluis sambeek-midden inspectie 7. Technical report, NEBEST.
- [13] W. Rankine. *On the cause of unexpected breakage of the Journals of Railway Axles*. Proc. Inst. Civil Engrs, 1843.
- [14] Rijkswaterstaat. *Design of Locks - Part 1*. Bouwdienst Rijkswaterstaat, first edition, 2000.
- [15] Rijkswaterstaat. Datatabel iq fase 2a v20.xls, January 2013.
- [16] Rijkswaterstaat. Rijkswaterstaat organisation. http://www.rijkswaterstaat.nl/en/about_us/, Februari 2013.

- [17] Rijkswaterstaat. Scheepvaartinformatie hoofdvaarwegen : editie 2009. <http://www.rijksoverheid.nl/documenten-en-publicaties/rapporten/2009/08/01/scheepvaartinformatie-hoofdvaarwegen-editie-2009.html>, Februari 2013.
- [18] Rijkswaterstaat. Vaarwegenoverzicht. http://www.rijkswaterstaat.nl/water/feiten_en_cijfers/vaarwegenoverzicht/, Februari 2013.
- [19] Schijve. *Fatigue of structures and materials*. Springer Science+Business Media B.V., second edition, 2009.
- [20] W. Uijttewaal. Eulerse balansen. Technical report, TUDelft.
- [21] Det Norske Veritas. Nen-en 1993-1-9+c2; eurocode 3: Design of steel structures - part 1-9: Fatigue, September 2012.
- [22] A. Wholer. *Tests to Determine the Forces Acting on Railway Carriage Axles and the Capacity of Resistance of the Axles*. 1871.
- [23] Youtube. Riveting at hays street bridge.

Appendix A

Tables and Figures

Tabel 3.1 — Aanbevolen waarden voor de partiële factoren voor de vermoeiingssterkte

Beoordelingsmethode	Gevolgen van het bezwijken	
	Gering	Groot
Schade-tolerant	1,00	1,15
Veilige-levensduur	1,15	1,35

Figure A.1: Recommended partial safety factors for fatigue strength

Figure A.2: Example of a free hinge, old lock gate of Sambeek

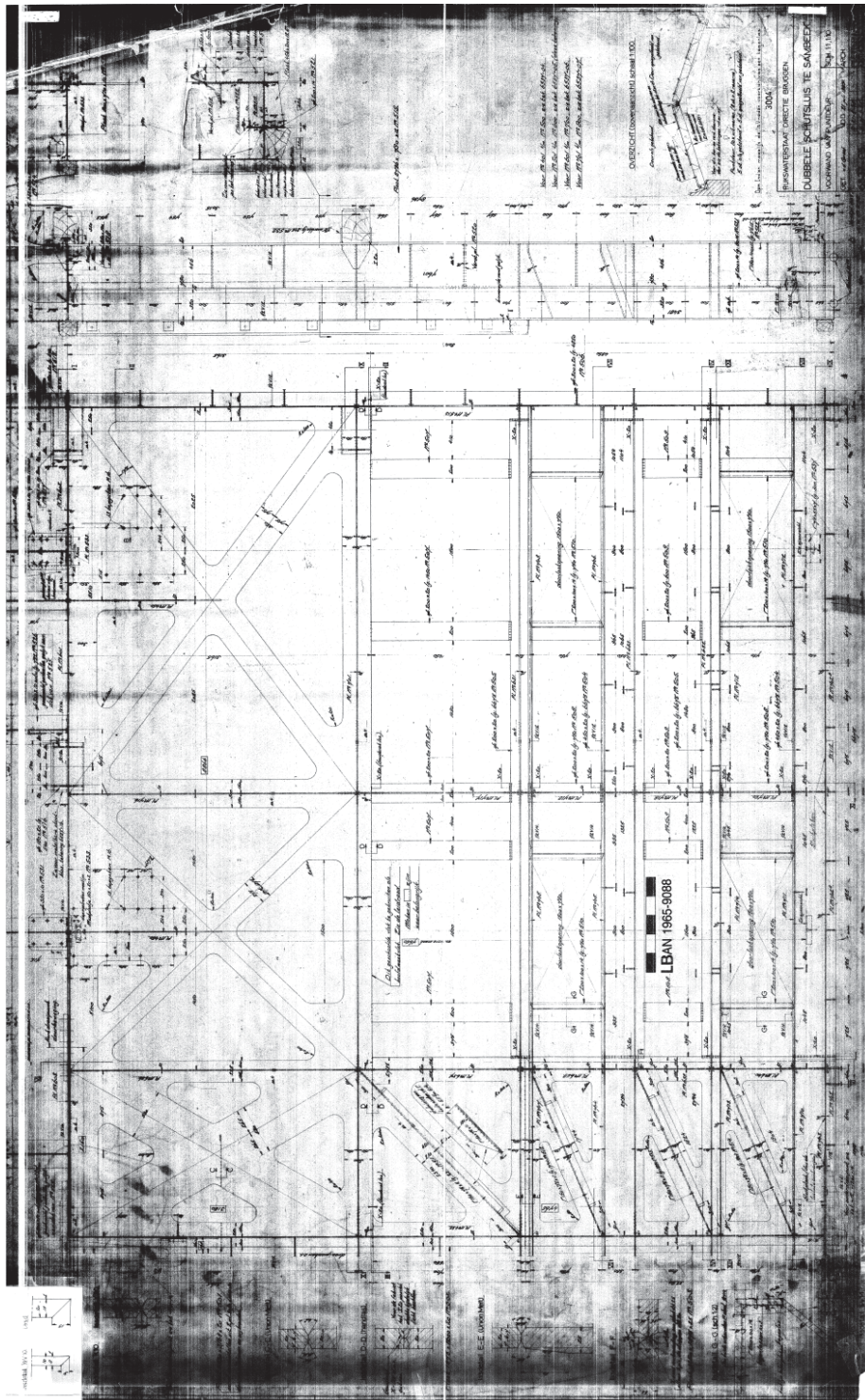


Figure A.3: Front view en cross-section old lock gate Sambeek

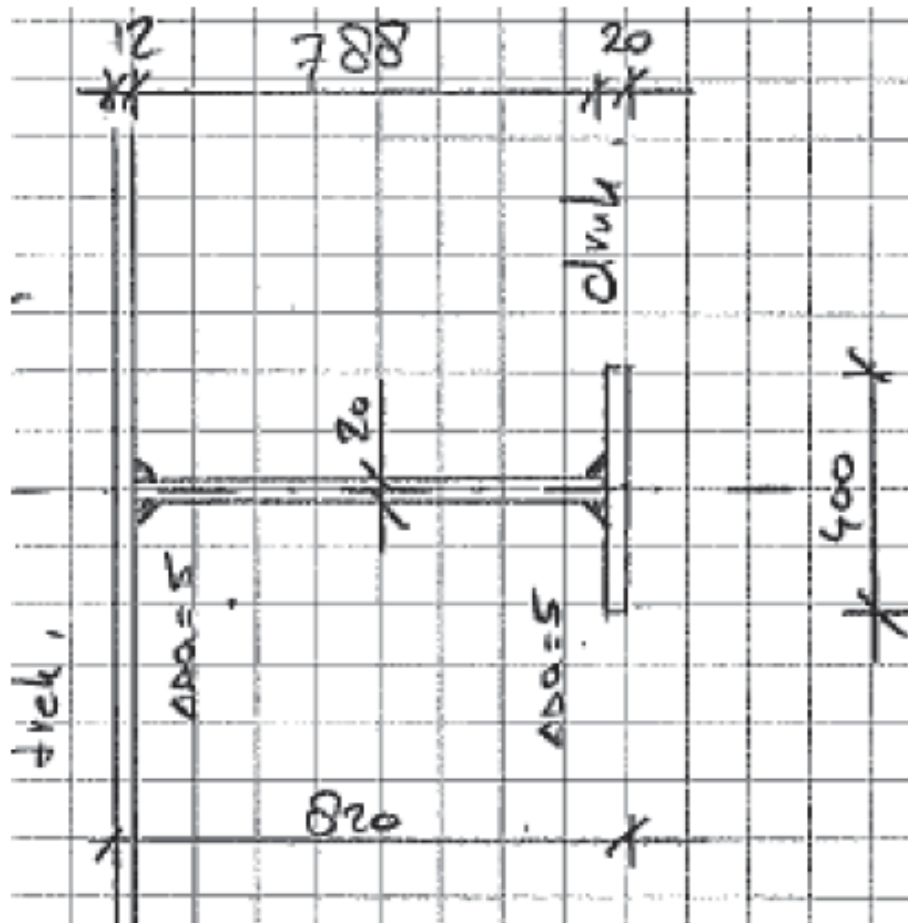


Figure A.5: Front view en cross-section new lock gate Sambeek

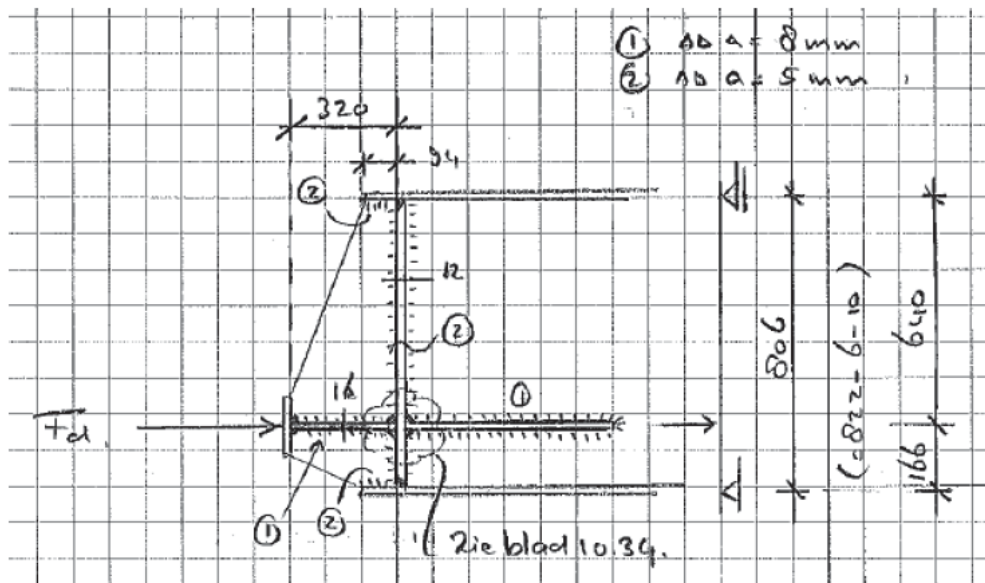


Figure A.6: Cross-section new lock Sambeek, eccentricity

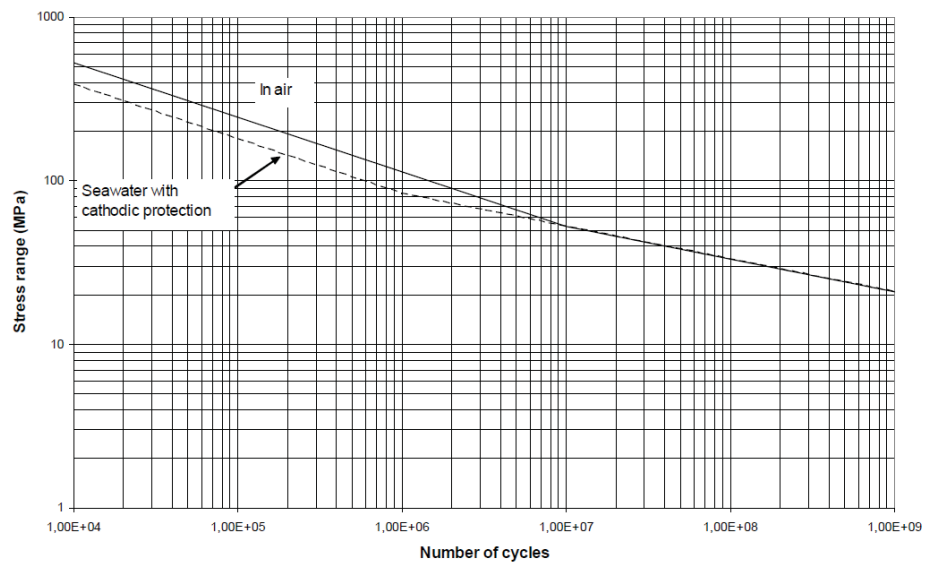
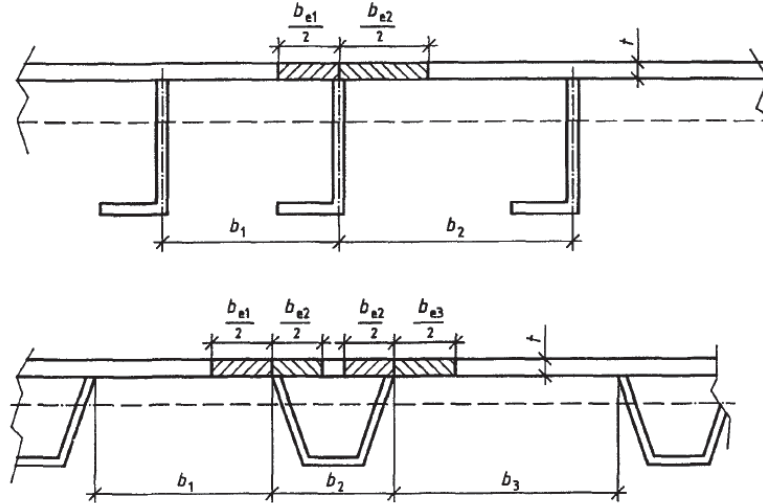


Figure A.7: DNV-RP-C203: Fatigue Design of Offshore Steel Structures

13.3 Geometrie van de verstijvingen

Bij het bepalen van de doorsnede grootheden van de verstijvingen moet gerekend zijn met het verstijvingsprofiel zelf tezamen met de meewerkende gedeelten van de te verstijven plaat (zie figuur 32).



Figuur 32 - Verstijvingen

Voor de meewerkende breedte b_e van een op druk belast plaatveld moet zijn aangehouden:

$$b_e = 1,33 t \sqrt{\frac{E_d}{f_{y,d}}} \leq b \text{ voor een vierzijdig scharnierend opgelegd plaatveld;} \quad (13.3-1)$$

$$b_e = 0,43 t \sqrt{\frac{E_d}{f_{y,d}}} \leq b \text{ voor een driezijdig scharnierend opgelegd plaatveld met één vrije langsrand;} \quad (13.3-2)$$

Figure A.8: Equation of the effective width according to NEN 6771 13.3

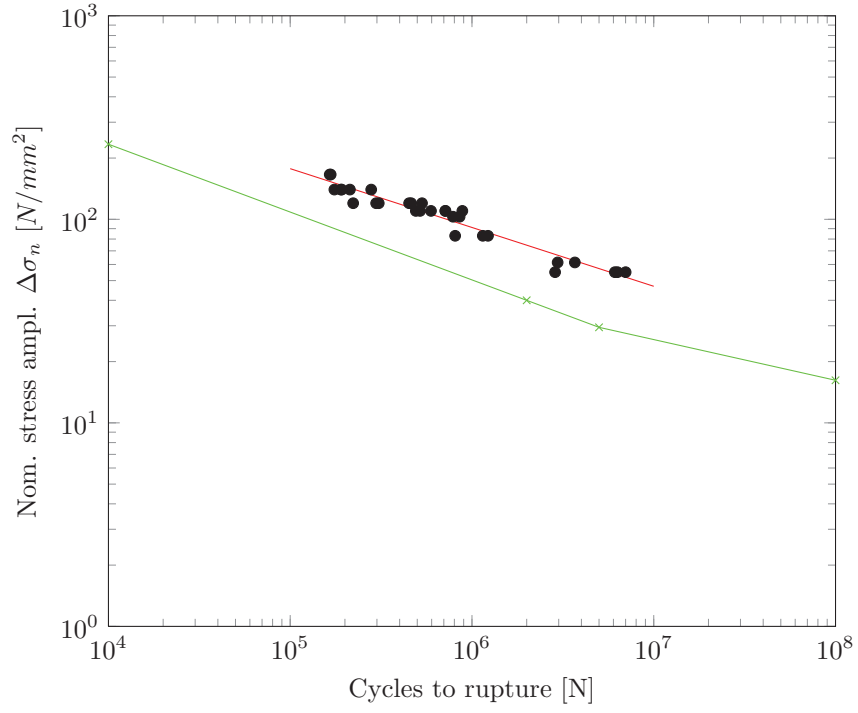


Figure A.9: Eurocode 3 S-N curve background document, data from experiments

The redline describes the mean value of the scatter. The value of the fatigue strength based on the scatter is 74.65 N/mm^2 at $2 \cdot 10^6$ cycles with a slope $m = 3.4602$. The green line indicated the characteristic value of the fatigue strength of 40 N/mm^2 at $2 \cdot 10^6$ cycles.

Appendix B

Examples fatigue calculation

B.1 Example calculation sensitivity

The fatigue damage is usually presented in a table to get an impression which part of the stress-spectrum has the most influence on the fatigue damage. In the next examples three different cases have been explained. For simplification we assume a fictitious number of 250 cycles in total and the stresses at the different waterlevels.

B.1.1 Example 1

Example 1 is loaded with 5 different waterlevel-differences according to Figure B.1. For simplification I have taken 5 fictitious stresses and number cycles according to the given values in Figure B.1.

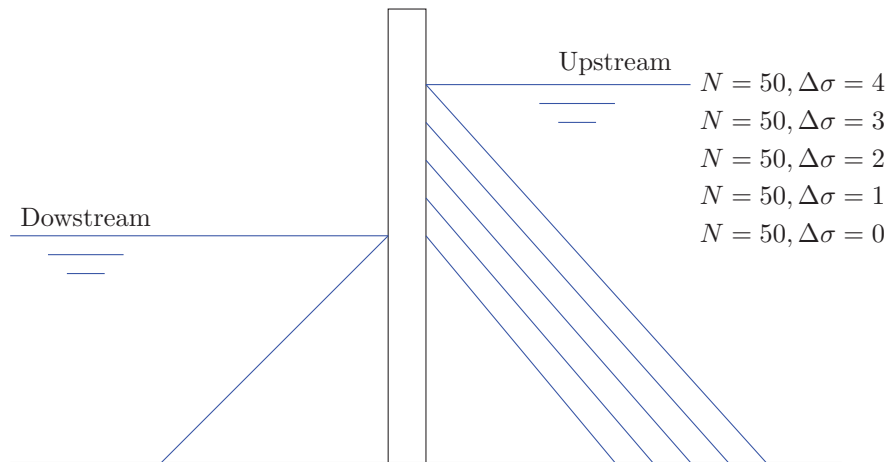


Figure B.1: Example 1: Load spectrum

For the calculation of the fatigue damage we use Equation 4.4, where N_{Ri} can be calculated with expression:

$$N_{Ri} = \left(\frac{\Delta\sigma_C}{\Delta\sigma_R} \right)^m \cdot N_{1,2} \quad (\text{B.1})$$

where:

- N_{Ri} = is the durability (in number of cycles) [-]
- $\Delta\sigma_C$ = the fatigue strength of the detail (in this example we assume a constant) [N/mm^2]
- $\Delta\sigma_R$ = the stress range [N/mm^2]
- m = slope in the S-N curve (in this example we assume a constant) [-]
- $N_{1,2,3}$ = Number of cycles of the part of the slope (in this example we assume a constant) [-]

By filling Equation B.1 into Equation 4.4 and rewriting we have the following expression:

$$D_d = \sum_{i=1}^n \frac{n_{Ei} \cdot (\Delta\sigma_R)^m}{(\Delta\sigma_C)^m \cdot N_{1,2,3}} \quad (\text{B.2})$$

In Equation B.2 the *denominator* is set as a constant en the *numerator* is the variable part depending on the stress and cycles of the load spectrum. The fatigue damage of the load spectrum of Figure B.1 is presented in Table B.1.

Stress spectrum			Fatigue strength		
Block	$\Delta\sigma_R$	N	m	N_R	N/N_R
0	0	50	3	-	$0 \cdot *C$
1	1	50	3	-	$50 \cdot *C$
2	2	50	3	-	$400 \cdot *C$
3	3	50	3	-	$1350 \cdot *C$
4	4	50	3	-	$3200 \cdot *C$
Damage					$5000 \cdot *C$

Table B.1: Example 1: Fatigue damage

$$*C = \frac{1}{(\Delta\sigma_C)^m \cdot N}$$

From Table B.1 we can see that the contribution of the largest stress, $\Delta\sigma_R = 4$, gives the largest influence on the fatigue damage. This is also to prove by Equation B.2. In the nominator the stress range is to the power m, $(\Delta\sigma_R)^m$, which implies that the the largest the stress range at the same cycles have the most influence on the fatigue damage.

B.1.2 Example 2

Now the same example as Figure B.1 is taken but now the number of blocks is been reduced to three, the total number of cycles stays the same (250) but is now distributed over the three block which gives each block 84 cycles . This can be seen in Figure B.2.

The same calculation now is made as in Example 1. The results are presented in Table B.2. From Example 1 the fatigue damage is increased with 20%. The reason for this increase is the contribution of the largest stress. Because the cycles of the largest stress range is increased, the contribution is now also increased.

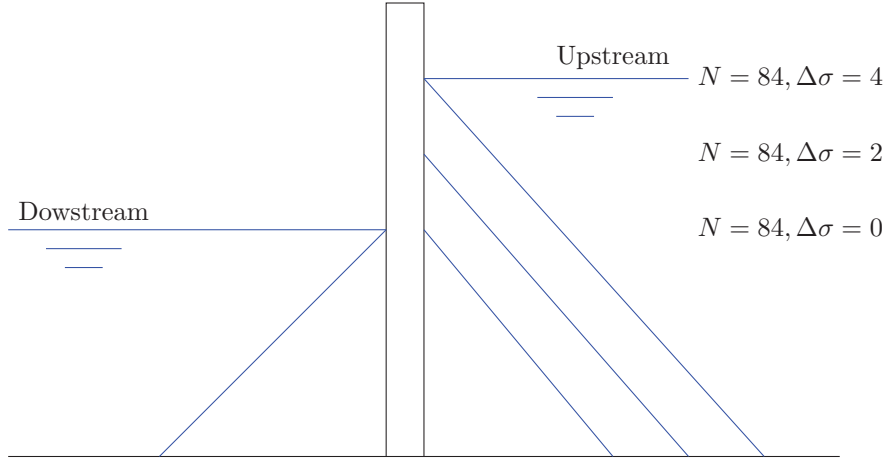


Figure B.2: Example 2: Load spectrum

Stress spectrum			Fatigue strength		
Block	$\Delta\sigma_i$	N	m	N_R	N/N_R
0	0	84	3	-	$0 \cdot *C$
2	2	84	3	-	$672 \cdot *C$
4	4	84	3	-	$5376 \cdot *C$
Damage					$6048 \cdot *C$

Table B.2: Example 2: Fatigue damage

$$*C = \frac{1}{(\Delta\sigma_C)^m \cdot N}$$

B.1.3 Example 3

A third Example is now threaded based on Figure B.1. In this case we assume that there is only one block with the total number of cycles as the summation of all the block in Example 1, 250 cycles. This can be seen in Figure B.3.

The same calculation now is made as in Example 1. The results are presented in Table B.3.

Stress spectrum			Fatigue strength		
Block	$\Delta\sigma_i$	N	m	N_R	N/N_R
2	2	250	3	-	$2000 \cdot *C$
Damage					$2000 \cdot *C$

Table B.3: Example 2: Fatigue damage

$$*C = \frac{1}{(\Delta\sigma_C)^m \cdot N}$$

Comparing the results from Example 3 of the results from Example 1 the fatigue damage is now decreased with 60%. The reason for this decrease is the contribution of the largest stress. Because now the stress range is halved, the contribution to the fatigue damage is

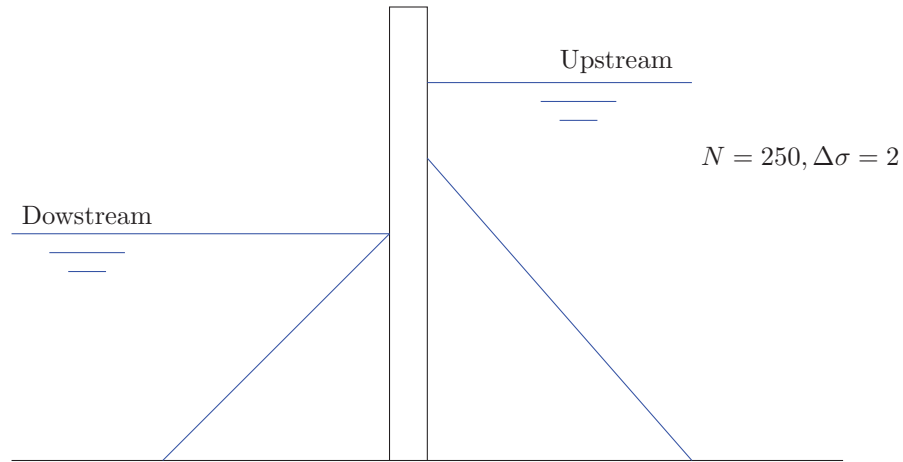


Figure B.3: Example 3: Load spectrum

now less than in Example 1.

For the calculation of the fatigue damage it is of importance that a correct load spectrum is used. In the next chapters two different cases will be treated. The first case consists of the locks of Sambeek. This is a lock in the River the Maas, the waterlevels have a daily value but fluctuates over the year. The second case consists of the locks of Terneuzen. This is a lock that lies in the west of the Netherlands in the Westerschelde, the waterlevel has daily fluctuation.

B.2 Fatigue damage; NEN 2063 - RINK Report

This section gives an overview of the fatigue damage calculation according to the RINK report. Table B.4 gives an overview of the different input parameters for the calculation of the fatigue damage. The life span that is taken of the lock gates is from 1968-2011, namely $N_{year} = 43$ year. In total 14.000 ship levellings take place a year, in one direction a value of $N = 7000$ levellings per year is taken. The detail category is compared with detail 501 of type 5 connection of the NEN 2063 as can be seen in Figure ?? In this case the detail category has a $\Delta\sigma_R = 30 \text{ N/mm}^2$. For the section modulus a value of $W_{backside} = 21.688 \cdot 10^6 \text{ mm}^3$ is taken, this values is calculated in the original design-report, page 9. For the gravitational force $g = 9.81 \text{ m/s}^2$ is taken.

Description	Sign	Value	Unit
Life span	N_{year}	43	year
Number of levellings	N	7000	per year
Detail category	$\Delta\sigma_C$	30	N/mm^2
Section modulus	$W_{backside}$	$21.688 \cdot 10^6$	mm^3
Effective width	b_{eff}	2.46	m
Length lock gate	L_{gate}	12.743	m
Gravitational force	g	9.81	m/s^2

Table B.4: Terneuzen RINK; Input values

B.2.1 Detail category

The characteristic value of the fatigue strength of the detail is based on the stress direction and the typical connection where the cracks have occurred. From the observation is was clear that cracks have occurred at sharp corners and round-off radii if the vertical and horizontal girders. The stresses in the girder at the connection are parallel and perpendicular to the welds. This is also shown in section 3.1.1. The fatigue damage calculation in the RINK report is based on the NEN 2063. The typical connection of the founded cracks is compared with detail 501 of type 5 connection of the NEN 2063, the detail category can be seen in Figure ?. The detail category states $\Delta\sigma_R = 30 \text{ N/mm}^2$ at 10^7 cycles.

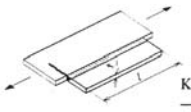
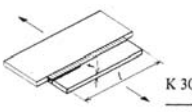
nr.	omschrijving	$\Delta\sigma_y$	$\Delta\sigma_z$	$\Delta\tau_{zy}$
501	Lassen zonder spleet Plaat met recht- hoekige beëindiging $l \leq 10 t$ $l > 10 t$	 K 35 K 30	 K 30* K 30	K 30 K 30

Figure B.4: Cracks in weld perpendicular and parallel to stress direction

*Detail 501 of type 5 connection, NEN 2063 Arc-welding

B.2.2 Waterlevel spectrum

The calculation in the RINK reports states that the waterlevel upstream does not fluctuates very much so an average waterlevel of +2.13m is taken. For the waterlevel downstream two scenarios have been investigated. The first scenario states that there is a fixed waterlevel at -1.90m NAP where 7000 ship levellings take place. The second scenario states that 50% of the 7000 ship levellings take place at -1.90m NAP and the other 50% takes place at +0.30m NAP (AWL). An overview of the situation can be seen in Figure 6.4.

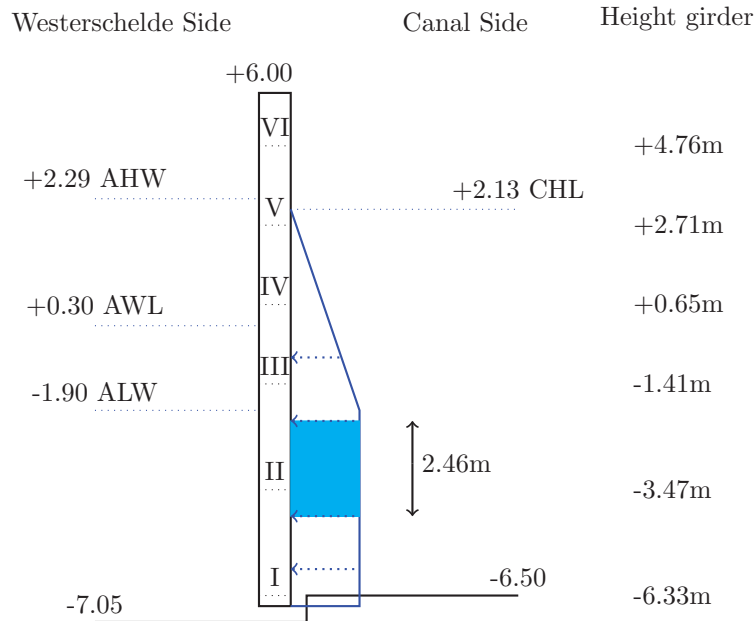


Figure B.5: Schematic situation

*CHL = Canal Waterlevel, AHW = Average High Waterlevel, ALW = Average Low Waterlevel

Figure B.5 shows an simplified overview of the situation. In this case on the left side an waterforce is taken from ALW and on the rights an waterforce of CHL is taken. Figure B.5 shows the resulting waterforce on the lock gate. From this figure it is clear that only the lower part of the lock gate is subjected to the highest waterforce. Because the bottom of the lock gate can touch the bottom rule by bending of the gate, this girder is not interesting to calculate. From girder III and above the waterforce reduces to zero, so the only interesting girder to be checked is the second girder. In the RINK report the second girder is checked.

B.2.3 Fatigue damage

The stress calculation is based on equations 2.1, 2.2, 2.6, 2.3, 2.5 and 2.8. From the waterlevel-difference the distributed force is calculated. This force is directly used in the moment equation and equation to determine the stresses. With equations 4.4, 4.5 and 4.5 the fatigue damage is determined.

The fatigue damage of scenario is calculated as following:

The distributed force on the second horizontal girder can be calculated by taken the water-level difference multiplied by the density and gravitational force. This can be written as:

$$q = (CHL - (-ALW)) \cdot \rho_{water} \cdot g$$

$$q = (2.13 - (-1.90)) \cdot 1.025 \cdot 9.81 = 41.3kN/m^2$$

The representative distributed force can be calculated by multiplying the distributed force with the height. This can be written as:

$$q_{rep} = b_{eff} \cdot q$$

$$q_{rep} = 2.46 \cdot 41.3 = 101.6kN/m^1$$

In this case the the representative distributed force is multiplied with a safety factor $\gamma = 1.25$. This can be written as:

$$q_d = \gamma \cdot q_{rep}$$

$$q_d = 1.25 \cdot 101.6 = 127.0kN/m^1$$

Calculating the maximum moment in the girder is simplifying the girder as a beam on two supports. The moment can be calculated with $\frac{1}{8} \cdot q_d \cdot L^2$. This can be written as:

$$M_d = \frac{1}{8} \cdot q_d \cdot L_{gate}$$

$$M_d = \frac{1}{8} \cdot 127.0 \cdot 12.743 = 2578kNm$$

The maximum stress in the girder is calculated by dividing the moment by the section modulus. This can be written as:

$$\Delta\sigma_{i,backwall,d,GLW} = \frac{M_d}{W_{backside}}$$

$$\Delta\sigma_{i,backwall,d,GLW} = \frac{2578 \cdot 10^6}{21.688 \cdot 10^6} = 118.9N/mm^2$$

For the fatigue damage the following equation are used:

$$N_i = \left(\frac{\Delta\sigma_k}{\Delta\sigma_i} \right)^m \cdot N_{1,2}$$

$$N_i = \left(\frac{30}{118.9} \right)^3 \cdot 10^7 = 1.61 \cdot 10^5$$

The fatigue damage be calculated according to:

$$D = \frac{n_i}{N_i}$$

$$D = \frac{43 \cdot 7000}{1.61 \cdot 10^5} = 1.87$$

<i>Stress spectrum</i>			<i>Fatigue strength</i>		
<i>Block</i>	$\Delta\sigma_i$	N	m	N_R	N/N_R
1	118.9	$3.01 \cdot 10^5$	3	$1.61 \cdot 10^5$	1.87
Damage					1.87

Table B.5: Terneuzen RINK; Fatigue damage, steps of 10cm , 100% ship levellings at ALW

*ALW = Average Low Waterlevel

The calculated value is presented in a Table B.5. The fatigue damage number of 1.87 is higher than the allowable 1. So this calculation shows that fatigue will occur. From perspective point this calculation is very conservative because not all ship levellings take place at the maximum average low waterlevel. This same calculation is also been done in a the second scenario.

The ship levelling are spread to 50% ship levellings at ALW and 50% at the average waterlevel of +0.30m NAP. The stress at AWL is lower, this value is calculated as $\Delta\sigma_i = 53.8 \text{ N/mm}^2$. The new fatigue damage is calculated. The values are given in table B.6.

<i>Stress spectrum</i>			<i>Fatigue strength</i>		
<i>Block</i>	$\Delta\sigma_i$	N	m	N_R	N/N_R
1	118.9	$1.51 \cdot 10^5$	3	$1.61 \cdot 10^5$	0.94
2	53.8	$1.51 \cdot 10^5$	3	$1.73 \cdot 10^6$	0.09
Damage					1.03

Table B.6: Terneuzen RINK; Fatigue damage, steps of 10cm, 50% ship levellings at ALW, 50% ship levellings at AWL

*ALW = Average Low Waterlevel, AWL = Average Waterlevel

Comparing these fatigue damage calculation with each other it is clear that the by changing the waterlevel spectrum from 1 spectrum into two spectrum the fatigue damage almost reduces by half. It is of importance that the prediction of the waterlevel spectrum should be as close as possible to the real waterlevel spectrum.

Appendix C

Fatigue damage calculations of case 1 and case 2

C.1 Fatigue damage calculations of case 1

This section gives an overview of the fatigue damage calculation of case 1. One waterlevel difference is chosen that contributes the most to the fatigue damage. In this case the waterlevel of 328cm contributes the most to the fatigue damage value.

Distributed load closed position:

$$q_d = \rho g \Delta h \cdot h_q$$
$$q_d = 1.0 \cdot 9.81 \cdot 3.28 \cdot 0.875 = 28.15 kN/m$$

Moment due to distributed load:

$$M_{dist} = \frac{1}{8} q_d L^2$$
$$M_{dist} = \frac{1}{8} \cdot 28.15 \cdot 8.9 = 278.77 kNm$$

Distributed load after opening:

$$q_d = 1.0 \cdot 9.81 \cdot 0.10 \cdot 0.875 = 0.86 kN/m$$

Moment just after opening:

$$M_{dist} = \frac{1}{8} \cdot 0.86 \cdot 8.9 = 8.50 kNm$$

Total resulting waterforce on the cross-section:

$$F_W = \rho g A \Delta h$$

$$F_W = 1.0 \cdot 9.81 \cdot (0.875 \cdot 8.9) \cdot 3.18 = 251 kN$$

Normal force in the cross-section

$$F_N = \frac{F_W}{2 \cdot \tan(\alpha)}$$

$$F_N = \frac{251}{2 \cdot \frac{1}{3}} = 376 kN$$

Moment due to the normal force

$$M_{nor,force} = -F_N \cdot e$$

$$M_{nor,force} = -376 \cdot 0.215 = -112 kNm$$

Stress in the cross-section:

$$\sigma = \left(\frac{M}{W} \right) + \left(\frac{F_N}{A} \right)$$

$$\sigma = \left(\frac{278.77}{4416438} + \frac{8.50}{4416438} - \frac{-112}{4416438} \right) + \left(\frac{376}{18136} \right) \cdot 10^{-3} = 71.22 N/mm^2$$

Number of cycles to lifetime:

$$N_{Ri} = \left(\frac{\Delta \sigma_C}{\Delta \sigma_i} \right)^m \cdot 2 \cdot 10^6$$

$$N_{Ri} = \left(\frac{74.65}{71.22} \right)^{3.4602} \cdot 2 \cdot 10^6 = 2353524$$

Fatigue damage:

$$D_d = \frac{n_{Ei}}{N_{Ri}}$$

$$D_d = \frac{28205}{2353524} = 0.012$$

This value can be validated in Appendix D Table D.2.

C.2 Fatigue damage calculations of case 2

This section gives an overview of the fatigue damage calculation of case 2. One waterlevel difference is chosen that contributes the most to the fatigue damage. In this case the waterlevel of 396cm contributes the most to the fatigue damage value.

Distributed load closed position:

$$q_d = \rho g \Delta h \cdot h_q$$

$$q_d = 1.0 \cdot 9.81 \cdot 3.96 \cdot 2.46 = 99.85 kN/m$$

Moment due to distributed load:

$$M_{dist} = \frac{1}{8} q_d L^2$$

$$M_{dist} = \frac{1}{8} \cdot 99.85 \cdot 12.743 = 2206 kNm$$

Distributed load after opening:

$$q_d = 1.0 \cdot 9.81 \cdot 0.35 \cdot 2.46 = 8.8 kN/m$$

Moment just after opening:

$$M_{dist} = \frac{1}{8} \cdot 8.8 \cdot 12.743 = 179 kNm$$

Total resulting waterforce on the cross-section:

$$F_W = \rho g A \Delta h$$

$$F_W = 1.0 \cdot 9.81 \cdot (2.46 \cdot 12.743) \cdot 3.96 = 556 kN$$

Normal force in the cross-section

$$F_N = \frac{F_W}{2 \cdot \tan(\alpha)}$$

$$F_N = \frac{556}{2 \cdot \frac{1}{3}} = 834 kN$$

No eccentric moment is applied.

Stress in the cross-section:

$$\sigma = \left(\frac{M}{W} \right) + \left(\frac{F_N}{A} \right)$$

$$\sigma = \left(\frac{2206}{21688000} + \frac{179}{21688000} \right) + \left(\frac{834}{46560} \right) \cdot 10^{-3} = 127.88 \text{ N/mm}^2$$

Number of cycles to lifetime:

$$N_{Ri} = \left(\frac{\Delta\sigma_C}{\Delta\sigma_i} \right)^m \cdot 2 \cdot 10^6$$

$$N_{Ri} = \left(\frac{74.65}{127.88} \right)^{3.4602} \cdot 2 \cdot 10^6 = 310527$$

Fatigue damage:

$$D_d = \frac{n_{Ei}}{N_{Ri}}$$

$$D_d = \frac{8642}{310527} = 0.028$$

This value can be validated in Appendix D Table E.3.

Appendix D

Tables and Figures case Sambeek

D.1 Sambeek Waterlevel-difference spectrum, step of 10cm, based on measurements

Wat. difference [cm]	Waterlevels [N/5years]	Percentage [%]	Ship Levelling [N/year]
488	1	0,00	2
478	0	0,00	0
468	0	0,00	0
458	0	0,00	0
448	2	0,00	4
438	1	0,00	2
428	0	0,00	0
418	0	0,00	0
408	0	0,00	0
398	1	0,00	2
388	0	0,00	0
378	0	0,00	0
368	0	0,00	0
358	0	0,00	0
348	3	0,00	6
338	36	0,01	77
328	306	0,09	656
318	459	0,14	984
308	408	0,12	875
298	335	0,10	718
288	191	0,06	409
278	185	0,06	397
268	139	0,04	298
258	107	0,03	229
248	77	0,02	165
238	78	0,02	167
228	72	0,02	154
218	69	0,02	148
208	60	0,02	129
198	65	0,02	139
188	46	0,01	99
178	55	0,02	118
168	35	0,01	75
158	38	0,01	81
148	41	0,01	88
138	25	0,01	54
128	33	0,01	71
118	33	0,01	71
108	30	0,01	64
98	37	0,01	79
88	15	0,00	32
78	9	0,00	19
68	23	0,01	49
58	28	0,01	60
48	39	0,01	84
38	63	0,02	135
28	134	0,04	287
18	9	0,00	19
8	0	0,00	0

Table D.1: Sambeek Waterlevel-difference spectrum, step of 10cm, based on measurements

D.2 Sambeek Old lock gate; Fatigue damage based on mean value

Fatigue dam. over	50 year(s)	Fatigue Damage			0,07
<i>Wat.difference</i>	$\Delta\sigma_i$	N	m	N_R	N/N_R
[cm]	[N/mm]	[-]	[-]	[-]	[-]
488	104,87	92	3,4602	616875	0,000
478	102,77	0	3,4602	661671	0,000
468	100,66	0	3,4602	710749	0,000
458	98,56	0	3,4602	764623	0,000
448	96,46	184	3,4602	823877	0,000
438	94,35	92	3,4602	889185	0,000
428	92,25	0	3,4602	961321	0,000
418	90,15	0	3,4602	1041182	0,000
408	88,04	0	3,4602	1129803	0,000
398	85,94	92	3,4602	1228391	0,000
388	83,84	0	3,4602	1338354	0,000
378	81,73	0	3,4602	1461340	0,000
368	79,63	0	3,4602	1599289	0,000
358	77,53	0	3,4602	1754492	0,000
348	75,42	277	3,4602	1929666	0,000
338	73,32	3318	3,4602	2128051	0,002
328	71,22	28206	3,4602	2353525	0,012
318	69,11	42308	3,4602	2610759	0,016
308	67,01	37608	3,4602	2905407	0,013
298	64,91	30879	3,4602	3244354	0,010
288	62,81	17605	3,4602	3636036	0,005
278	60,70	17052	3,4602	4090858	0,004
268	58,60	12812	3,4602	4621742	0,003
258	56,50	9863	3,4602	5244864	0,002
248	54,39	7098	3,4602	5980629	0,001
238	52,29	7190	3,4602	6855010	0,001
228	50,19	6637	3,4602	7901374	0,001
218	48,08	6360	3,4602	9163023	0,001
208	45,98	5531	3,4602	10696780	0,001
198	43,88	5991	3,4602	12578098	0,000
188	41,77	4240	3,4602	14908500	0,000
178	39,67	5070	3,4602	17826549	0,000
168	37,57	3226	3,4602	21524384	0,000
158	35,46	3503	3,4602	26273143	0,000
148	33,36	3779	3,4602	32462979	0,000
138	31,26	2304	3,4602	40667722	0,000
128	29,15	3042	3,4602	51752451	0,000
118	27,05	3042	3,4602	67058484	0,000
108	24,95	2765	3,4602	88733774	0,000
98	22,84	3410	3,4602	120349306	0,000
88	20,74	1383	3,4602	168109090	0,000
78	18,64	830	3,4602	243372808	0,000
68	16,53	2120	3,4602	368310139	0,000
58	14,43	2581	3,4602	589753615	0,000
48	12,33	3595	3,4602	1017167408	0,000
38	10,22	5807	3,4602	1943147790	0,000
28	8,12	12351	3,4602	4311152410	0,000
18	6,02	830	3,4602	12162193393	0,000
8	3,91	0	3,4602	53851991167	0,000

Table D.2: Sambeek Old lock gate; Fatigue damage based on mean value

Appendix E

Tables and Figures case Terneuzen

E.1 Terneuzen Waterlevel-difference spectrum, step of 10cm, based on measurements

Wat. difference [cm]	Waterlevels [N/5years]	Percentage [%]	Ship Levelling [N/year]
526	5	0,0000	0
516	4	0,0000	0
506	13	0,0000	0
496	33	0,0001	1
486	78	0,0003	2
476	191	0,0007	6
466	442	0,0017	14
456	879	0,0033	28
446	1672	0,0064	53
436	2484	0,0094	79
426	3517	0,0134	112
416	4745	0,0180	152
406	5607	0,0213	179
396	6295	0,0239	201
386	6955	0,0264	222
376	7272	0,0276	232
366	7602	0,0289	243
356	7501	0,0285	239
346	7473	0,0284	239
336	7242	0,0275	231
326	7184	0,0273	229
316	6781	0,0258	217
306	6536	0,0248	209
296	6248	0,0237	199
286	6076	0,0231	194
276	5777	0,0220	184
266	5524	0,0210	176
256	5384	0,0205	172
246	5190	0,0197	166
236	4927	0,0187	157
226	4776	0,0182	152
216	4764	0,0181	152
206	4429	0,0168	141
196	4399	0,0167	140
186	4289	0,0163	137
176	4139	0,0157	132
166	4191	0,0159	134
156	4003	0,0152	128
146	4204	0,0160	134
136	4006	0,0152	128
126	4204	0,0160	134
116	4220	0,0160	135
106	4422	0,0168	141
96	4617	0,0175	147
86	4733	0,0180	151
76	5138	0,0195	164
66	5248	0,0199	168
56	5756	0,0219	184
46	5876	0,0223	188
36	5872	0,0223	187
26	5829	0,0222	186
16	5759	0,0219	184
6	3354	0,0127	107

Table E.1: Terneuzen Waterlevel-difference spectrum, step of 10cm, based on measurements

E.2 Terneuzen Waterlevel-difference spectrum, step of 10cm, based on new prediction model

Wat. difference [cm]	Time [min]	Percentage [%]	Ship Levelling [N/year]
426	69	0,092	774
416	29	0,039	324
406	22	0,030	252
396	19	0,026	215
386	17	0,023	191
376	16	0,021	175
366	14	0,019	163
356	14	0,018	153
346	13	0,017	146
336	12	0,017	140
326	12	0,016	135
316	12	0,016	130
306	11	0,015	127
296	11	0,015	124
286	11	0,014	121
276	11	0,014	119
266	10	0,014	117
256	10	0,014	116
246	10	0,014	114
236	10	0,013	113
226	10	0,013	112
216	10	0,013	112
206	10	0,013	111
196	10	0,013	111
186	10	0,013	111
176	10	0,013	111
166	10	0,013	112
156	10	0,013	112
146	10	0,013	113
136	10	0,014	114
126	10	0,014	115
116	10	0,014	117
106	11	0,014	119
96	11	0,014	121
86	11	0,015	123
76	11	0,015	126
66	12	0,015	130
56	12	0,016	134
46	12	0,017	139
36	13	0,017	145
26	14	0,018	152
16	14	0,019	162
6	9	0,012	102

Table E.2: Terneuzen Waterlevel-difference spectrum, step of 10cm, based on new prediction model

E.3 Terneuzen Old lock gate; Fatigue damage based on mean value

Fatigue dam. over	50 year(s)	Fatigue Damage				0,39
<i>Wat.difference</i>	$\Delta\sigma_i$	N	m	N_R	N/N_R	
[cm]	[N/mm]	[-]	[-]	[-]	[-]	
526	172,0	7	3,4602	111312	0,000	
516	168,6	5	3,4602	119261	0,000	
506	165,2	18	3,4602	127957	0,000	
496	161,8	45	3,4602	137488	0,000	
486	158,4	107	3,4602	147954	0,001	
476	155,0	262	3,4602	159470	0,002	
466	151,6	607	3,4602	172167	0,004	
456	148,2	1207	3,4602	186199	0,006	
446	144,9	2296	3,4602	201740	0,011	
436	141,5	3410	3,4602	218994	0,016	
426	138,1	4829	3,4602	238198	0,020	
416	134,7	6515	3,4602	259629	0,025	
406	131,3	7698	3,4602	283611	0,027	
396	127,9	8643	3,4602	310527	0,028	
386	124,5	9549	3,4602	340827	0,028	
376	121,1	9984	3,4602	375049	0,027	
366	117,7	10437	3,4602	413831	0,025	
356	114,3	10298	3,4602	457941	0,022	
346	110,9	10260	3,4602	508303	0,020	
336	107,5	9943	3,4602	566036	0,018	
326	104,1	9863	3,4602	632507	0,016	
316	100,7	9310	3,4602	709390	0,013	
306	97,3	8973	3,4602	798755	0,011	
296	93,9	8578	3,4602	903175	0,009	
286	90,5	8342	3,4602	1025875	0,008	
276	87,1	7931	3,4602	1170933	0,007	
266	83,7	7584	3,4602	1343545	0,006	
256	80,3	7392	3,4602	1550403	0,005	
246	77,0	7125	3,4602	1800206	0,004	
236	73,6	6764	3,4602	2104398	0,003	
226	70,2	6557	3,4602	2478209	0,003	
216	68,2	6541	3,4602	2731506	0,002	
206	66,9	6081	3,4602	2923286	0,002	
196	65,6	6039	3,4602	3132781	0,002	
186	64,2	5888	3,4602	3362035	0,002	
176	62,9	5683	3,4602	3613379	0,002	
166	61,6	5754	3,4602	3889477	0,001	
156	60,3	5496	3,4602	4193379	0,001	
146	58,9	5772	3,4602	4528593	0,001	
136	57,6	5500	3,4602	4899160	0,001	
126	56,3	5772	3,4602	5309755	0,001	
116	55,0	5794	3,4602	5765802	0,001	
106	53,6	6071	3,4602	6273617	0,001	
96	52,3	6339	3,4602	6840580	0,001	
86	51,0	6498	3,4602	7475350	0,001	
76	49,7	7054	3,4602	8188126	0,001	
66	48,3	7205	3,4602	8990975	0,001	
56	47,0	7903	3,4602	9898234	0,001	
46	45,7	8067	3,4602	10927023	0,001	
36	44,4	8062	3,4602	12097884	0,001	
26	43,0	8003	3,4602	13435598	0,001	
16	41,7	7907	3,4602	14970227	0,001	
6	40,0	4605	3,4602	17345924	0,000	

Table E.3: Terneuzen Old lock gate; Fatigue damage based on mean value

